PB84-143148

Study of the Steam Gasification of Organic Wastes

Princeton Univ., NJ

Prepared for

Industrial Environmental Research Lab.
Research Triangle Park, NC

Jan 84

U.S. Department of Commerce
National Technical Information Service
NTIS

PB84-143148

EPA-600/7-84-009
January 1984

A STUDY OF THE STEAM GASIFICATION OF ORGANIC WASTES

by

Michael J. Antal, Jr.
William E. Edwards
Henry L. Friedman
Frank E. Rogers

Department of Mechanical and Aerospace Engineering
Princeton University
Princeton, New Jersey 08544

University Grant No. R804836010

Project Officer

Walter W. Liberick, Jr.
U.S. Environmental Protection Agency
Industrial Environmental Research Laboratory
Cincinnati, Ohio 45268

INDUSTRIAL ENVIRONMENTAL RESEARCH LABORATORY
OFFICE OF RESEARCH AND DEVELOPMENT
U.S. ENVIRONMENTAL PROTECTION AGENCY
CINCINNATI, OHIO 45268

REPRODUCED BY
NATIONAL TECHNICAL
INFORMATION SERVICE
U.S. DEPARTMENT OF COMMERCE
SPRINGFIELD, VA. 22161

TECHNICAL REPORT DATA
(Please read Instructions on the reverse before completing)

1. REPORT NO. EPA-600/7-84-009	2.
3. RECIPIENT'S ACCESSION NO. PB84 143148	
4. TITLE AND SUBTITLE A Study of the Steam Gasification of Organic Wastes	5. REPORT DATE January 1984 6. PERFORMING ORGANIZATION CODE
7. AUTHOR(S) Michael J. Antal, Jr., William E. Edwards, Henry L. Friedman, Frank E. Rogers	8. PERFORMING ORGANIZATION REPORT NO.
9. PERFORMING ORGANIZATION NAME AND ADDRESS Department of Mechanical & Aerospace Engineering Princeton University Princeton, NJ 08544	10. PROGRAM ELEMENT NO. 11. CONTRACT/GRANT NO. R804836010
12. SPONSORING AGENCY NAME AND ADDRESS Industrial Environmental Research Laboratory--IERL-Ci Office of Research and Development U.S. Environmental Protection Agency Cincinnati, OH 45268	13. TYPE OF REPORT AND PERIOD COVERED 14. SPONSORING AGENCY CODE EPA/600/12
15. SUPPLEMENTARY NOTES	

16. ABSTRACT

Chemical kinetic data describing the pyrolysis/gasification characteristics of organic waste (biomass) materials is needed for the design of improved conversion reactors. Unfortunately, little data is available in the literature on the pyrolysis kinetics of waste materials, and essentially no data has been published on the rates and products of the secondary, gas phase reactions. The objective of this research was to determine the effects of various reactor conditions (residence time, temperature, and heating rate) on the rates of the primary pyrolysis reactions, and the rates and products of the secondary gas phase reactions.

17. KEY WORDS AND DOCUMENT ANALYSIS

a. DESCRIPTORS	b. IDENTIFIERS/OPEN ENDED TERMS	c. COSATI Field/Group

18. DISTRIBUTION STATEMENT Release Unlimited	19. SECURITY CLASS *(This Report)* Unclassified	21. NO. OF PAGES 106
	20. SECURITY CLASS *(This page)* Unclassified	22. PRICE

EPA Form 2220-1 (Rev. 4-77) PREVIOUS EDITION IS OBSOLETE

NOTICE

This document has been reviewed in accordance with U.S. Environmental Protection Agency policy and approved for publication. Mention of trade names or commercial products does not constitute endorsement or recommendation for use.

FOREWORD

When energy and material resources are extracted, processed, converted, and used, the related pollutional impacts on our environment and even on our health often require that new and increasingly more efficient pollution control methods be used. The Industrial Environmental Research Laboratory-Cincinnati (IERL-Ci) assists in developing and demonstrating new and improved methodologies that will meet these needs both efficiently and economically.

This study investigated the chemical kinetic data describing the pyrolysis/gasification characteristics of organic waste materials. The results will be useful for the design of improved conversion reactors. For further information, contact the Oil Shale and Energy Mining Branch of the Energy Pollution Control Division.

David G. Stephan
Director
Industrial Environmental Research
Laboratory-Cincinnati

TYPING GUIDE SHEET
BEGIN FIRST LINE OF TEXT HERE
CENTER OF PAGE
TOP OF IMAGE AREA
DROPPED HEAD, BEGIN SECTIONS HERE
BEGIN LAST LINE OF TEXT
BOTTOM OF IMAGE AREA; OUTSIDE DIMENSION FOR TABLES AND ILLUSTRATIONS
3/8"
PAGE NUMBER
EPA-287 (Cin.) (4-76)

ABSTRACT

Chemical kinetic data describing the pyrolysis/gasification characteristics of organic waste (biomass) materials is needed for the design of improved conversion reactors. Unfortunately, little data is available in the literature on the pyrolysis kinetics of waste materials, and essentially no data has been published on the rates and products of the secondary, gas phase reactions. The objective of this research was to determine the effects of various reactor conditions (residence time, temperature, and heating rate) on the rates of the primary pyrolysis reactions, and the rates and products of the secondary gas phase reactions.

Because steam was known to be a good gasification/fuel conversion medium for various liquid and gaseous hydrocarbons, coal and peat, the experimental studies described here focused on the steam gasification of organic waste (biomass) materials. However, no attempt was made to study the water gas or Boudouard reactions, which require higher temperatures than used in this research. As discussed in Section II, the chemistry of biomass gasification differs considerably from that of coal or peat.

The most important result of this research was the discovery that pyrolytic volatile matter cracks very rapidly in the gas phase at temperatures above 650°C to yield a hydrocarbon rich synthesis gas. At temperatures above 700°C, rates of ethylene formation are second only to carbon monoxide in magnitude. Consequently, organic waste materials appear to be excellent, low priced cracking feedstocks for olefin production. More research is recommended to detail reaction mechanisms and improve product slates.

ACKNOWLEDGMENTS

Both undergraduate and graduate students at Princeton greeted the opportunity to participate in this research with great enthusiasm. The following students made significant contributions to the research described in this report: T. Mattocks, V. Kothari, R. Novak, D. Wu, F. Connor, D. Urban, J. Huffman, R. Grayson, D. Keyes, C. Okoh and G. Haddon. The authors wish to acknowledge the contributions they made to this work.

The quartz reactors used in our work were skillfully fabricated by Mr. H. Olson, the University Glassblower. Finally, it is a pleasure to acknowledge the expert assistance of Ms. P. Berger in typing and assembling this report.

CONTENTS

	Page
Abstract	iv
Acknowledgements	v
Figures	vii
Tables	x
I. Introduction	1
II. Summary and Conclusions	2
III. Recommendations	4
IV. Thermochemical Predictions	5
V. Primary Pyrolysis Kinetics	16
VI. Secondary, Gas Phase Reaction Kinetics	53
VII. Model Compound Studies	75
VIII. Pressurized Steam Gasification Studies	84
References	89
Appendix I	95

FIGURES

Number		Page
1.	Thermochemical predictions of the weight fraction and gas calorific value of the products of cellulose pyrolysis as a function of temperature at a pressure of 0.1013 bars (0.1 atmosphere)	8
2.	Thermochemical predictions of the weight fraction and gas calorific value of the products of cellulose pyrolysis as a function of temperature at a pressure of 1.013 bars (1 atmosphere)	9
3.	Thermochemical predictions of the weight fraction and gas calorific value of the products of cellulose pyrolysis as a function of temperature at a pressure of 10.13 bars (10 atmospheres)	10
4.	Thermochemical predictions of the weight fraction and gas calorific value of the products of cellulose pyrolysis as a function of temperature at a pressure of 101.3 bars (100 atmospheres)	11
5.	Thermochemical predictions of the weight fraction and gas calorific value of the products of cellulose pyrolysis in steam (7 moles steam per mole cellulose) as a function of temperature at a pressure of 0.1013 bars (0.1 atmosphere)	12
6.	Thermochemical predictions of the weight fraction and gas calorific value of the products of cellulose pyrolysis in steam (7 moles steam per mole cellulose) as a function of temperature at a pressure of 1.013 bars (1 atmosphere)	13
7.	Thermochemical predictions of the weight fraction and gas calorific value of the products of cellulose pyrolysis in steam (7 moles steam per mole cellulose) as a function of temperature at a pressure of 10.13 bars (10 atmospheres)	14
8.	Thermochemical predictions of the weight fraction and gas calorific value of the products of cellulose pyrolysis in steam (7 moles steam per mole cellulose) as a function of temperature at a pressure of 101.3 bars (100 atmospheres)	15
9.	Schematic of TGA Quartz Tube modified for use of steam	21
10.	Thermogravimetric curves for the pyrolysis of cellulose in nitrogen (50 ml/min) at various heating rates	22

Number		Page
11.	Thermogravimetric curves for the pyrolysis of cellulose in steam at various heating rates	23
12.	Plot of the activation energy vs. weight fraction remaining for the pyrolysis of cellulose in steam (o) and Nitrogen (•)	26
13.	Experimental and calculated thermogravimetric curves for the pyrolysis of cellulose in steam	27
14.	Experimental and calculated thermogravimetric curves for the pyrolysis of cellulose in nitrogen.	28
15.	Experimental and calculated thermogravimetric curves for the pyrolysis of cellulose in steam and nitrogen.	31
16.	Thermogravimetric curves for the pyrolysis of N.Y. Times newsprint in nitrogen	34
17.	Thermogravimetric Curves for the pyrolysis of Wall Street Journal newsprint in nitrogen	35
18.	Activation energy vs. weight fraction for pyrolysis of newsprint from The Wall Street Journal in nitrogen.	36
19.	Activation energy vs. weight fraction for pyrolysis of newsprint from The New York Times in nitrogen	37
20.	Thermogravimetric curves for the pyrolysis of hardwood in nitrogen	40
21.	Thermogravimetric curves for the pyrolysis of softwood in nitrogen	41
22.	Activation energy vs. weight fraction for pyrolysis of hardwood in nitrogen	42
23.	Activation energy vs. weight fraction for pyrolysis of softwood in nitrogen	43
24.	Thermogravimetric curves for the pyrolysis of hardwood and its components in nitrogen	46
25.	Thermogravimetric curves for the pyrolysis of softwood and its components in nitrogen	47
26.	Thermogravimetric curves for the pyrolysis of cow manure in nitrogen	50
27.	Activation energy vs. weight fraction for pyrolysis of cow manure in nitrogen	52
28.	Schematic of the tubular quartz reactor experiment	55
29.	Temperature map of tubular plug flow reactor	56
30.	Non-hydrocarbon gas production vs. residence time for various gas phase temperatures	65

Number		Page
31.	Paraffinic hydrocarbon gas production vs. residence time for various gas phase temperatures	66
32.	Olefinic hydrocarbon gas production vs. residence time for various gas phase temperatures	67
33.	Carbon, hydrogen and oxygen efficiency vs. residence time for various gas phase temperatures.	68
34.	Arrhenius plot of the gas phase production rate for various gas species	71
35.	Arrhenius plot of the gas phase production rate for various gas species	72
36.	Flowchart of CDS system	76
37.	Pressurized DSC reactor system schematic.	86
38.	Tubular reactor schematic	87

TABLES

Number		Page
1.	Pyrolysis Kinetics Derived from Experiments Utilizing Small (< 1 g) Samples	18
2.	Kinetic Parameters for Cellulose Pyrolysis in N_2	30
3.	Kinetic Parameters for Cellulose Pyrolysis in H_2O	30
4.	Kinetic Parameters for The New York Times in Nitrogen-Single Reaction Model	38
5.	Kinetic Parameters for The Wall Street Journal in Nitrogen-Single Reaction Model	38
6.	Kinetic Parameters for Hardwood HW-1 in Nitrogen-Triple Reaction Model	44
7.	Kinetic Parameters for Softwood SW-2 in Nitrogen-Triple Reaction Model	45
8.	Kinetic Parameters for Hardwood HW-1 in Nitrogen-Single Reaction Model	49
9.	Kinetic Parameters for Softwood SW-2 in Nitrogen-Single Reaction Model	49
10.	Kinetic Parameters for Cow Manure in Nitrogen-Single Reaction Model	51
11.	Various Parameters Used to Calculate Gas Phase Residence Time	62
12.	Selected Gasification Results for Cellulose.	69
13.	Apparent Low Temperature ($500°C \leq T \leq 675°C$) Activation Energy (E_j) for Various Gas Species.	70
14.	Numerical Values Used in the Gas Phase Kinetic Model	74
15.	Setaram Differential Scanning Calorimeter (DSC).	85
16.	Cellulose Gasification Results at Atmospheric and Elevated Pressures	88

SECTION I

INTRODUCTION

In an age of diminishing fossil fuel reserves, reflected in rapidly escalating prices for fluid fuels, local shortages of gasoline and fuel oil, and large imbalances in international trade, attention has recently focused on fluid fuel production from renewable biomass* resources. Pyrolysis is one attractive method for converting biomass to more useful fuel forms. Unfortunately, the product slate of most pyrolysis processes includes significant quantities of relatively valueless tars, oils, pitches, liquors and some water soluble organic compounds. These low value products of conversion processes adversely affect process economics because they result in reduced conversion efficiencies, and they require more complicated equipment for their handling and ultimate disposal.

The primary goal of this research was to experimentally determine the conditions required for the conversion of these valueless products into a hydrocarbon rich synthesis gas. To accomplish this goal the research effort focused primarily on a careful elucidation of the chemistry of waste pyrolysis/gasification in steam. Since kinetic information is absolutely required for the development of improved gasification systems, all experiments were designed and conducted to provide carefully characterized rate data. When possible, this data was interpreted using Arrhenius kinetics, and mathematical models were developed to fit the experimental data. Although these models were not intended to be of fundamental import, they are expected to be of great use to the chemical engineer involved with the design of advanced gasification systems.

*Throughout this report the words "biomass" and "organic wastes" are used interchangeably, since their thermochemical properties are similar.

SECTION II

SUMMARY AND CONCLUSIONS

The gasification characteristics of biomass differ considerably from those of coal, lignite, peat and other fossil fuels. Research described in this report has shown biomass gasification to be a three-step process:

1. Pyrolysis. At modest temperatures (300° to 500°C) biomass materials lose between 70% to 90% of their weight by pyrolysis, forming gaseous volatile matter and solid char. Biomass materials contain much more volatile matter than coal, and biomass loses weight more rapidly than coal by pyrolysis.

2. Cracking/Reforming of the Volatile Matter. At somewhat higher temperatures (600°C or more) the volatile matter evolved by the pyrolysis reactions (step 1) reacts in various ways to form a hydrocarbon rich synthesis gas. These reactions happen very rapidly (seconds or less) and can be manipulated to favor the formation of various hydrocarbons (such as ethylene).

3. Char Gasification. At even higher temperatures (800°C or more) char gasification occurs by reactions

$$C + H_2O \rightarrow CO + H_2$$
$$C + CO_2 \rightarrow 2CO$$
$$C + \tfrac{1}{2} O_2 \rightarrow CO$$
$$C + O_2 \rightarrow CO_2$$

These reactions can be used to describe coal gasification, but proceed more slowly and under more demanding conditions than those required for steps 1 and 2. Since step 1 produces less than 30% by weight char, these char gasification reactions play a minor role in biomass gasification.

Although each of these three steps play a role in commercial reactors designed for biomass gasification, the ultimate product slate of the reactor is largely determined by the second step of the gasification process. Careful control of reactor conditions (i.e., gas phase residence time and temperature) can favor the production of valuable hydrocarbons (olefins and paraffins) from biomass over a less valuable synthesis gas (CO and H_2), or valueless tars, liquors and oils. The focus of this report is the determination of those conditions which favor the formation of hydrocarbons from biomass using thermochemical conversion techniques. The conclusion

is that surprisingly mild conditions are required to effect the conversion of biomass to hydrocarbons.

Those familiar with petrochemical technologies will recognize similarities between the results given in this report and comparable results for steam cracking naphthas and gas oils to ethylene. In fact, biomass may be a more desirable source of olefins than feedstocks traditionally used by the petrochemical industry. Data given in this report indicate that from a thermochemical viewpoint biomass is a much more desirable solid fuel feedstock for the production of fluid fuels and chemicals than coal, lignite, or peat.

During the past two years over 60% of the Princeton research effort on biomass and waste conversion has focused on elucidating the rates and products of the secondary, gas phase reactions of pyrolytic volatile matter in steam (step 2 described earlier). Results of our research in this area are described in Section VI of this report. It represents the first detailed study of secondary, gas phase reaction rates and products reported in the literature. The most important conclusion resulting from this aspect of the research is that the secondary, gas phase reactions are dominated by cracking chemistry. At temperatures above 700°C these cracking reactions reach completion in less than one second. Thus the technologies developed for steam cracking naphthas and gas oils are applicable to biomass conversion, and may prove to be the favored conversion route as conversion technologies develop and mature.

A significant effort was also made to study the effects of increased pressure on the products and rates of the primary and secondary pyrolysis reactions. Numerous difficulties were encountered which substantially impeded our progress; nevertheless some early results are reported here.

The remaining fraction of Princeton's research effort was divided between kinetic studies of the solid phase pyrolysis reactions (step 1 described earlier), and some exploratory model compound studies aimed at providing an insight into the gas phase chemistry. In spite of the great variety of biomass materials studied, their rates and mechanisms of weight loss by pyrolysis were reasonably similar from an engineering point of view. Kinetic weight loss models, developed to describe the solid phase pyrolysis reactions, are presently being used in a reactor design effort going on at Princeton. The model compound studies focused on the gas phase pyrolysis of ethanol, used to simulate the cracking chemistry of cellulose volatiles. Competitive reactions forming ethylene, or CH_4, CO and H_2 were studied. Cracking rates were measured, and found to compare favorably with literature values. Future research on model compounds will be aimed at determining those conditions which give rise to maximum production of olefins from biomass by offering an insight into the gas phase cracking chemistry.

SECTION III

RECOMMENDATIONS

Since the research described in this report indicates that biomass and wastes may be more desirable than coal, peat, or lignite as gasification feedstocks, they should be thoroughly investigated as synfuel sources. A more thorough investigation of the thermochemical conversion chemistry of biomass and wastes to useful fluid fuels would be necessary before final economic and environmental judgments can be made. These efforts should include studies of gasification mechanisms, kinetics, and catalysis. More attention should be given to the secondary, gas phase reactions of pyrolytic volatile matter. Novel reactors, designed specifically to study the gas phase chemistry, should be developed. Without a better insight into the gas phase chemistry, biomass gasification reactor design efforts will continue to result in 19th and early 20th century concepts, rather than the 21st century processes needed to compete with today's sophisticated hydrocarbon processing industry.

SECTION IV

THERMOCHEMICAL PREDICTIONS*

Thermochemical calculations have been made to predict the potential products of cellulose pyrolysis. These calculations also serve to increase knowledge of the dependence of those products on the conditions (pressure and temperature) prevalent within a reactor, and a helpful background for understanding the gasification data described in Chapter VI.

The thermochemical predictions rely on a computer program developed by NASA* for calculating complex equilibrium compositions, rocket performance, incident and reflected shocks, and Chapman-Jouquet detonations. The program minimizes the Gibb's free energy of a mixture of chemical species subject to the mass balance constraint. Lagrangian multipliers are introduced, partial derivatives taken and set equal to zero, and the Newton-Raphson method is used to determine roots of the resultant equations. These roots correspond to the equilibrium composition of the mixture for a specific temperature and pressure.

In the temperature range of interest, char exists in equilibrium with the other products of cellulose pyrolysis. As a first approximation, char can be represented by carbon. Using the chemical formula of cellulose ($C_6H_{10}O_5$) to establish the relative amounts of the elements present in the system, and assuming the thermodynamic properties of char can be adequately represented by carbon, the NASA program was used to calculate the equilibrium composition of the mixture as a function of temperature and pressure. The rationale for this approach rests on the fact that char is observed to be in chemical equilibrium with the pyrolysis products at elevated temperatures. The only role cellulose plays in the process is to supply the chemical elements found in the system. Cellulose is not present in the system as a species at elevated temperatures.

Figures 1-4 indicate the effects of pressure and temperature on the products of cellulose pyrolysis. (Note: Calculations of the equilibrium composition were made at 300°, 400°, 500°, 600°, and 800°C. Lines connecting points indicating the equilibrium composition at these temperatures serve only to identify the calculated points. The lines are not intended to be used for interpolation between the points.) The amount of carbon (char) in equilibrium with the other pyrolysis products is reduced by increasing temperature and increased by increasing pressure. These figures

*This material was published in References 10, 11, 12 and 13.

also indicate the calorific value of the evolved gases on a Gj/Mg of cellulose pyrolyzed basis. Carbon monoxide and hydrogen production are favored by high temperatures and low pressures; whereas methane, carbon dioxide, and water are favored by low temperatures and high pressures. The calorific value of the gas is increased by higher temperatures and lower pressures. These results are easily understood in terms of the following reactions:

Reaction	$T(k_p \sim 1)$	
$C + H_2O \rightarrow CO + H_2$	670°C	(1)
$C + CO_2 \rightarrow 2CO$	690	(2)
$CH_4 + 2H_2O \rightarrow CO_2 + 4H_2$	610	(3)
$CO + 3H_2 \rightarrow CH_4 + H_2O$	650	(4)
$2CO + 2H_2 \rightarrow CH_4 + CO_2$	630	(5)
$C + 2H_2 \rightarrow CH_4$	540	(6)
$CO + H_2O \rightarrow H_2 + CO_2$	830	(7)

The temperature listed indicates where the value of the equilibrium constant at atmospheric pressure approximately equals one. The first three reactions produce hydrogen and/or carbon monoxide. These reactions are endothermic and are favored by high temperatures. Consequently, the calorific value (Gj/Mg) of the gas is increased by these reactions as the pyrolysis temperature increases. The stoichiometry of these equations indicates that low pressures favor the formation of gaseous products. Similarly, Reactions (4)-(7) are exothermic and are favored by low temperatures and high pressures. These reactions are the source of methane, water, and/or carbon dioxide. Thus, the results of the complex equilibrium calculations agree with an intuitive understanding of the constituent reactants.

Some interesting conclusions can be drawn from these results. Although higher hydrocarbon species (i.e., C_2H_2, C_2H_4, C_2H_6) were considered in the calculation, they were not found present in equilibrium for any of the pressures or temperatures indicated. Evidently, the presence of higher hydrocarbons in the products of cellulose pyrolysis indicates that those products did not have sufficient time to reach an equilibrium composition. These results suggest the important effects of residence time, heating rate, and catalysis on the products of pyrolysis.

Similar calculations were made to describe the resultant products of cellulose pyrolysis in steam. Predictions of the equilibrium chemical composition for one mole of cellulose pyrolyzed with seven moles of available water are given in Figs. 5-8. These predictions indicate that the use of steam as a gasification medium should decrease the amount of char residue formed, and should generally increase the amounts of carbon monoxide and hydrogen present in the gas (assuming that the steam is condensed following pyrolysis and pressurized over one atmosphere). The calorific value of the

gas (Gj/Mg) should also be increased. These predictions can also be understood in terms of Eqs. 1-7. The presence of steam enhances hydrogen production by Reactions 1 and 3 which are endothermic, yielding a gas of higher calorific value (Gj/Mg). Reaction 7 is also enhanced, but the calorific value of the gas (Gj/Mg) is lowered due to the exothermicity of the reaction.

These calculations suggest steam to be a useful medium for pyrolysis, yielding increased quantities of gaseous fuels with a more useful chemical composition. Comparisons of experimental results with thermochemical predictions will be made to determine how closely equilibrium conditions are obtained during pyrolysis.

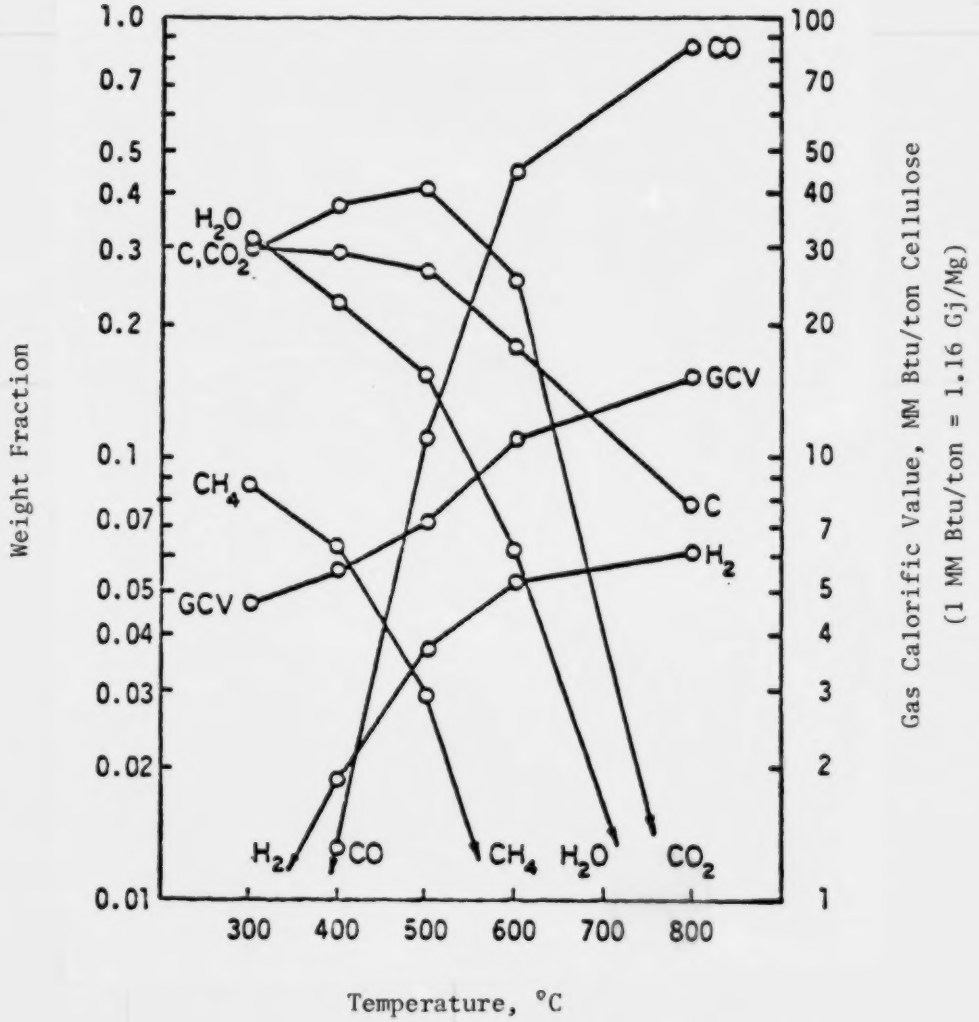

Figure 1. Thermochemical predictions of the weight fraction and gas calorific value of the products of cellulose pyrolysis as a function of temperature at a pressure of 0.1013 bars (0.1 atmosphere).

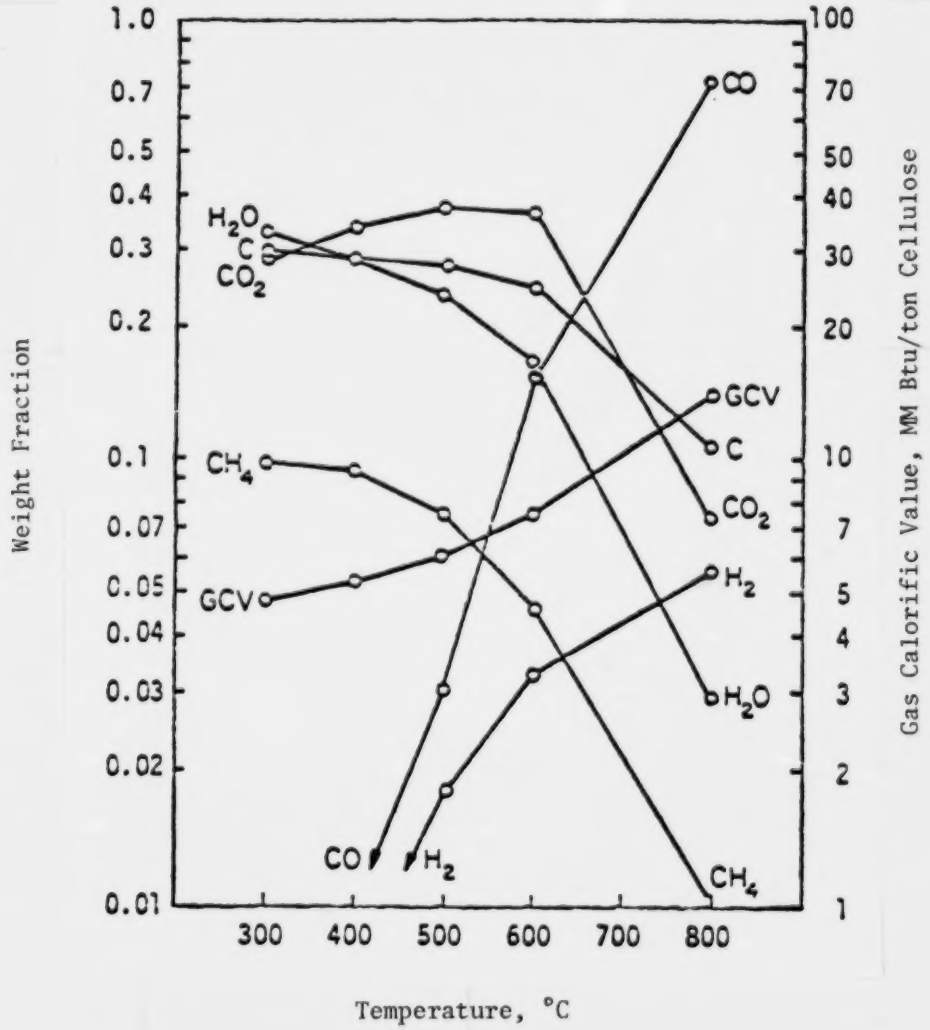

Figure 2. Thermochemical predictions of the weight fraction and gas calorific value of the products of cellulose pyrolysis as a function of temperature at a pressure of 1.013 bars (1 atmosphere).

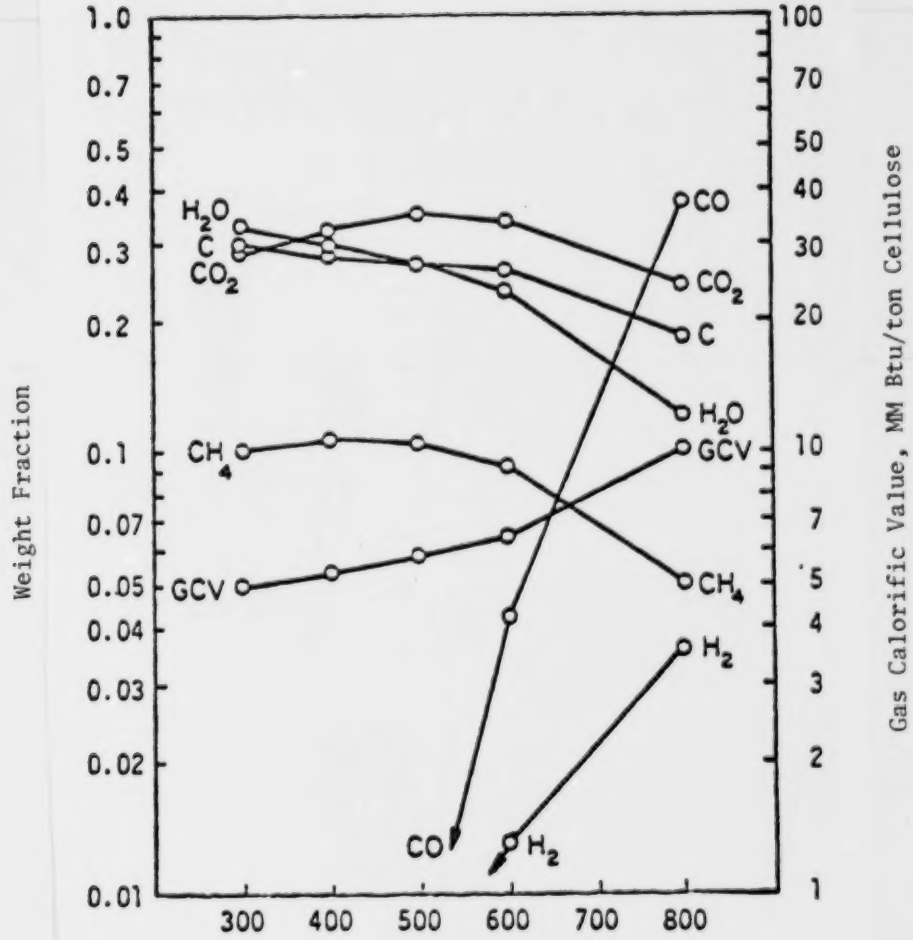

Figure 3. Thermochemical predictions of the weight fraction and gas calorific value of the products of cellulose pyrolysis as a function of temperature at a pressure of 10.13 bars (10 atmospheres).

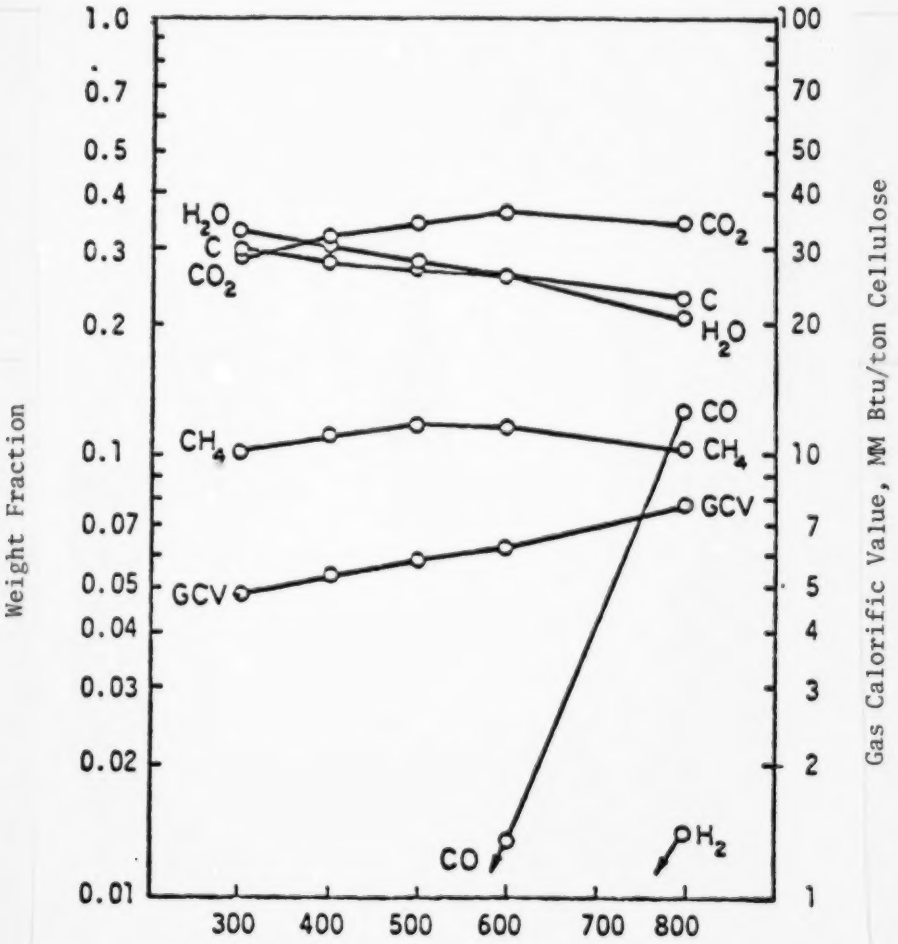

Figure 4. Thermochemical predictions of the weight fraction and gas calorific value of the products of cellulose pyrolysis as a function of temperature at a pressure of 101.3 bars (100 atmospheres).

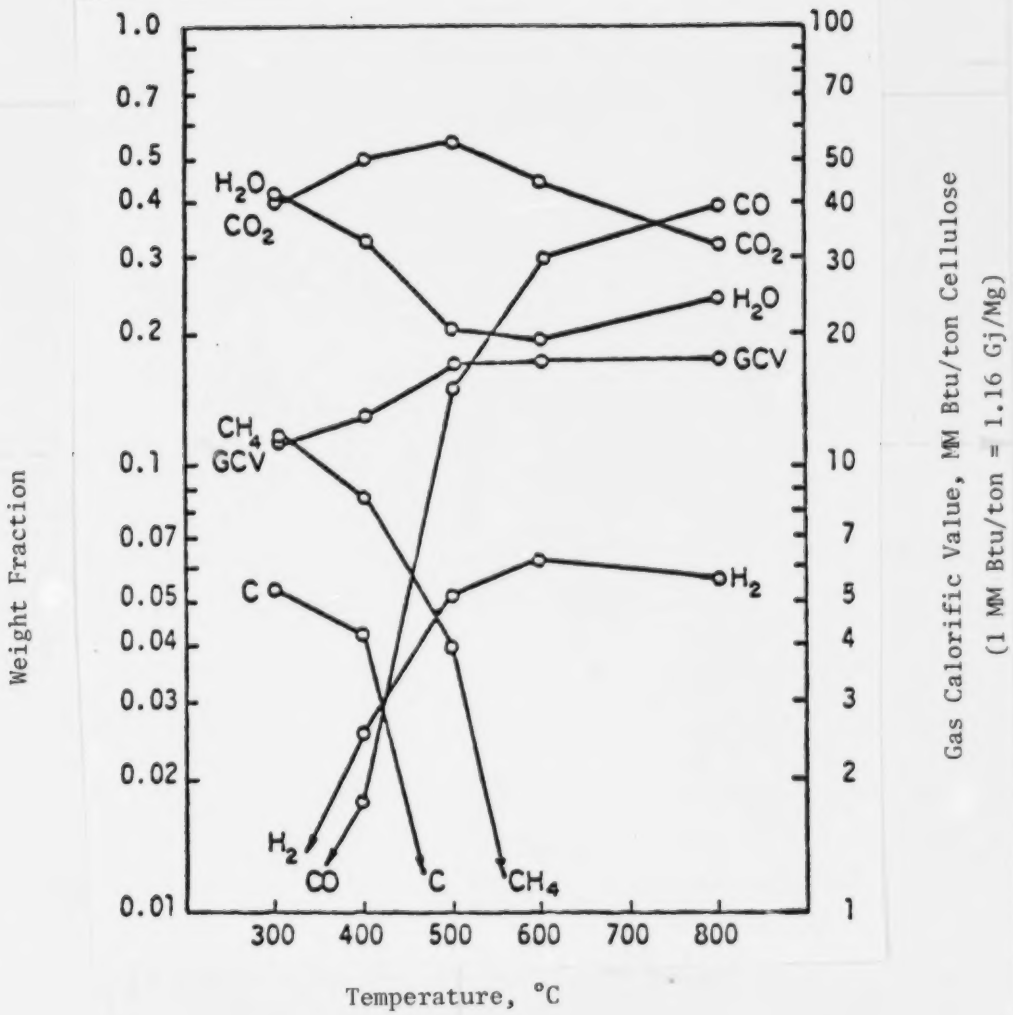

Figure 5. Thermochemical predictions of the weight fraction and gas calorific value of the products of cellulose pyrolysis in steam (7 moles steam per mole cellulose) as a function of temperature at a pressure of 0.1013 bars (0.1 atmosphere).

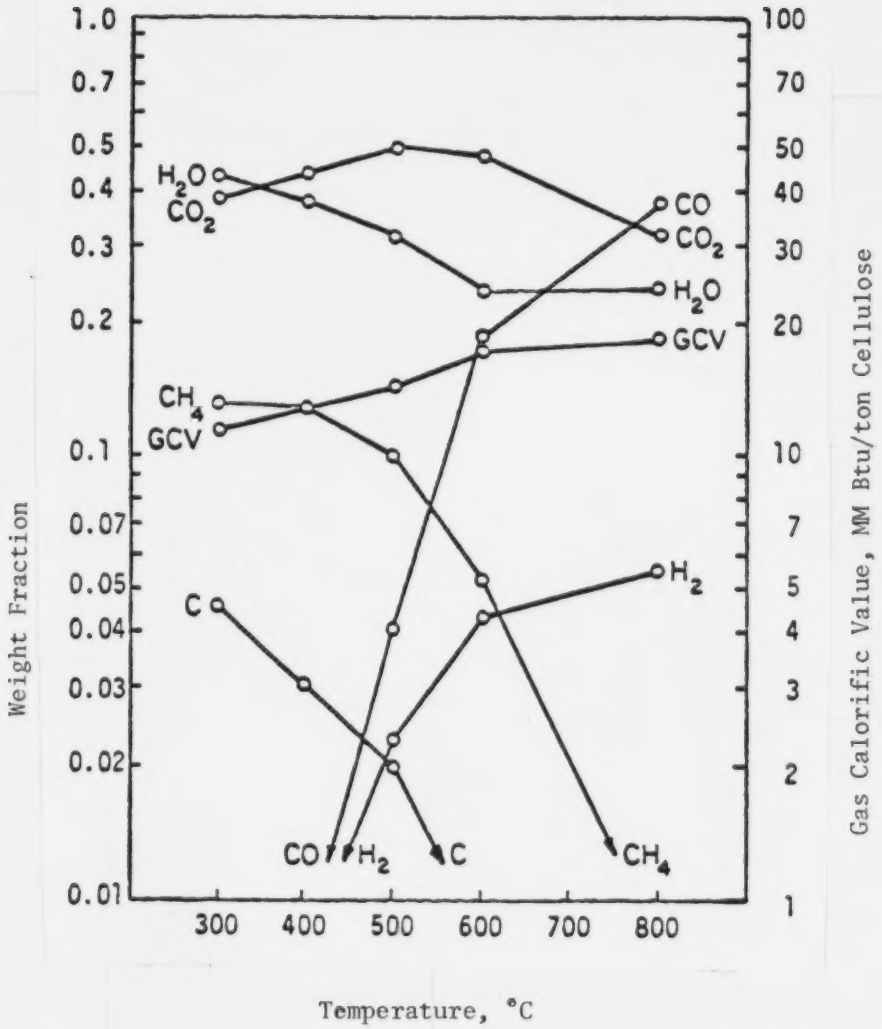

Figure 6. Thermochemical predictions of the weight fraction and gas calorific value of the products of cellulose pyrolysis in steam (7 moles steam per mole cellulose) as a function of temperature at a pressure of 1.013 bars (1 atmosphere).

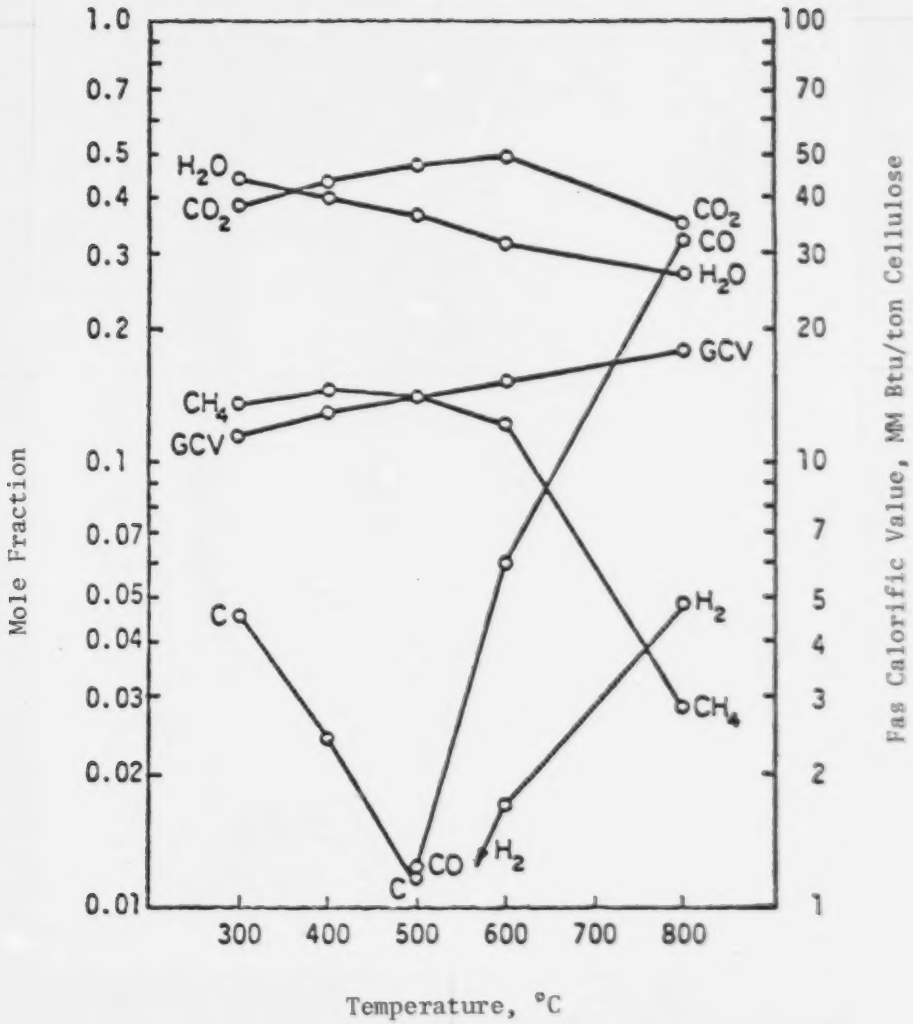

Figure 7. Thermochemical predictions of the weight fraction and gas calorific value of the products of cellulose pyrolysis in steam (7 moles steam per mole cellulose) as a function of temperature at a pressure of 10.13 bars (10 atmospheres).

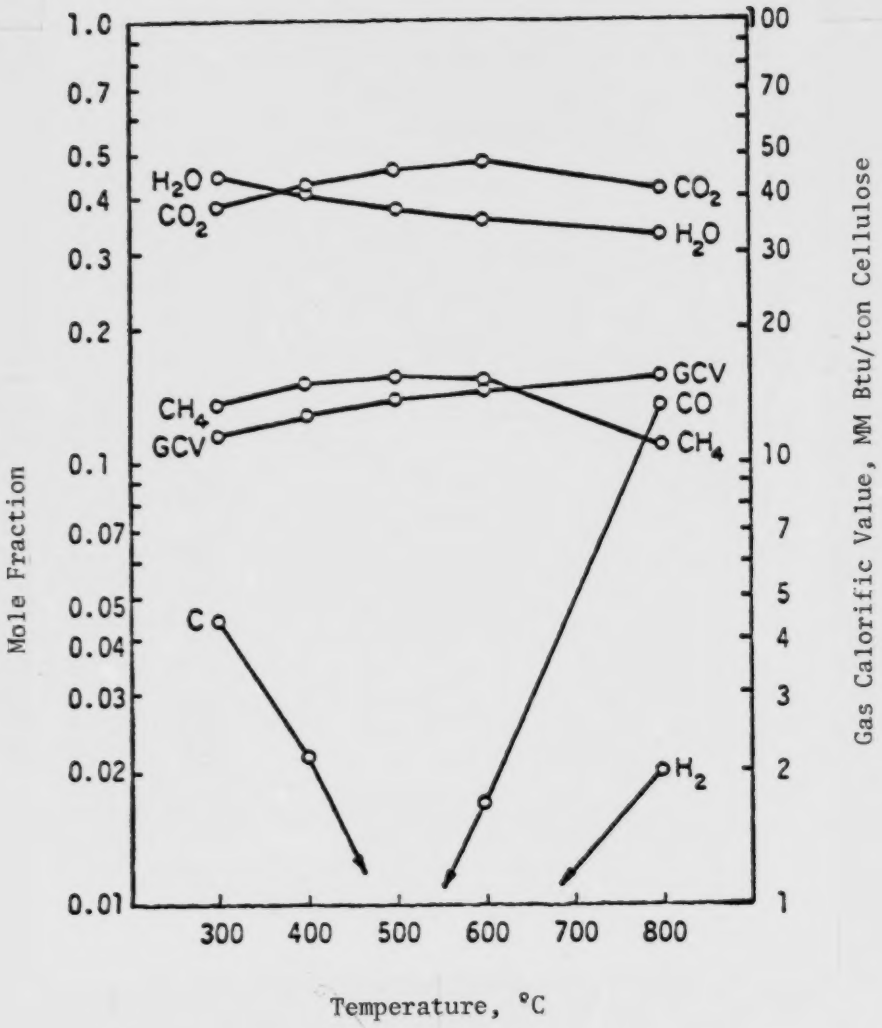

Figure 8. Thermochemical predictions of the weight fraction and gas calorific value of the products of cellulose pyrolysis in steam (7 moles steam per mole cellulose) as a function of temperature at a pressure of 101.3 bars (100 atmospheres).

SECTION V

PRIMARY PYROLYSIS KINETICS

INTRODUCTION

Organic materials have attracted considerable attention as a potentially inexhaustible resource for synthetic fuel production[2-4]. Conversion processes often rely on pyrolysis to produce gaseous and/or liquid fuels[5,6]. Pyrolysis also plays an important role in the steam gasification of organic wastes, which has recently been shown to be a potentially attractive method for the production of a hydrocarbon-rich synthesis gas from biomass[7-15]. Consequently, fundamental studies of pyrolysis phenomena in steam and inert atmospheres are needed to provide data for the design and optimization of chemical reactors and other process equipment used for biomass conversion.

This section focuses on the measurement of kinetic parameters useful for the engineering design of large chemical reactors. As such, the experimental results are not analyzed with the intent of describing the fundamental chemical mechanism of pyrolysis. Nevertheless, the results presented here do offer an insight into some not widely recognized difficulties faced by those studying pyrolysis mechanisms.

CELLULOSE

A substantial background of material exists on cellulose pyrolysis in nitrogen and other inert atmospheres, but only one paper has appeared describing cellulose pyrolysis in steam[16]. The thermal degradation of cellulose in nitrogen has attracted widespread interest due to its importance in the fields of fire research, fabric flammability, nuclear weapons effects, waste incineration, and aerospace technology. Four reasonably complete reviews of the English literature have been published in recent years[17-20], and a substantial body of knowledge exists in the Russian literature as well[21]. This section presents a brief review of the English literature to serve as both a foundation and a point of departure for the results reported here.

Prior Research on Cellulose Pyrolysis

The chemical products produced by the pyrolysis of cellulose have been studied extensively and summarized by Madorsky[22]. Compounds identified in the product mixture include CO, CO_2, levoglucosan (1, 6 anhydro-b-D-glucopyranose), H_2, char, and a host of aldehydes, ketones, and organic acids[23-30]. These latter products generally have a low molecular weight, and may be

present only in trace amounts. Many are highly reactive at elevated temperatures and support the flaming combustion of cellulosic materials.

The mechanism of cellulose pyrolysis has also been intensively investigated. There is some agreement[31-37] that this mechanism consists of two competitive reactions: the dehydration of cellulose to form anhydro-cellulose which further decomposes to yield gases and char, and the depolymerization of cellulose at somewhat high temperatures, producing levoglucosan which decomposes via secondary reactions to yield tars, gases, and char.

McCarter[38], Chatterjee[39], and Chatterjee and Conrad[40] presented evidence suggesting that the depolymerization reaction proceeds by a sequential process. Some workers[23,24,26,41,42] have reported levoglucosan to be the intermediate result of cellulose depolymerization during pyrolysis. The levoglucosan may then participate in two competing reactions: repolymerization to form char or further pyrolysis to form tars, gases and char.

Other workers[29,43-45] prefer to describe the mechanism as a two- or three-stage process: an initial, degradation step followed by a zero order depolymerization, devolatilization step, and a first order step leading to the final char. A schematized summary of these mechanisms is given in Appendix I.

Substantial disagreement exists in the literature on the measured rates of cellulose pyrolysis. Experiments utilizing both "small" (< 1 g) and large samples have been reported; however, this section focuses on the results of those studies utilizing "small" samples. The analysis of results from large samples[25,46-51] is complicated by heat and mass transfer phenomena and secondary reactions, all of which tend to obscure the interpretation of the experiment.

Table 1 lists values of the activation energy for the dominant high temperature reaction observed by various workers studying small samples. Usually this reaction was said to be the depolymerization reaction discussed earlier. The results are grouped according to the degree of the decoupling which existed between the thermocouple used to measure the sample temperature, and the sample temperature itself.

Experiments performed in vacuum with the thermocouple not in contact with the sample are the most badly decoupled, and exhibit activation energies ranging from 36 to 60 kcal/gmol. Experiments with the sample and thermocouple in a flowing inert gas but not in direct thermal contact are less decoupled, and exhibit activation energies ranging between 33 and 50 kcal/gmol. Finally, experiments with the sample in direct contact with the thermocouple displayed activation energies ranging between 26 and 33 kcal/gmol.

At first the present authors were surprised that these results fell into natural groups according to the coupling of the temperature sensor with the sample, and although this observation may not be the explanation for the wide disparity of results in earlier studies, it is consistent with phenomena observed in this research.

TABLE 1. PYROLYSIS KINETICS DERIVED FROM EXPERIMENTS UTILIZING SMALL (< 1 g) SAMPLES

SAMPLE	REFERENCE	EXPERIMENT	E(kcal/gmol)
Cellulose	Akita and Kase (1967)	TGA, TC in vacuum	53.5
Cotton	Madorsky, Hart and Straus (1956)	TGA, TC in vacuum	50.
Cellulose	Ramiah (1970)	TGA, TC in vacuum	36.-60.
Cellulose	Tang (1964)	TGA, TC in vacuum	56.
Cellulose	Tand and Neil (1964)	TGA, TC in vacuum	53.-56.
Cellulose	Arseneau (1971)	TGA, Flowing N_2	45.4
Wood	Browne and Tang (1963)	TGA, Flowing N_2	35.8
Cotton	Chatterjee and Conrad (1966)	TGA, Flowing He	33.
Cotton	Mack and Donaldson (1967)	TGA, Flowing N_2	48.8
Cellulose	Lipska and Parker (1966)	Fluidized Bed	50.
Cellulose	Chatterjee (data of Lipska and Parker) (1965)	Fluidized Bed	42.
Cellulose	Lipska and Wodley (1969)	Fluidized Bed	42.
Cellulose	McCarter (1972)	Evolved Gas	40.5
Cellulose	Murphy (1962)	Evolved Gas	39.4
Cellulose	Martin (1965)	Radiation	30.
Cellulose	Shivadev and Emmons (1974)	Radiation	26.
Cellulose	Lewellen, Peters and Howard (1976)	Electrically heated screen	33.4

Experimental Apparatus and Procedure

For the pyrolysis studies reported here, measurements of weight loss on a mass fraction basis vs. temperature, weight loss vs. time, and temperature vs. time were obtained using the DuPont 951 Thermal Gravimetric Analyzer (TGA) as a part of the DuPont 990 Thermal Analysis System. In using the DuPont 990 System several operational features were noted which have a significant influence on calculated kinetics.

First, the nominal heating rates indicated on the instrument generally were lower than the experimental heating rates measured during the course of an experiment.

Second, although the instrument simultaneously plots the time derivative of the weight loss curve, it was observed to be inaccurate at nominal heating rates exceeding 10°C/min. To avoid this problem, the experimental curves of weight loss vs. temperature generated by the TGA were digitized and read into Princeton's interactive computer system using a Tektronix graphic tablet. A curve fitting cubic spline polynomial was passed through the digitized experimental data and used to calculate the derivative as a function of time.

Third, strong temperature gradients were observed along the length of the TGA furnace. Since the "sample" thermocouple also senses the furnace temperature, the penetration distance within the furnace of the quartz tube containing the sample pan and sample thermocouple was observed to affect weight loss vs. temperature results. This distance was set so that the melting points of aluminum, tin and zinc fell within the accuracy of the type K thermocouple used in the DuPont system.

For the experiments reported here, small samples (2 to 3 mg) of Whatman No. 1 filter paper, with an ash content of 0.1% by weight, were introduced into the platinum sample pan, and the instrument was subsequently purged for one hour using flowing nitrogen (50 ml/min) to reduce the concentration of oxygen within the system to below detectable limits. The sample was then dried to constant weight at 110°C, and heated to 600°C in the flowing nitrogen at nominal linear rates of 2°, 5°, 10°, 20°, and 50°C/min.

At least two experiments at each heating rate were performed: the first provided data on weight loss vs. temperature and the second on weight loss vs. time and temperature vs. time. The weight loss vs. temperature curve provided a precise measurement of temperature since the temperature scale could be stretched over 30 inches; whereas the weight loss and temperature vs. time measurement offered an insight into the variability of the heating rate over the temperature range of interest. Agreement of the two curves to within 8°C at equal weight loss was always obtained, and a study of many experiments indicated the degree of precision in the temperature measurement for a given weight loss to be ± 5°C.

A number of procedural factors were observed to effect the experimental results. Oxygen concentrations greater than ½% reduced the observed temperatures at which pyrolysis occurred. Increased rates of inert purge gas

flow through the system also reduced the observed temperature due to increased convective heat transfer. Variation of sample size between 2 and 10 mg had no effect on the observed results.

In order to use steam as the pyrolysis medium, the DuPont TGA was modified in a manner similar to that described by Ruth et al.[52]. Oxygen free, distilled water was pumped by a peristaltic pump into a tubular boiler and then through a packed bed heat exchanger before entering the modified quartz TGA reactor vessel (see Figure 9). The steam flowed over the sample through the baffle, and reversing direction mixed with the nitrogen purge gas and exited through a blowhole. Experiments using air as a purge gas in place of nitrogen showed no evidence of the effects of oxygen on pyrolysis; hence the pyrolysis atmosphere present in the TGA was assumed to be essentially pure steam.

Other experiments were made using nitrogen in place of water in the steam reactor system with a nominal heating rate of 20°C/min. These experiments were originally intended to serve as a "control" to lend greater credence to the steam results. A discussion of the results of these control experiments is given in the following section.

Results and Discussion

Figures 10 and 11 give weight loss vs. temperature curves of cellulose pyrolyzed in nitrogen and steam. For a given weight fraction, the corresponding temperature for pyrolysis in steam is about 20°C lower than that in nitrogen. These results could lead one to believe that steam has a marked effect on the rates of pyrolysis. As discussed in the previous section, a series of control experiments using nitrogen in place of water in the steam generator were also performed. Apart from a rapid initial weight loss in the steam experiments due to moisture desorbed from the cellulose, the nitrogen experiments in the steam reactor system were in perfect agreement with the steam experiments.

Further experiments showed that the displaced curves in nitrogen were not due to increased gas flow rates within the steam reactor, nor were they due to either the preheating of the inert gas stream or the smaller sample pan used with the steam system. The only remaining explanation was the placement of the thermocouple relative to the sample. In the steam system the thermocouple is downstream of the sample; whereas in its usual position the thermocouple is upstream of the sample.

A final experiment was performed using the customary TGA system with the thermocouple extended past the sample pan to lie downstream of the sample. The observed temperature at which the sample reached a given degree of conversion, with the thermocouple downstream of the sample, was 25°C lower than the temperature observed when the thermocouple was upstream of the sample. Evidently a large temperature gradient exists in the neighborhood of the sample pan during pyrolysis.

A few simple heat transfer calculations are sufficient to confirm the existence of a large temperature gradient around the sample during pyrolysis.

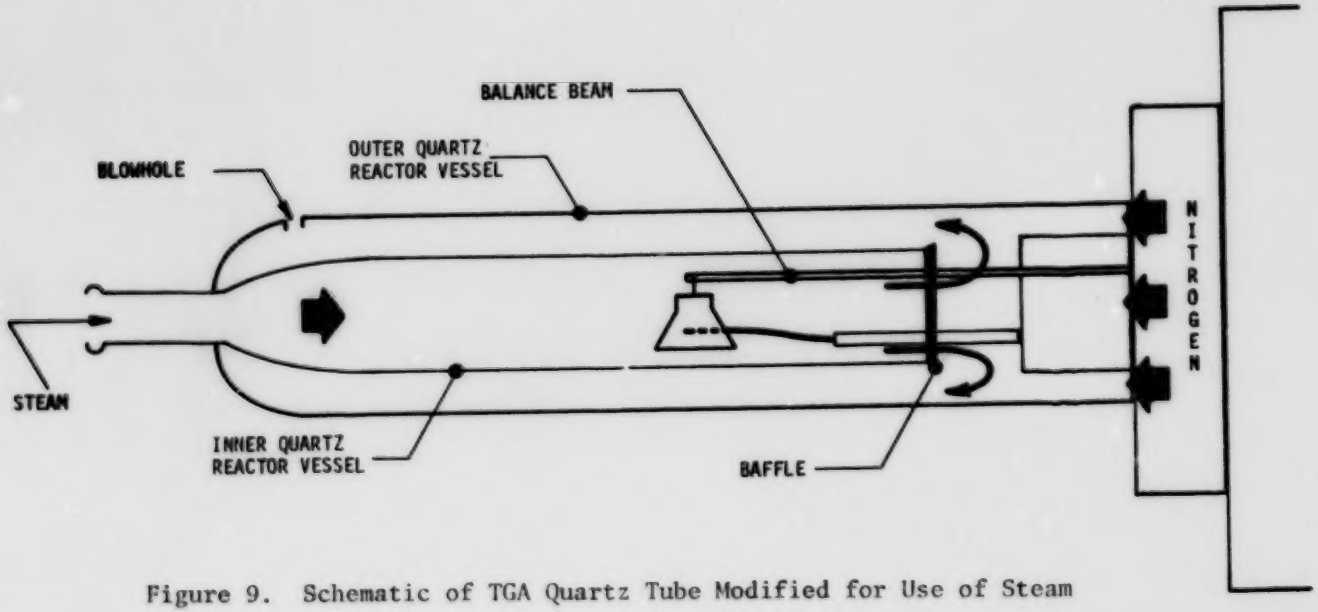

Figure 9. Schematic of TGA Quartz Tube Modified for Use of Steam

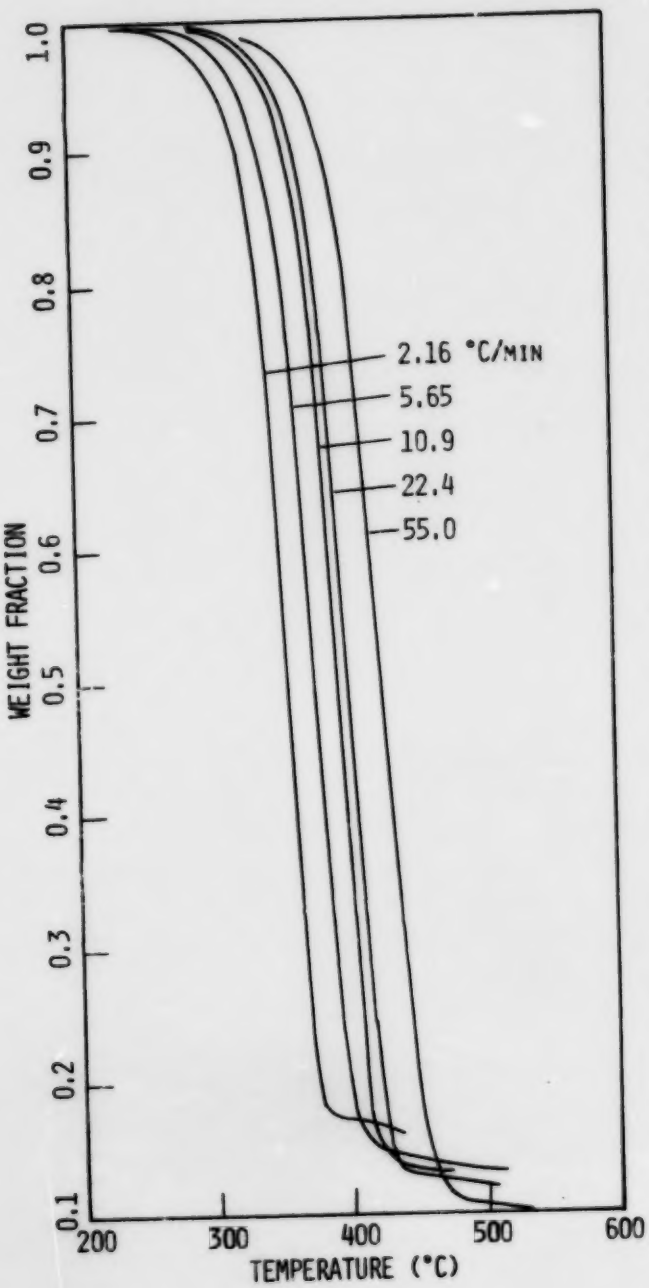

Figure 10. Thermogravimetric Curves for the Pyrolysis of Cellulose in Nitrogen (50 ml/min) at Various Heating Rates.

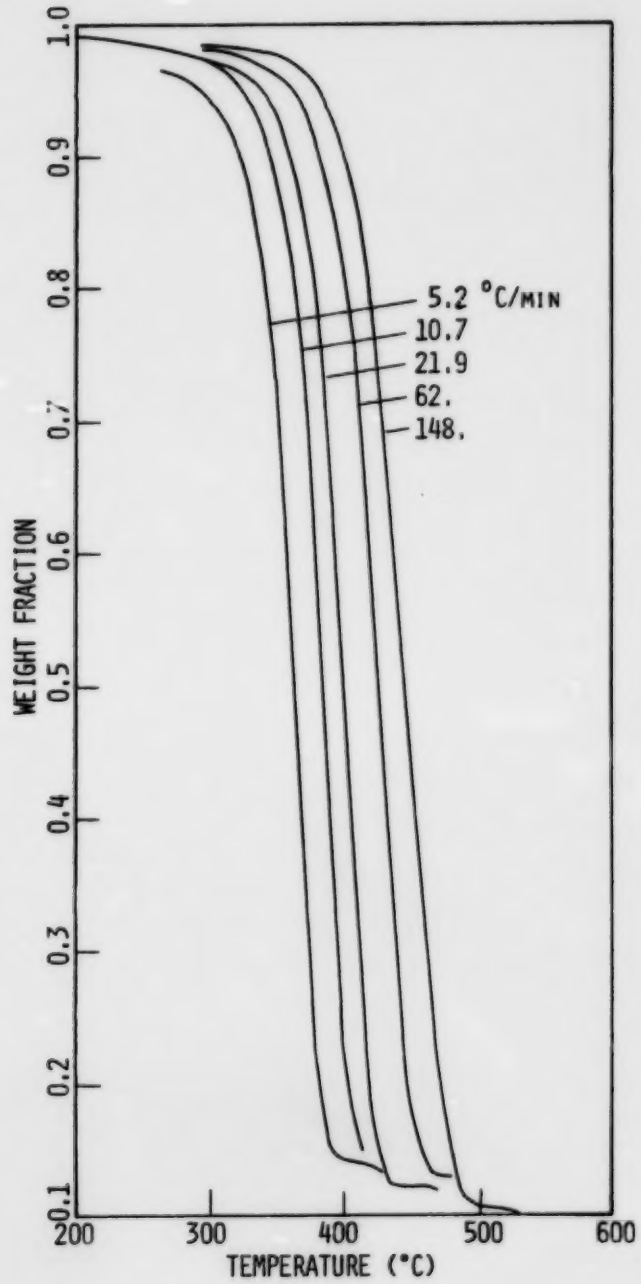

Figure 11. Thermogravimetric Curves for the Pyrolysis of Cellulose in Steam at Various Heating Rates.

At a nominal heating rate of 20°C/min the maximal rate of heat demanded by the endothermic pyrolysis reactions was measured to be 0.88 mcal/sec/mg at 386°C. For the total flow of nitrogen through the system to supply this heat, the gas temperature would drop 14°C when passing over the sample; consequently the actual temperature drop is expected to be much larger. For conduction to supply the heat, a temperature drop of 34°C is required. If the emissivity of the paper at 386°C is assumed to be 0.5, then radiation will supply the heat required with a temperature drop of about 30°C. Clearly, there is good reason to expect a large temperature gradient to exist in the vicinity of the sample during pyrolysis.

There are two ways to reduce the inaccuracy in temperature measurement due to this gradient: bring the thermocouple into contact with the sample, or reduce the sample size. The first method is not possible with most TGA's, including the DuPont System. In order to implement the second method, it is important to note that the surface-to-volume ratio scales as the 2/3 power; consequently it is necessary to reduce the sample weight by a factor of 32 in order to reduce the temperature gradient by a factor of 10. Therefore, sample sizes of cellulose below 0.1 mg are necessary to reduce the temperature gradient below 2°C. Difficulties in obtaining a representative sample for analysis would be greatly aggravated by the need for such a small sample. It would appear that the manufacturers of instruments for thermal analysis should place a much greater emphasis on obtaining temperature measurements with thermocouples in direct contact with the sample for applications that require kinetic analysis.

Recognizing the inherent inaccuracies present in the data, kinetic parameters were obtained for engineering purposes. The derivation of kinetic data from weight loss curves obtained under non-isothermal conditions has received considerable attention, and a complete review is available[53]. The derivation of suitable kinetic parameters is not made any easier by the fact that there are at least 16 theoretical kinetic equations which represent reaction mechanisms in the solid state[54].

Four of these theoretical equations are summarized by

$$\frac{dC}{dt} = k(1-C)^n \qquad (8)$$

$$k = A^{(-E/RT)}$$

where the order of the reaction n takes on the values 0, 1/2, 2/3, or 1. In Equation (1), $C = (w_i - w)/(w_i - w_f)$ where w_i is the initial sample weight, w_f the final sample weight, w the time dependent sample weight, A the pre-exponential constant, E the apparent activation energy, R the universal gas constant, and T the time dependent absolute temperature. Methods for deriving these parameters from the more complex equations have recently appeared in the literature[55,56].

The approach to the kinetic analysis of the curves (Figures 10 and 11) taken in this paper consists of the following steps:

a) Calculate the activation energy (E) as a function of cellulose conversion to determine if E is sufficiently constant throughout the reaction to justify further analysis by a simple model.

b) Use the master curves method of Criado[57] to find the appropriate kinetic equation to describe the pyrolysis reaction.

c) Assuming the pyrolysis mechanism is reasonably insensitive to heating rate variations, derive a single set of E, A, and n for all the TG curves.

d) Calculate the kinetic parameters for each TG curve separately using the Freeman-Carroll method.

Several methods are available for assessing the constancy of the activation energy E during the course of pyrolysis[58-60]. Figure 12 gives plots of E vs. conversion fraction using the Friedman method[58] for cellulose pyrolysis in nitrogen and steam. From Figure 12 it is seen that the value of E remains relatively constant at about 37.5 kcal/gmol for cellulose pyrolysis in nitrogen with $0.2 \leq C \leq 0.7$. Similarly, for cellulose pyrolysis in steam E takes the relatively constant value 34 kcal/gmol for $0.2 \leq C \leq 0.8$. The relative constancy of E in each case for a major part of the decomposition range indicates that an adequate formal description of the TG curves can be approximated by a single reaction model.

Next, the method of Criado[57] was used to determine which kinetic equation best describes the weight loss data. Criado[57] has developed a series of master curves for quick analysis of the particular kinetic equation describing the thermal decomposition reaction of solids from DTG data. This method does not discriminate among all 16 equations but does narrow the choices considerably. Using this approach the pyrolyses in steam and nitrogen were found to fit the mechanism given in Equation (1) in which $n = \frac{1}{2}$.

Having established the range of E's and the appropriate equation, the next step was to calculate the best set of kinetic parameters which fit the experimental curves shown in Figures 10 and 11. The method due to Chen and Fong[56] was used to obtain these fits. Results for cellulose pyrolysis in steam at nominal heating rates of 5°, 10°, 20°, and 50°C/min are given below.

	Steam	N_2
A(sec^{-1})	1.67×10^9	6.06×10^9
E (kcal/gmol)	34.2	36.6
n	0.512	0.464

As expected from the Criado method, the best solution for all the TG curves comes with an n close to ½. The small difference in E for the steam and nitrogen pyrolysis is an artifact of the experimental procedure, reflecting a change in the flow direction of the purge gas and the position of the thermocouple relative to the sample. Figures 13 and 14 compare the

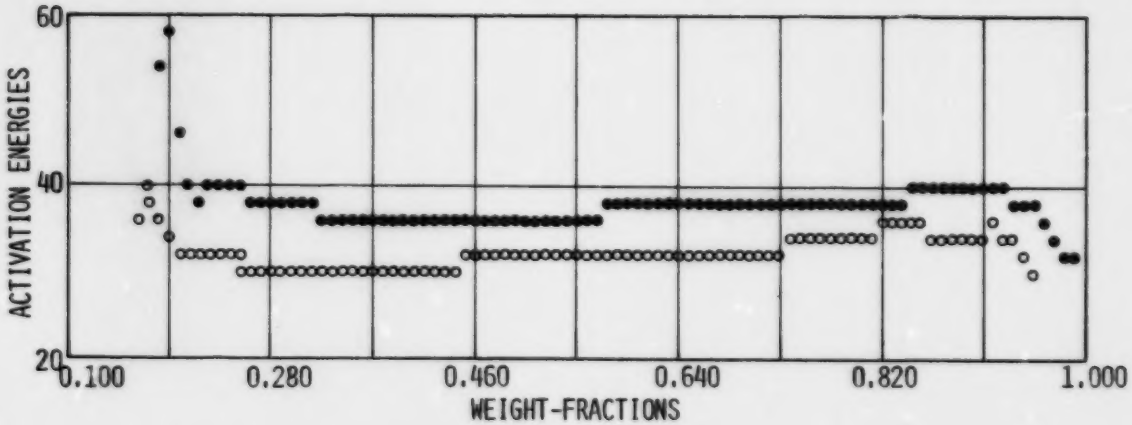

Figure 12. Plot of the Activation Energy vs. Weight Fraction Remaining for the Pyrolysis of Cellulose in Steam (o) and Nitrogen (•).

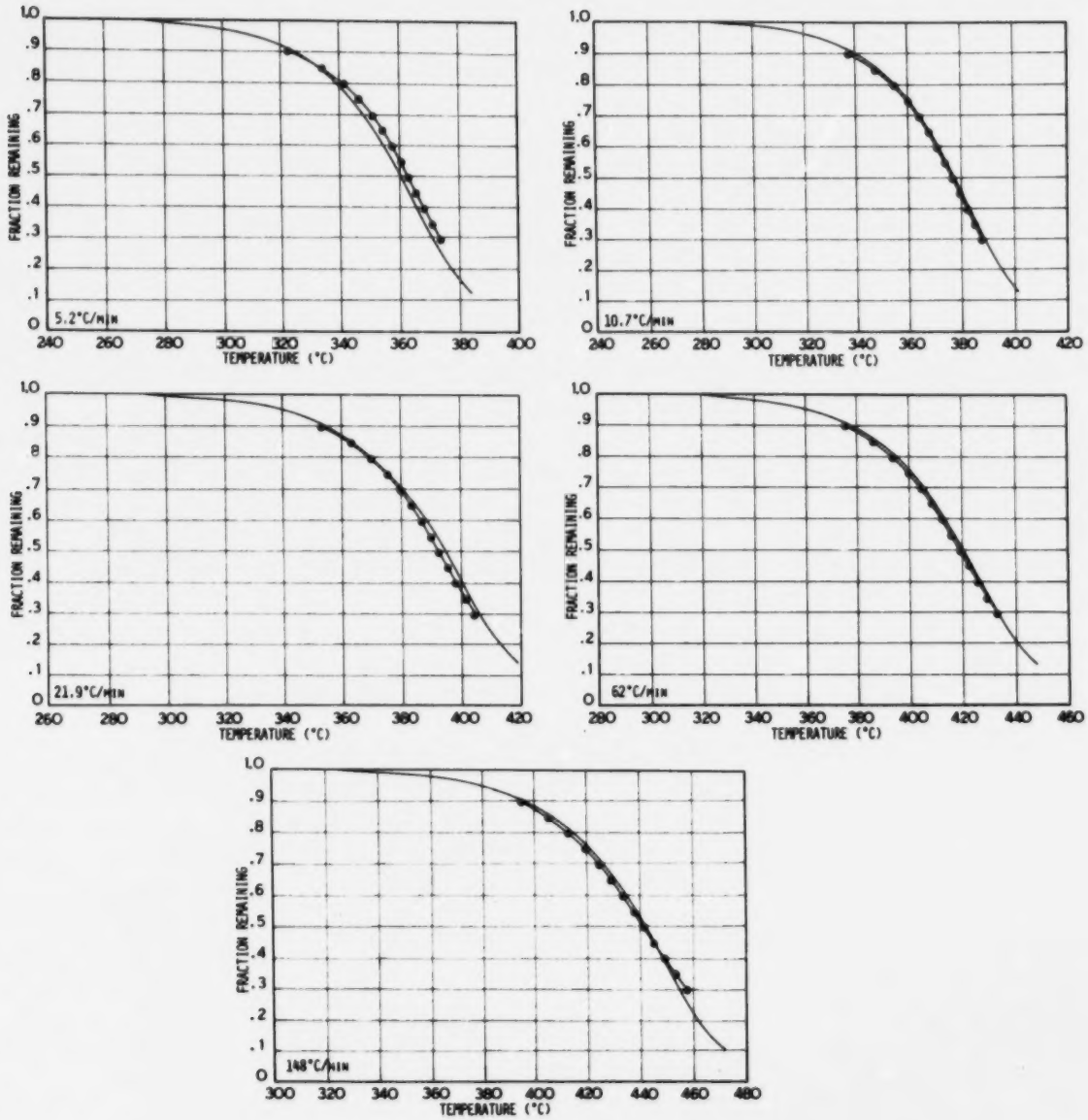

Figure 13. Experimental (circles) and Calculated (solid line) Thermogravimetric Curves for the Pyrolysis of Cellulose in Steam. Calculated Curves Based on E = 34.2 kcal/mol, A = 1.67×10^9 sec^{-1} and n = 0.512. Heating Rates Appear in Lower Left Corner.

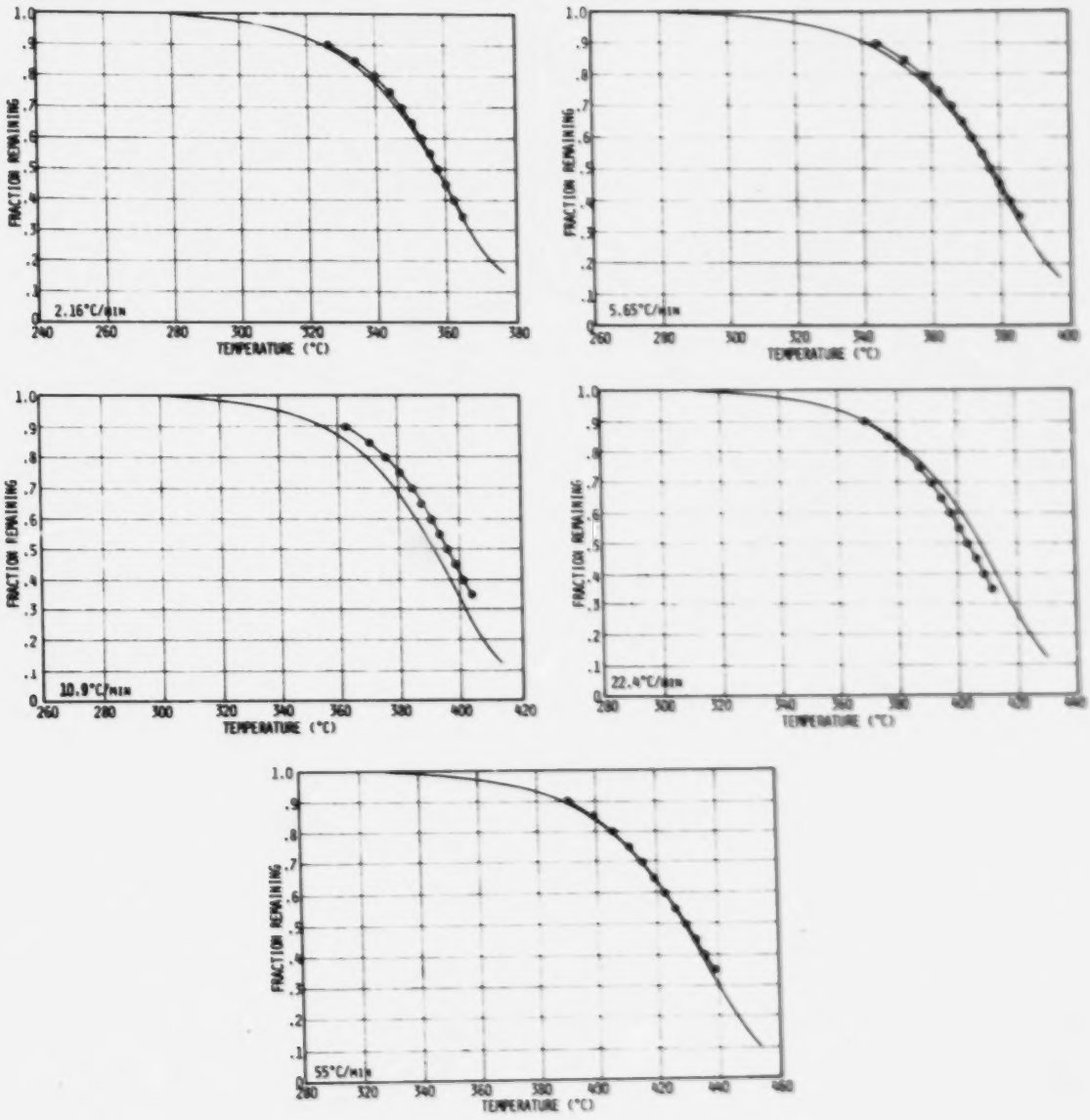

Figure 14. Experimental (circles) and Calculated (solid line) Thermogravimetric Curves for the Pyrolysis of Cellulose in Nitrogen. Calculated Curves Based on E = 36.6 kcal/mol, A = 6.06 x 10^9 sec^{-1} and n = 0.464. Heating Rates Appear in Lower Left Corner.

experimental points and the theoretical curve calculated from the kinetic parameters given above. The fit to the steam pyrolysis data is quite satisfactory over the entire heating range, but is less satisfactory for the weight loss curves in nitrogen. In the latter case, the extent of the discrepancy is about 5°C at a heating rate of 10.9°C/min (i.e., E is underestimated by about 1% for this case). If we assume, for the moment, that the difference in kinetic parameters for steam and nitrogen are real rather than a reflection of variations in experimental procedure, the predicted rate constants can be compared as follows:

	$k(sec^{-1})$	
Temp. (°C)	Steam	N_2
300	15×10^{-5}	6.7×10^{-5}
500	0.36	0.27
800	180	212

The relative agreement of the rate constants in the temperature range of 300 - 800°C does not support any important influence of steam on the course of pyrolysis. However, the use of steam as a pyrolysis medium has been found to affect condensible tar and oil formation by secondary reactions of the volatile pyrolysis products.[14]

Kinetic parameters were also derived from the single TG curves by the Freeman and Carroll (FC) method. This widely used method[61] is the only one that permits direct determination of A, E, and n from a single measurement at one heating rate. Comparisons of the kinetic parameters derived from the FC and other methods appear in the literature. The TG curves were analyzed using the rate equation

$$dV/dt = k'(V^* - V)^n \qquad (9)$$

where $V^* = (w_i - w_f)/w_i$ and $V = (w_i - w)/w_i$. Equations (3) and (1) are related by the equation

$$A' = \left(\frac{w_i}{w_i - w_f}\right)^{n-1} A$$

and degenerate to the same equation when $n = 1$ or $w_f = 0$. Kinetic parameters for both steam and nitrogen at each heating rate are given in Tables 2 and 3. Values for E for pyrolysis in nitrogen range between 36 and 53 kcal/gmol; whereas the comparable values in steam range between 30 and 44 kcal/gmol. Typical fits of the solution of Equation (3) using the data from Tables 2 and 3 for low and high heating rates are displayed in Figure 15.

The lack of consistency in the FC kinetic parameters in spite of (a)

TABLE 2. KINETIC PARAMETERS FOR CELLULOSE PYROLYSIS IN N_2

Sample	0905771300	0807772330	0805771520	0807772200	090771015
Heating Rate (°C/min)	2.16	5.65	10.9	22.4	55.
$T_{initial}$ (°C)	110	110	110	110	110
T_{final} (°C)	600	600	600	600	600
n	1.0	1.0	1.0	1.0	0.9
E(kcal/gmol)	52.9	37.7	35.6	38.9	36.6
A(min^{-1})	$2.8x10^{17}$	$8.4x10^{11}$	$1.6x10^{11}$	$2.7x10^{12}$	$4.2x10^{11}$
V*	0.85	0.87	0.88	0.88	0.90

TABLE 3. KINETIC PARAMETERS FOR CELLULOSE PYROLYSIS IN H_2O

Sample	0717771800	0521771400	0520771300	0521771300	0521770900
Heating Rate (°C/min)	5.35	11.48	23.49	64.05	150.18
$T_{initial}$ (°C)	130	130	130	130	130
T_{final} (°C)	600	600	600	600	600
n	1.0	.667	.75	.75	.75
E(kcal/gmol)	40.3	39.7	44.0	38.1	29.6
A(min^{-1})	$1.7x10^{13}$	$9.5x10^{12}$	$2.4x10^{14}$	$2.2x10^{12}$	$4.0x10^{9}$
V*	0.86	0.86	0.86	0.86	0.90

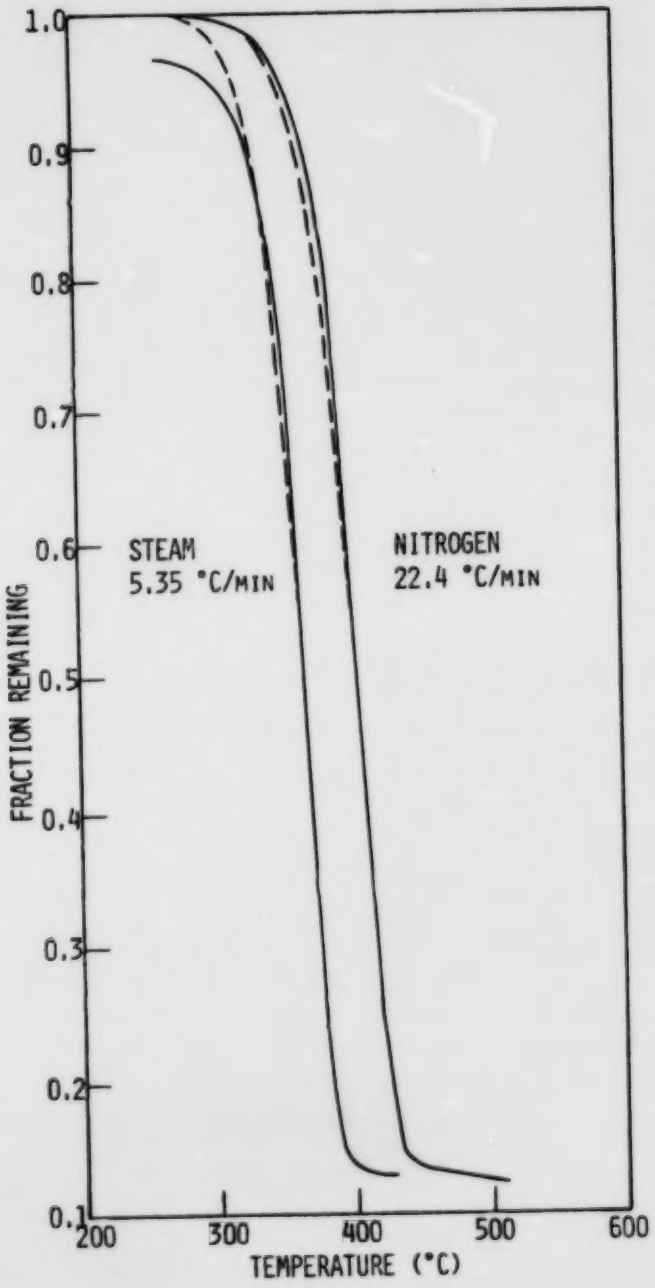

Figure 15. Experimental (solid line) and Calculated (dashed line) Thermogravimetric Curves for the Pyrolysis of Cellulose in Steam and Nitrogen. Calculated Curves Based on Kinetic Parameters of Tables 2 and 3 (Obtained by Freeman-Carroll Method).

the plateau regions shown in Figure 12 and (b) the good agreement in the experimental and theoretical curves for steam pyrolysis (Figure 13) is a measure of the sensitivity of the FC method to slope equation and experimental fluctuations which are always present in the TG curves[60,62]. The FC equations involve complex difference differential terms leading to scatter in the Arrhenius plots. For example, Sharp and Wentworth[63] found that the inclusion of the first part of a TG curve caused E and n to drop from 43 kcal/gmol and 0.55 to 36 kcal/gmol and -0.1, respectively. The FC method can be accurate if the random errors in the slope measurements are smoothed and calculations are based on the steeper parts of the TG curve. When a phenomenological description of a pyrolysis process at differing heat rates is desired, the Chen and Fong method used earlier is to be preferred over the FC method.

Conclusions

Thermogravimetric analysis has been used to measure rates of weight loss for cellulose pyrolysis in nitrogen and steam at nominal heating rates of 2° (nitrogen only), 5°, 10°, 20°, 50°, and 100°C/min (steam only). The apparent activation energy, frequency factor, and order for each heating rate were determined by the methods of Chen and Fong, and Freeman and Carroll, and the variation in activation energy as a function of conversion was determined by the method of Friedman. A single rate equation was found to be capable of simulating the cellulose weight loss data for all the heating rates studied in this section. Due to the poor heat transfer characteristics of the TGA, temperature gradients as large as 20° to 25°C were observed to exist in the vicinity of the sample at a heating rate of 20°C/min. Consequently, within the accuracy of the experiment, no difference was detected in the results of cellulose pyrolysis in nitrogen and steam. The wide range of activation energies for cellulose pyrolysis reported by previous workers may reflect the apparent difficulty in measuring the temperature of the cellulose due to inadequate heat transfer during pyrolysis. Future research should give adequate attention to the problems of heat transfer associated with chemical measurements.

OTHER ORGANIC WASTE MATERIALS

Pyrolysis kinetics of other organic waste materials were studied as part of this project. Since steam was not observed to affect the rates of cellulose pyrolysis, and because the steam system was difficult to use, weight loss was studied in flowing inert nitrogen. Results for cellulose pyrolysis suggest that the weight loss curves presented in this section are displaced to higher temperatures than would be the case if more accurate sample temperature measurements could be obtained.

The materials discussed in the following subsections were studied using the experimental techniques described earlier in this section; consequently only a summary of the results will be presented. A more detailed discussion of wood and manure gasification will be given in the forthcoming M.S.E. theses of Messrs. Timothy Mattocks and Virendra Kothari.

Newsprint

Samples of newsprint from The Wall Street Journal and The New York Times were pyrolyzed at nominal heating rates of 5°, 10°, 20°, 50°, and 100°C/min in nitrogen. Initially, reference samples from a single page of each newspaper were studied, and then the behavior of samples from other issues of the newspaper were compared to the reference samples. Although this study is far from comprehensive, no significant differences in pyrolysis behavior were detected between different issues of the same newspaper. However, newsprint used by The Wall Street Journal was observed to undergo pyrolysis in a somewhat different manner than The New York Times. This can be confirmed by a careful comparison of Figures 16 and 17, which display weight loss curves as a function of heating rate for the two types of newsprint. Kinetic analysis of the weight loss curves using the Friedman method are given in Figures 18 and 19, and kinetic parameters derived using the Freeman and Carroll method are presented in Tables 4 and 5.

Hard and Soft Woods

Grab samples of southern yellow pine (a softwood) and cherry (a hardwood) were obtained from industrial sources. These wood samples were ground and sieved to reduce their particle size below 50μ and to ensure sample homogeneity. Small samples weighing 2 - 3 mg were taken from these larger samples and analyzed on the TGA in flowing nitrogen at heating rates of 5°, 10°, 20°, 50°, and 100°C/min between 110° and 600°C. Results of typical analyses at the five heating rates are given in Figures 20 and 21. These figures portray the best, most representative results of many experiments.

Before discussing these results, it is helpful to develop an understanding of the chemical composition of wood. The following discussion relies in part on the excellent thesis of Beall[64].

Cellulose is the relatively crystalline polymer of high molecular weight that has been previously studied on this project. In wood, it is found in elementary fibrils (35A in diameter) which are bound with other fibrils to form microfibrils up to 300A in diameter. Timell[65] claims all wood types average 43 ± 2% cellulose except where reaction wood is found.

Much like cellulose, except for its largely amorphous physical shape, lower molecular weight and greater diversity of sub-species is hemicellulose, another polysaccharide associated with the cellulose in the wood cells and walls. A large number of compounds exist in this genre. Differing tree species contain differing amounts and combinations of hemicelluloses. The major type found in hardwoods is a partially acidic xylan (0-acetyl-4-0-methyl-glucuronoxylan) making up 20 - 35% of the wood. Softwood contains, on the average, less hemicellulose than hardwood. The principal types are the galactoglucomannans which comprise 10 - 20% of the wood.

The last major substance, lignin, differs from the above polymers by its reactive properties and irregular chemical structure. Lignin first forms outside the wood cell walls. Later the primary and secondary walls and middle lamellae become liquefied at which time the cell dies. Lignin

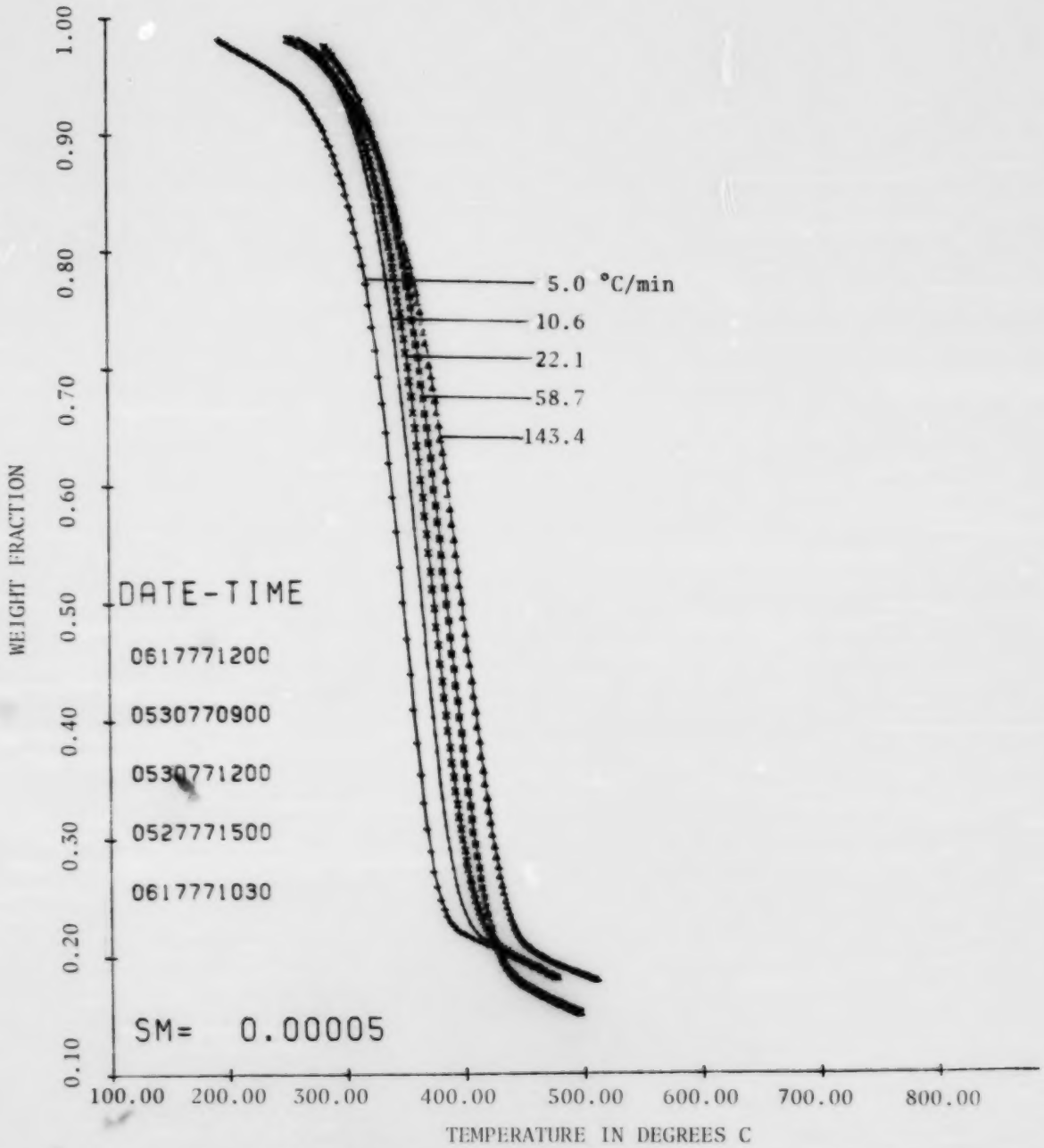

Figure 16. Thermogravimetric Curves for the Pyrolysis of New York Times newsprint in Nitrogen (50 ml/min) at Various Heating Rates.

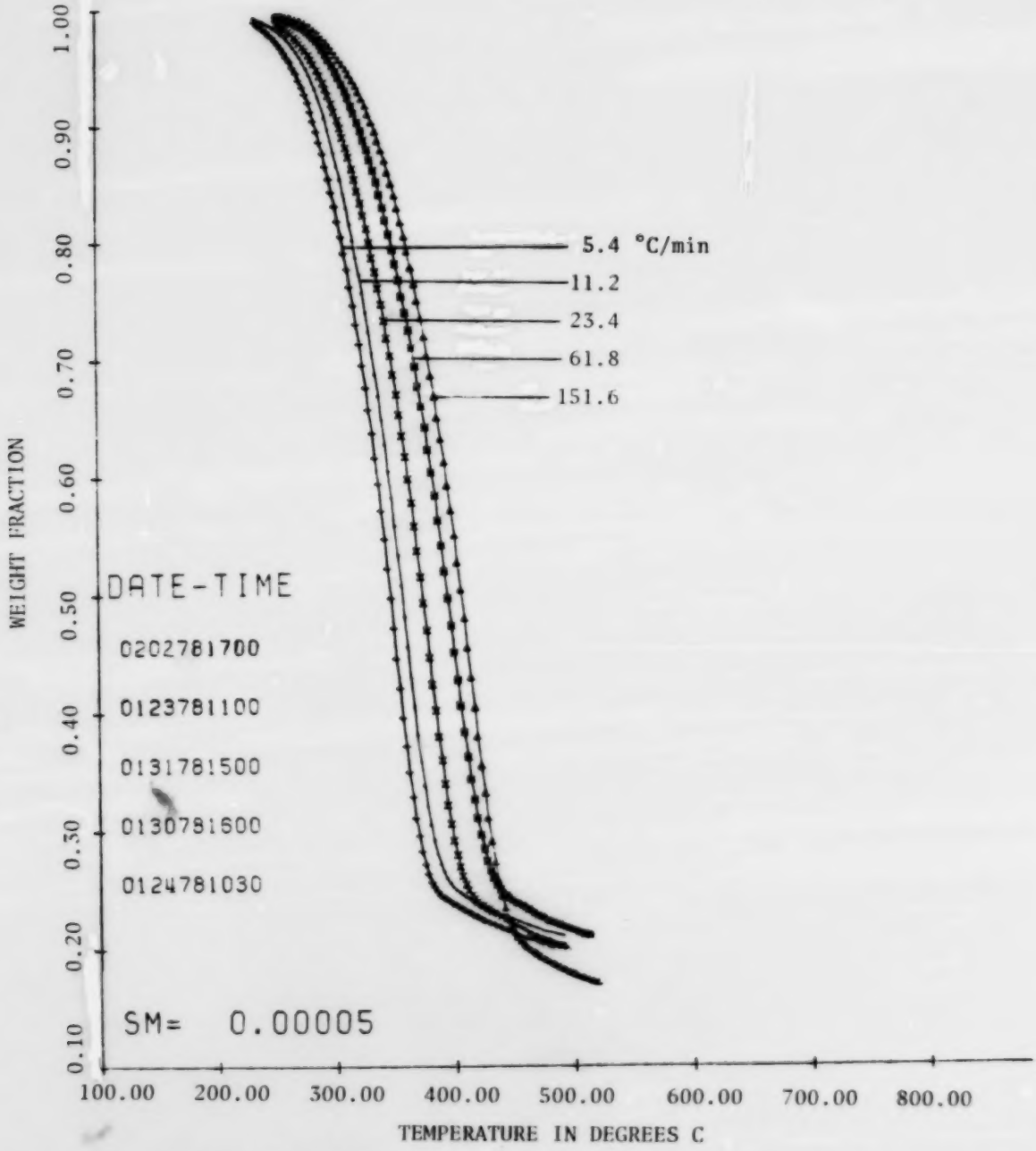

Figure 17. Thermogravimetric Curves for the Pyrolysis of Wall Street Journal newsprint in Nitrogen (50 ml/min) at Various Heating Rates.

ACTIVATION ENERGY VS WEIGHT FRACTION FOR PYROLYSIS OF NEWSPRINT FROM *THE WALL STREET JOURNAL* IN NITROGEN

Figure 18

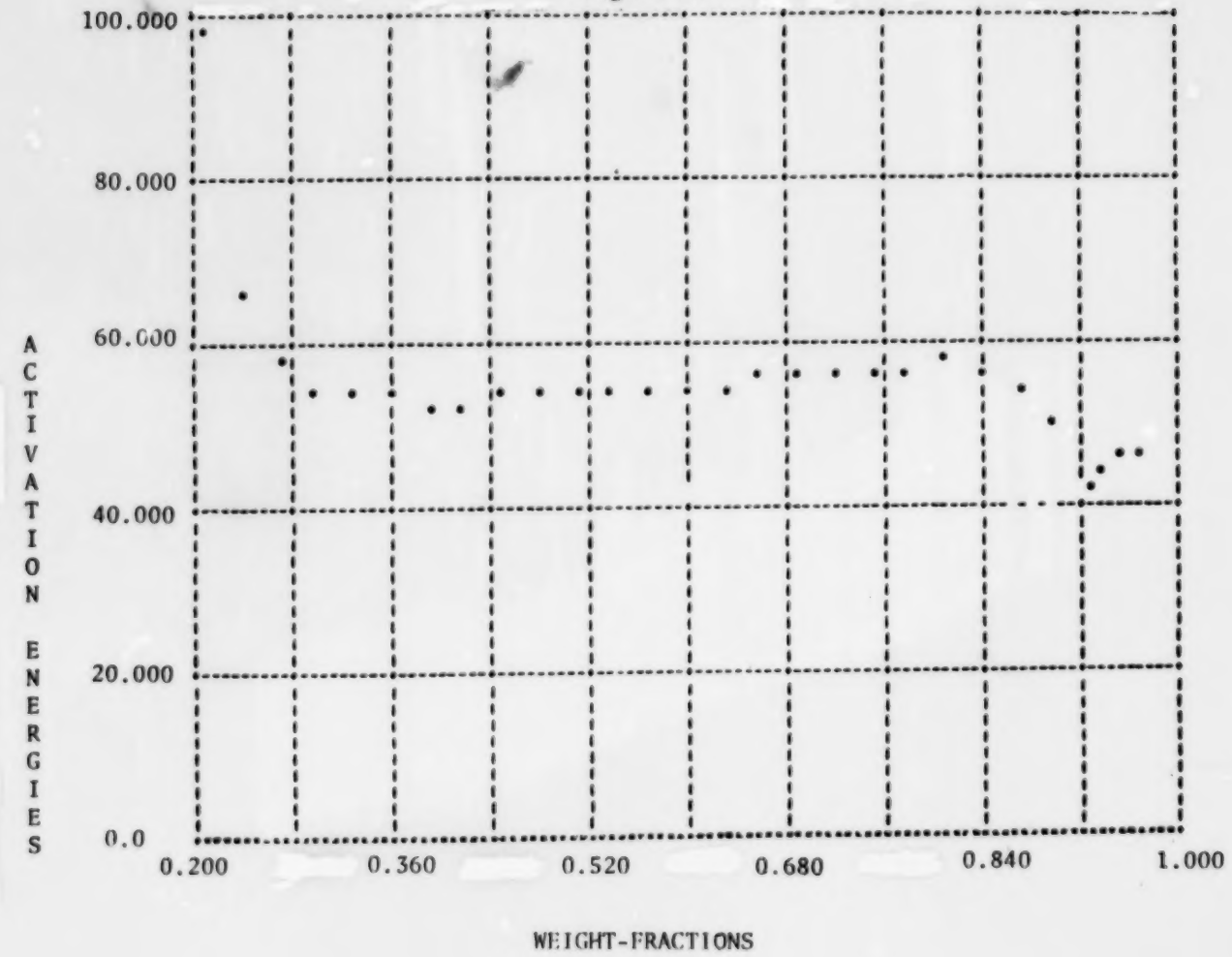

ACTIVATION ENERGY VS WEIGHT FRACTION FOR PYROLYSIS OF NEWSPRINT FROM *THE NEW YORK TIMES* IN NITROGEN

Figure 19

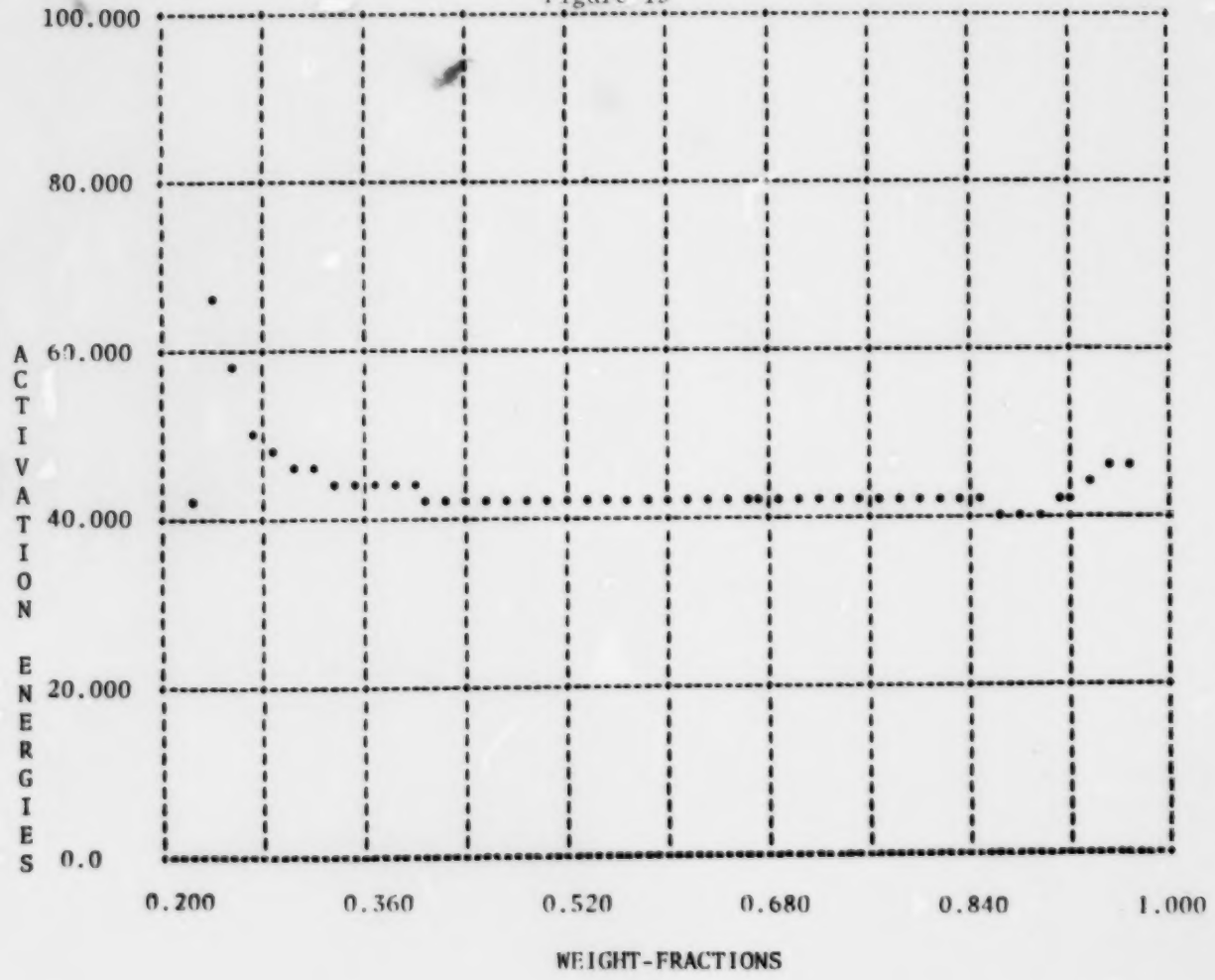

TABLE 4. KINETIC PARAMETERS FOR *THE NEW YORK TIMES* IN NITROGEN-SINGLE REACTION MODEL

Sample	0617771200	0530771100	0530771200	0527771500	061771030
Heating Rate (°C/min)	5.35	10.6	22.1	58.74	143.43
$T_{initial}$(°C)	110	110	110	110	110
T_{final}(°C)	600	600	600	600	600
n	.667	.667	.667	.667	.667
E(kcal/gmol)	21.60	22.62	20.45	20.48	18.39
A(min^{-1})	$5.02x10^6$	$1.31x10^7$	$3.67x10^6$	$5.73x10^6$	$2.12x10^6$
V*	.83	.84	.84	.87	.84

TABLE 5. KINETIC PARAMETERS FOR *THE WALL STREET JOURNAL* IN NITROGEN-SINGLE REACTION MODEL

Sample	0202781700	0123781100	0131781500	0130781600	0124781030
Heating Rate (°C/min)	5.40	11.2	23.4	61.8	151.6
$T_{initial}$(°C)	110	110	110	110	110
T_{final}(°C)	660	660	600	600	600
n	.25	.25	.25	.25	.25
E(kcal/gmol)	15.66	14.79	15.49	13.71	13.20
A(min^{-1})	$1.0x10^3$	$1.9x10^5$	$3.2x10^4$	$1.7x10^4$	$8.0x10^3$
V*	.81	.82	.82	.82	.83

accounts for 25 - 35% of softwoods and 15 - 25% of hardwoods.

At various times all of the above materials have been the subject of individual scrutiny or utilization. Thus, a whole methodology has been created for separating these materials. However, it is wrong to assume that pure components can be extracted by these chemical techniques since the extract is a function of the method used. For this reason, one cannot speak of a separated substance such as lignin without mentioning how it was obtained. This is an important scientific restraint which should be kept in mind when discussing the subject of wood and its components. In short, the differences between a compound in situ and extracted may be significant.

Results of the TGA analysis of hard and softwoods were given in Figures 20 and 21. The behavior of the decomposition at various heating rates led to a model with two or more independent reactions. The DuPont 330 Curve Resolver was used to separate the first derivative curves of weight loss into separate Arrhenius reactions. It was found that three independent curves added together were needed to accurately duplicate the experimental curves. From this the temperature of maximum reaction rate and integral percentage of each component was obtained.

The Friedman multiple heating rate method was then used to determine the prevalent activation energy during the three stages of decomposition (see Figures 22 and 23). By assuming a reaction order of n = 1, the pre-exponential constant A was calculated from the following application of the Arrhenius equation:

$$\ell n\ A = \frac{E}{RT_m} + \ell n\ \frac{\beta}{T_m^2} \qquad (10)$$

where T_m is the temperature at which the maximal rate of reaction occurs, and β is the heating rate.

To compare this model with the data, theoretical curves were generated from the experimental values of β, n, E, and A by a Runge-Kutta solution of the three independent Arrhenius type differential equations.

Due to possible non-uniqueness of solution by the curve resolver, a number of iterations were necessary before kinetic parameters were determined. "Best fit" values for the parameters A, E, n, and V* for the three constituents of both woods at 20°C/min, and also the hardwood run at 100°C/min were obtained. These values are given in Tables 6 and 7.

Various conclusions can be reached concerning this phase of the study. While non-uniqueness of the curve resolver might be argued, the three-component model of independent reactions seems to be able to universally duplicate the data. Indeed, this model predicts quite well not only the major portion of the reaction, but also the tail off at the end. Justification for this model can be found elsewhere as well. Beall[64] and others assert that the three major components of wood thermally decompose independent of each other. Figures 24 and 25 show our pure component decompositional curves

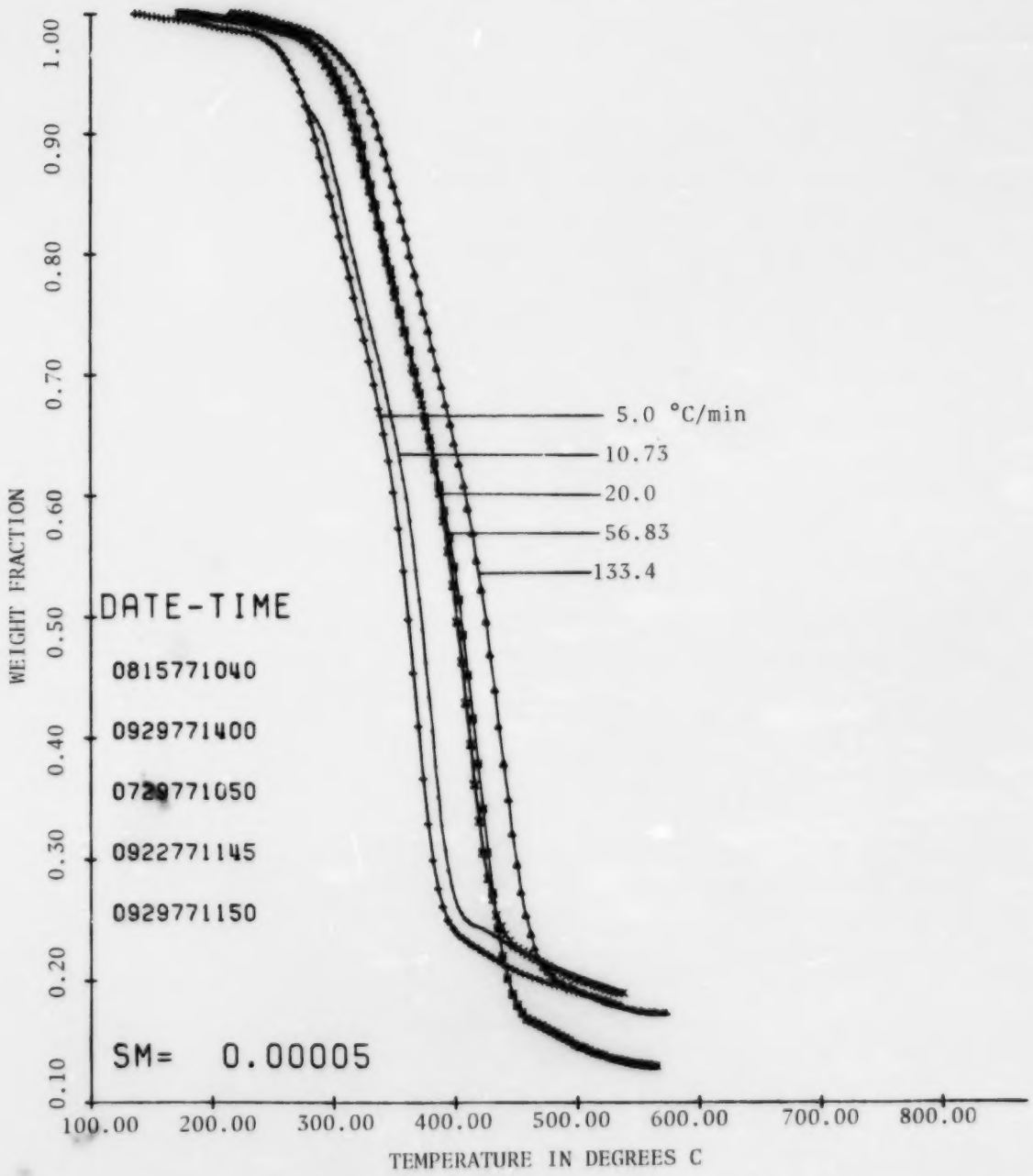

Figure 20. Thermogravimetric Curves for the Pyrolysis of Hardwood in Nitrogen (50 ml/min) at Various Heating Rates.

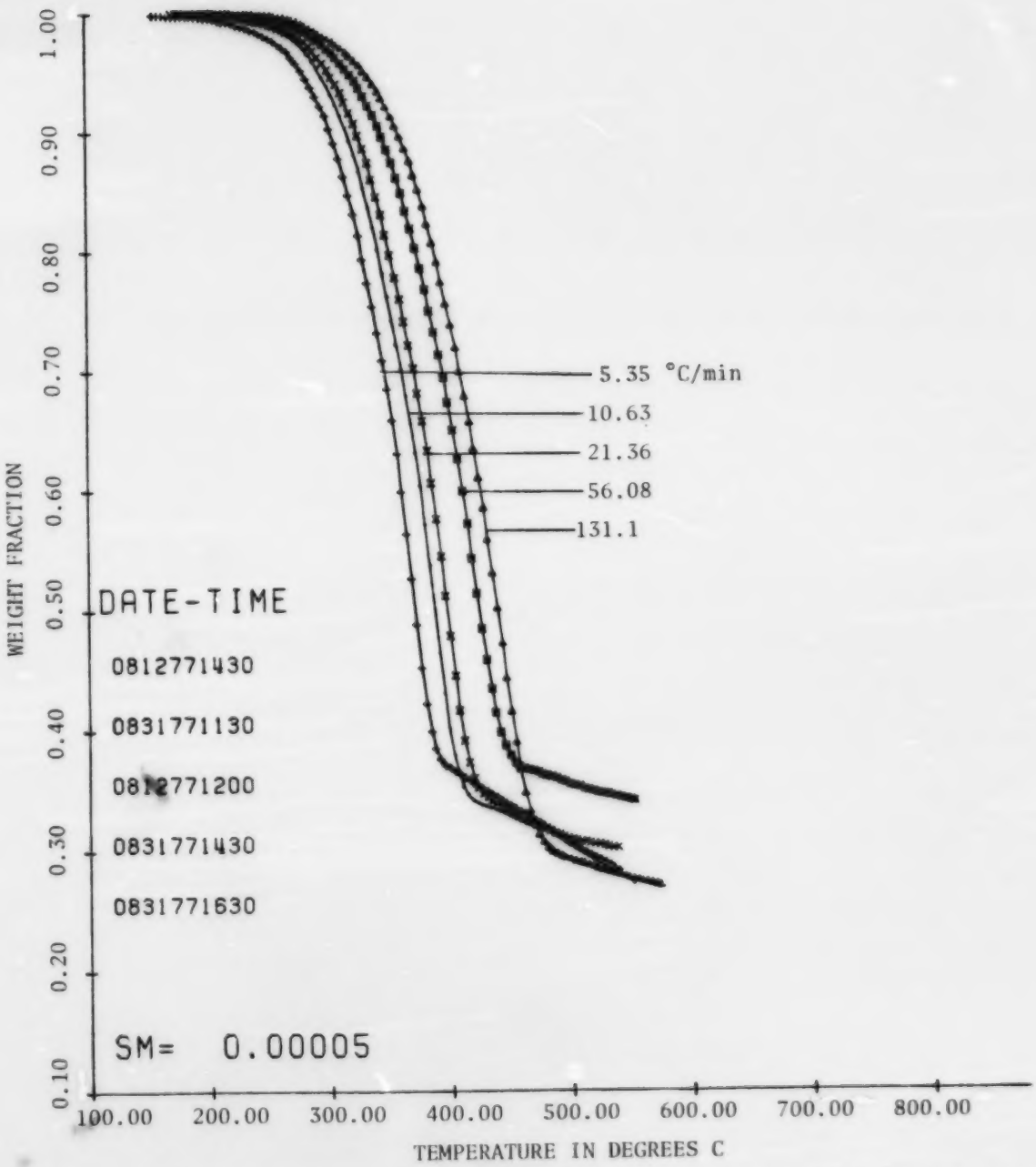

Figure 21. Thermogravimetric Curves for the Pyrolysis of Softwood in Nitrogen (50 ml/min) at Various Heating Rates.

ACTIVATION ENERGY VS WEIGHT FRACTION FOR PYROLYSIS OF HARDWOOD IN NITROGEN

Figure 22

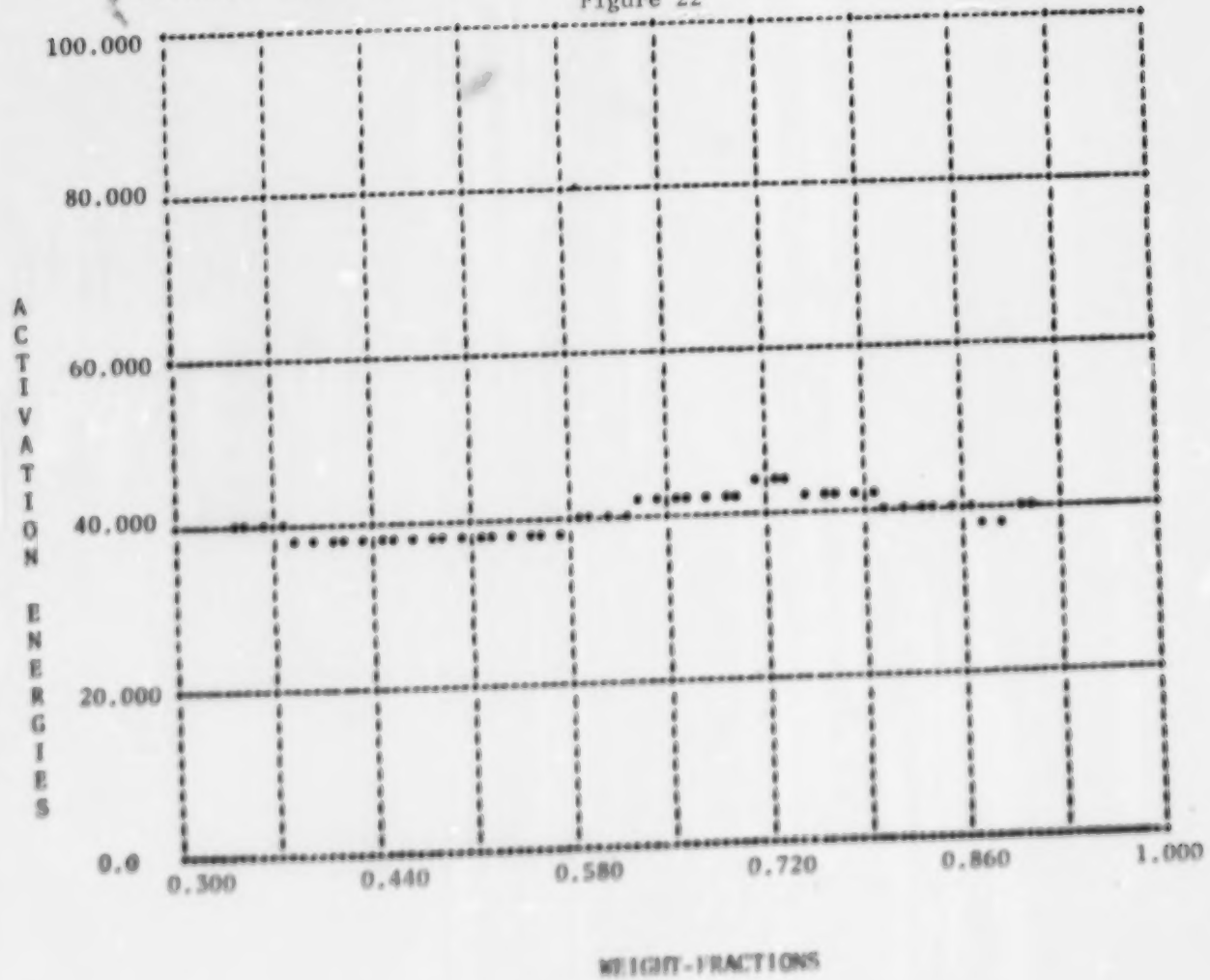

ACTIVATION ENERGY VS WEIGHT FRACTION FOR PYROLYSIS OF SOFTWOOD IN NITROGEN

Figure 23

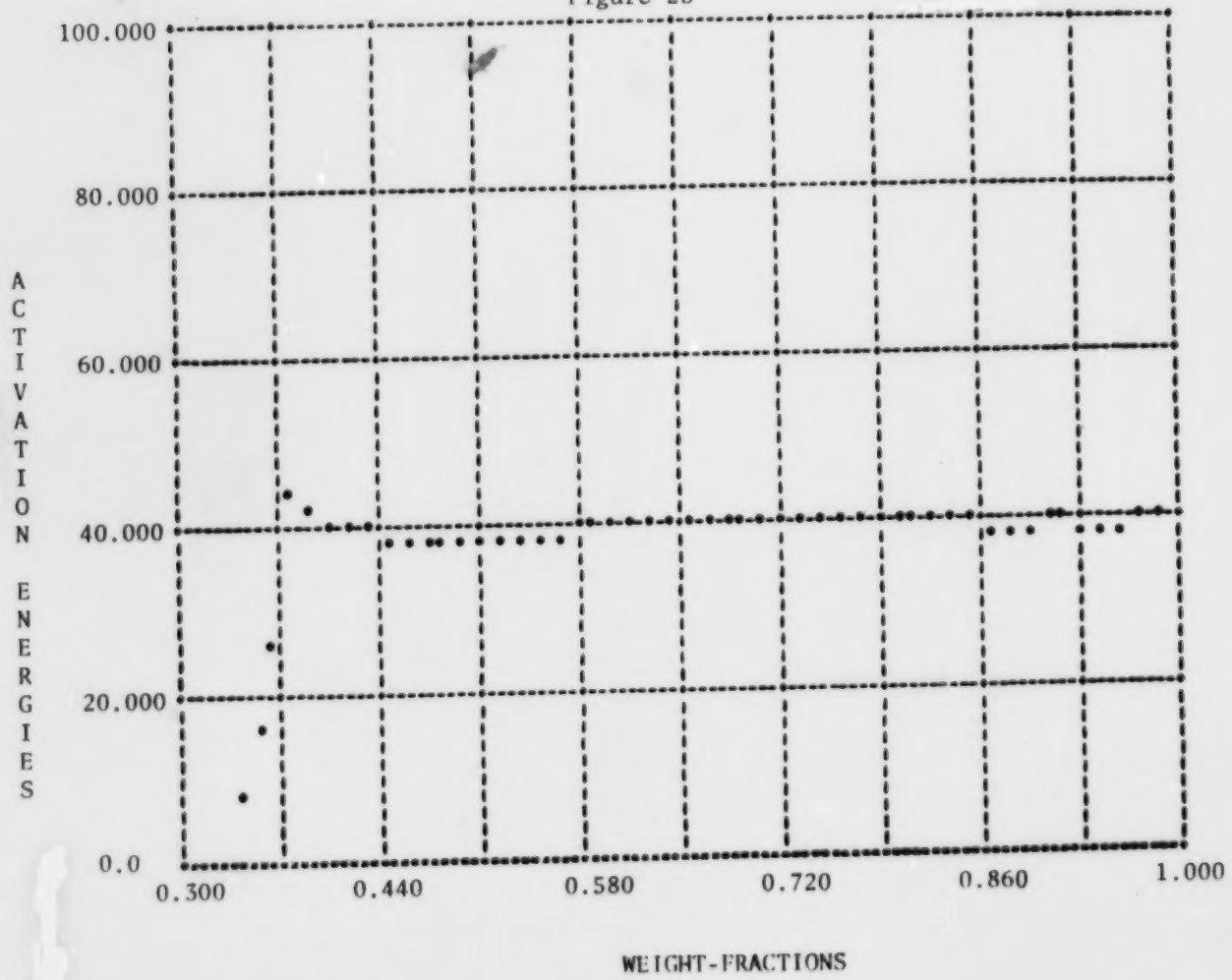

TABLE 6

KINETIC PARAMETERS FOR HARDWOOD HW-1 (CHERRY)
IN NITROGEN-TRIPLE REACTION MODEL

Sample 0929771150

Heating Rate (°C/min) 133.4

	Hemicellulose	Cellulose	Lignin
E(kcal/gmol)	40.0	34.0	2.0
A (min^{-1})	2.55×10^{14}	1.37×10^{11}	1.17
n	1.0	1.0	1.0
V*	0.9	0.9	0.9
% in sample	26	54	20

Sample 0729771050

Heating Rate (°C/min) 20.0

	Hemicellulose	Cellulose	Lignin
E(kcal/gmol)	40.0	34.0	2.0
A (min^{-1})	3.20×10^{14}	5.61×10^{10}	2.04×10^{-1}
n	1.0	1.0	1.0
V*	0.9	0.9	0.9
% in sample	15	62	22

TABLE 7

KINETIC PARAMETERS FOR SOFTWOOD SW-2 (SOUTHERN YELLOW PINE) IN NITROGEN-TRIPLE REACTION MODEL

Sample 0812771200

Heating Rate (°C/min) 21.36

	Hemicellulose	Cellulose	Lignin
E(kcal/gmol)	40.0	34.0	2.0
A (min^{-1})	$1.4x10^{14}$	$9.66x10^{14}$	$2.86x10^{-1}$
n	1.0	1.0	1.0
V*	0.80	0.85	0.6
% in sample	17%	53%	30%

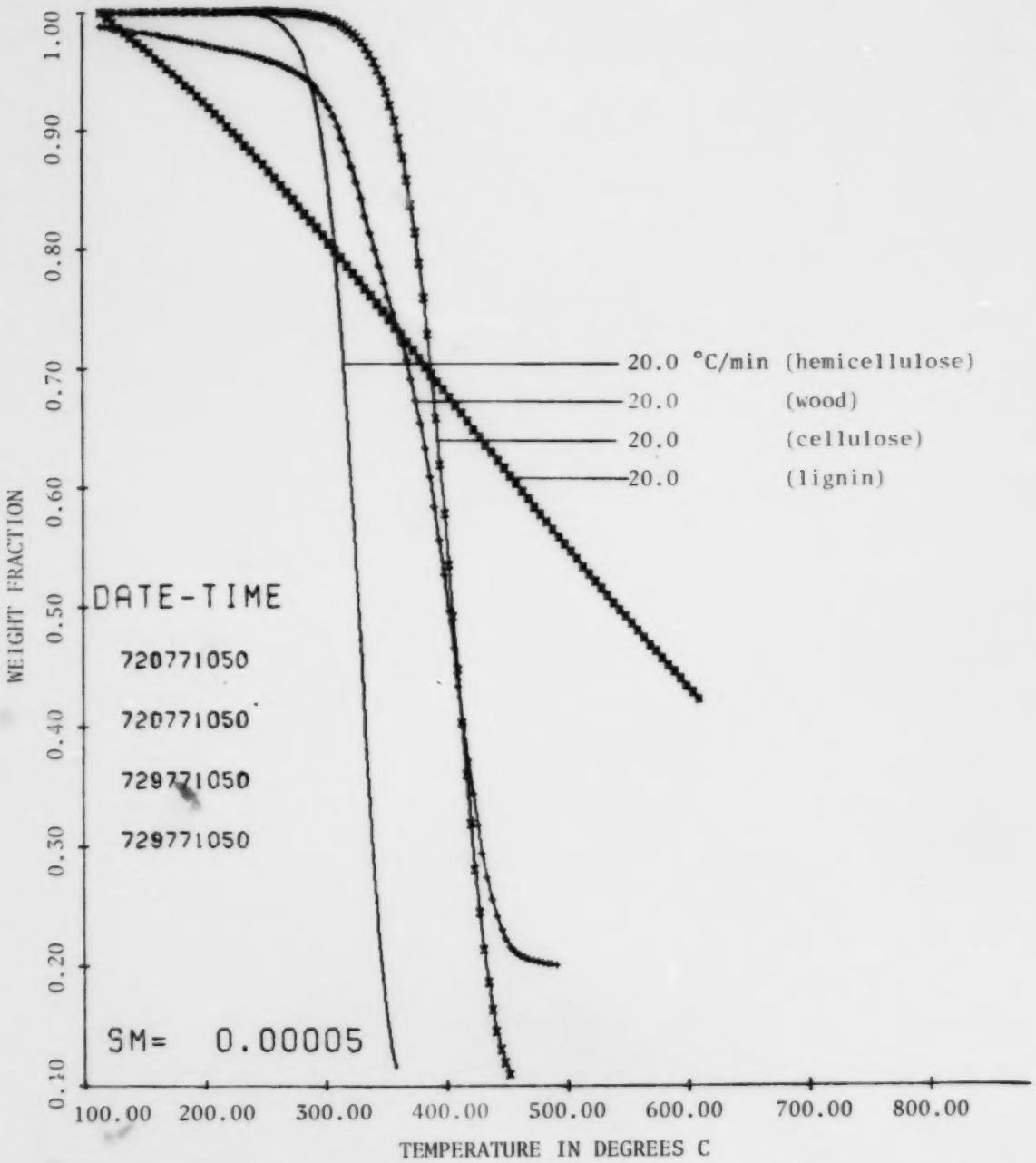

Figure 24. Thermogravimetric Curves for the Pyrolysis of Hardwood and Its Components in Nitrogen (50 ml/min) at Various Heating Rates.

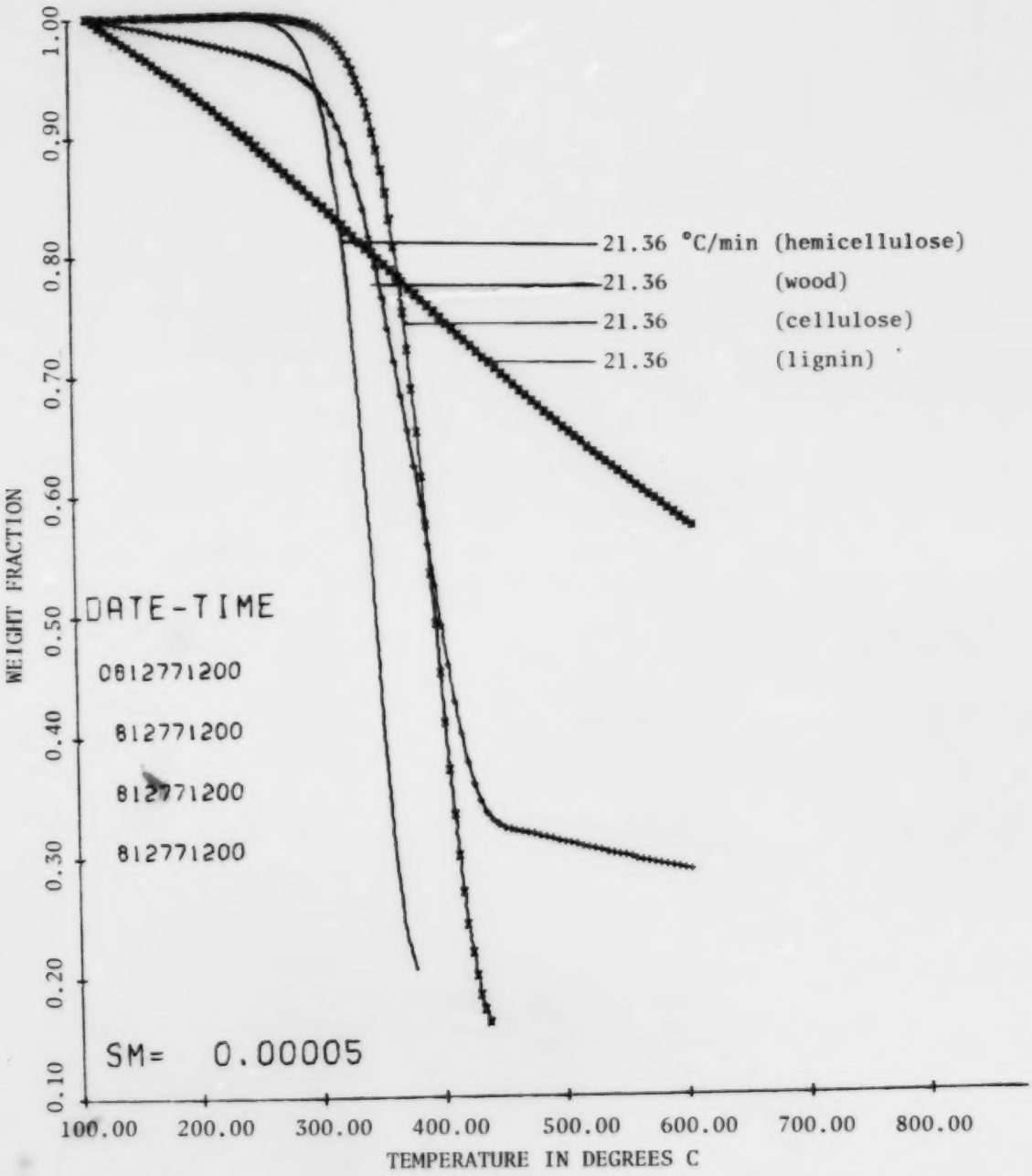

Figure 25. Thermogravimetric Curves for the Pyrolysis of Softwood and Its Components in Nitrogen (50 ml/min) at Various Heating Rates.

along with our theoretical wood curves. Similarly shaped experimental curves are found in Beall[64].

However, differences from previous work do exist. Percentages of components do not precisely fit the literature values. But because these values are determined by approximate separations, this study may be a more accurate measure of component percentages. Also, high surface temperatures or other alterations by the industrial treatment of the wood could have caused discrepancies by selectively reducing some compounds. Lastly, mere species or sample variation could be accountable for this difference.

Other differences such as percent residue, temperature of maximum reaction and activation energies are not outside the data range of the previous studies. In addition, the Arrhenius model does not seem to fit the initial and final regions perfectly. This seems to suggest that a more complex sequence of reactions is present early and late in the decomposition, possibly involving re-polymerization and/or dehydration.

Still, the basis of the model is sound. A migration of curves to the right with increasing heating rate, proper asymptotic residues and nearly perfect duplication of the zone of maximum reaction are produced by this model. Consistent activation energies for components between different woods are also good signs if independence of reaction is assumed. In transferring from one wood to another, the only major alteration done on the parameters involved changing percentages and residues of components, changes expected from the natural differences between soft and hardwoods.

For comparison sake, the experimental curve obtained from both the hard and softwoods at a heating rate of 20°C/min were fitted using the single step pyrolysis model [Equations (9) - (10)]. Results are given in Tables 8 and 9. This model may be more convenient for engineering calculations.

Cow Manure

Grab samples of Holstein Cow Manure were obtained from a dairy farm and analyzed on the DuPont TGA to determine the kinetic parameters for pyrolysis in nitrogen. The manure was first dried in an oven at 80°C to remove most of its moisture content. In order to obtain a homogeneous sample, approximately one pound of dried cow manure was first put in a grinding machine and then passed through a set of U.S.A. Standard Series Sieves. The finest sieve used was a No. 60 sieve (250 μm).

Samples weighing approximately 7-8 mg of the homogenized manure were further dried at 110°C for about 45 minutes in flowing nitrogen. The sample was then heated to 900°C at nominal rates of 5°, 10°, 20°, 50°, and 100°C/min in a nitrogen atmosphere. The weight-loss was recorded as a function of temperature. Results of typical analyses are given in Figure 26. Curves obtained at a given heating rate were surprisingly reproducible.

Kinetic analyses of the weight loss curves using the F-C method, are given in Table 10, and results of the Friedman multiple heating rate method of analysis for these curves are given in Figure 27.

TABLE 8

KINETIC PARAMETERS FOR HARDWOOD HW-1 (CHERRY) IN NITROGEN-SINGLE REACTION MODEL

Sample	0729771050
Heating Rate (°C/min)	20.0
E(kcal/gmol)	38.0
A (min^{-1})	$2.00x10^{12}$
n	1.0
V*	0.8

TABLE 9

KINETIC PARAMETERS FOR SOFTWOOD SW-2 (SOUTHERN YELLOW PINE) IN NITROGEN-SINGLE REACTION MODEL

Sample	0812771200
Heating Rate (°C/min)	21.36
E(kcal/gmol)	38.0
A (min^{-1})	$2.50x10^{12}$
n	1.0
V*	0.7

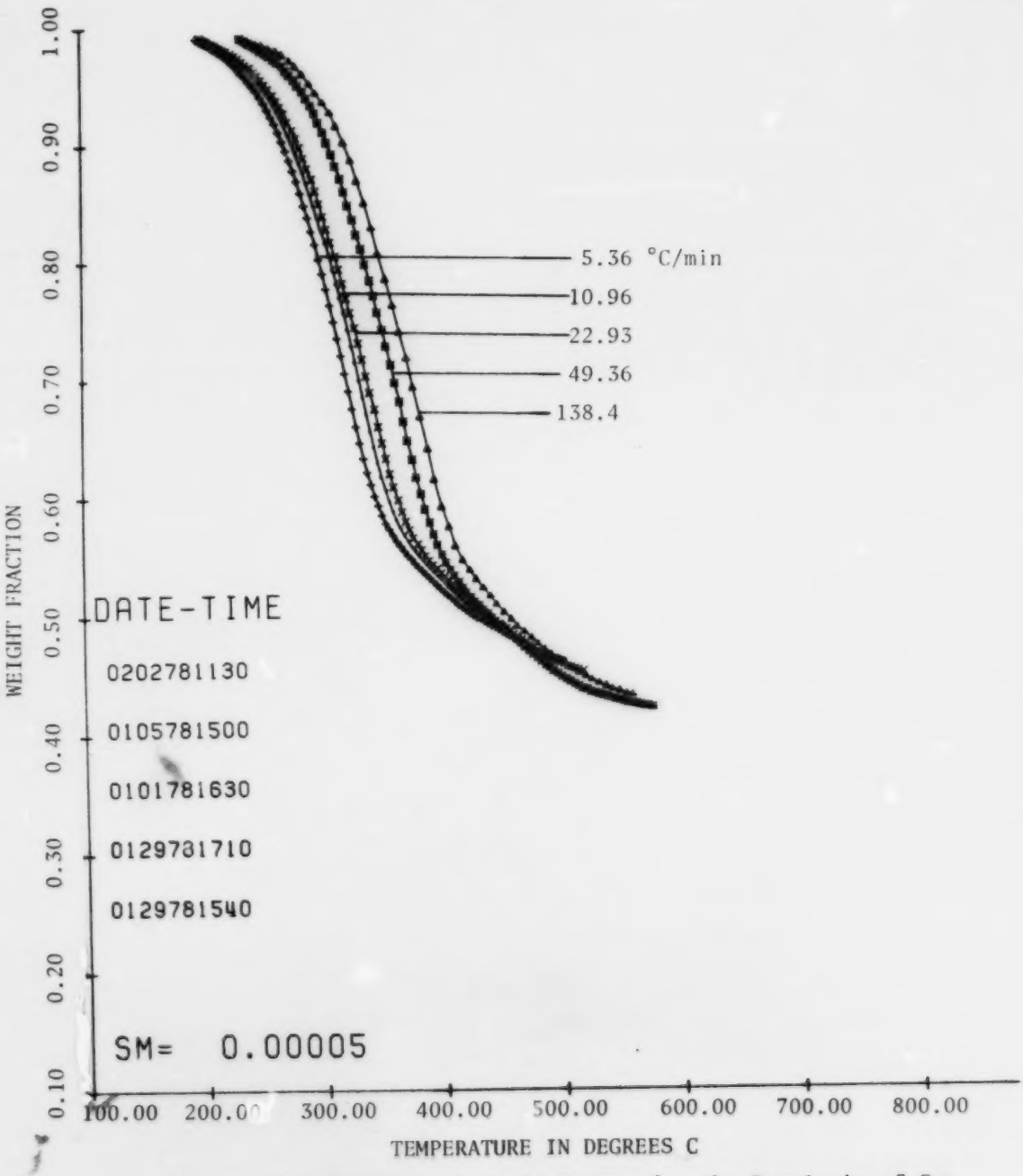

Figure 26. Thermogravimetric Curves for the Pyrolysis of Cow Manure in Nitrogen (50 ml/min) at Various Heating Rates.

TABLE 10

KINETIC PARAMETERS FOR COW MANURE IN NITROGEN-SINGLE REACTION MODEL

Sample	0202781130	0105781500	0101781630	0129781710	0129781540
Heating Rate (°C/min)	5.36	10.96	22.93	49.36	138.4
$T_{initial}$ (°C)	110	110	110	110	110
T_{final} (°C)	900	900	900	900	900
n	0.75	0.75	0.7	0.95	0.75
E(kcal/gmol)	13.7	12.8	13.77	13.14	13.26
A(min^{-1})	$7.0x10^3$	$5.0x10^3$	$2.4x10^4$	$2.1x10^4$	$4.0x10^4$
V*	0.619	0.614	0.602	0.615	0.605

ACTIVATION ENERGY VS WEIGHT FRACTION FOR PYROLYSIS OF COW MANURE IN NITROGEN

Figure 27

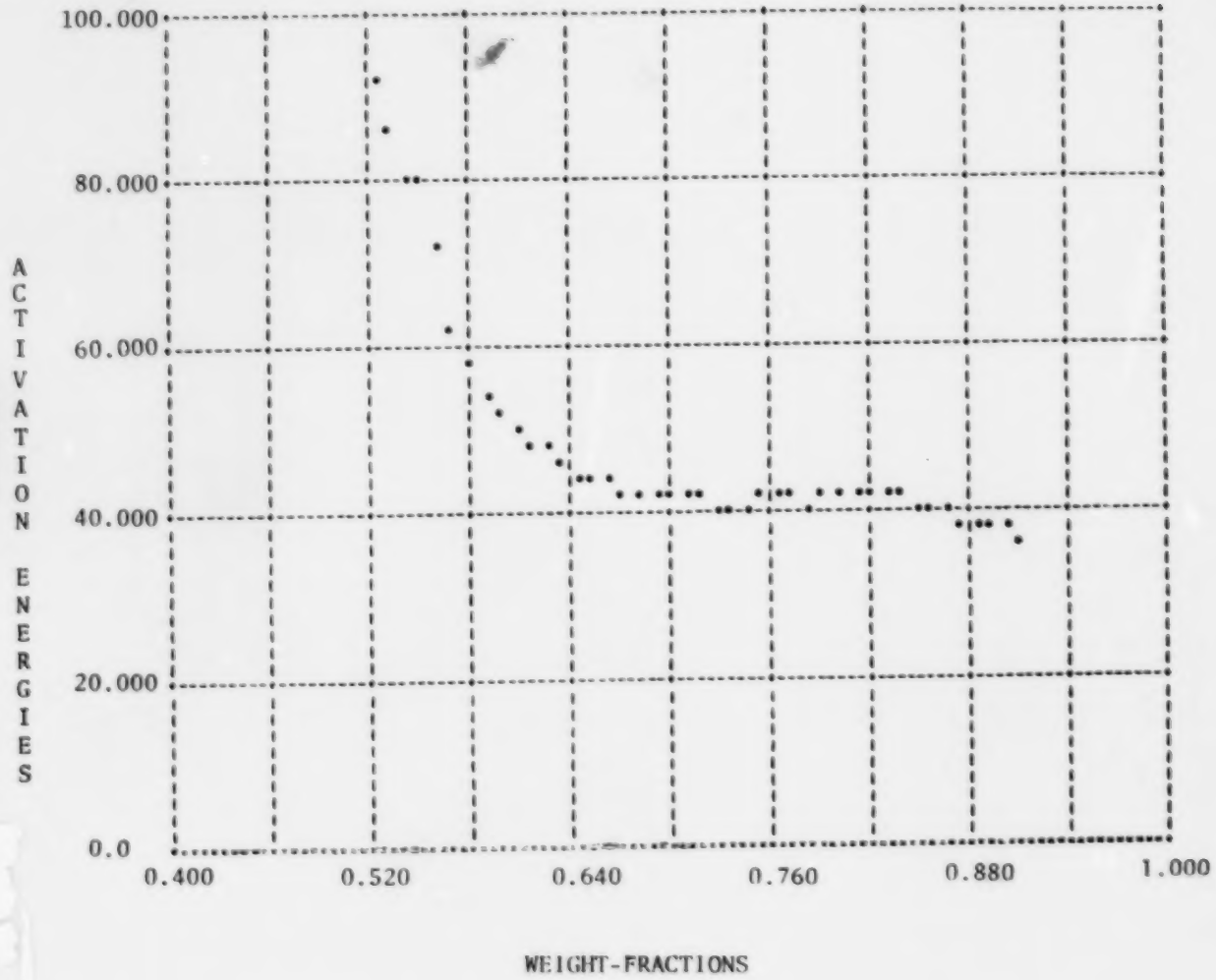

SECTION VI

SECONDARY, GAS PHASE REACTION KINETICS*

INTRODUCTION

As described in the preceding section, from 60% to over 90% of organic waste material is volatile matter. This contrasts with about 40% volatile matter for coal and 12% volatile matter for oil shale. Because the bulk of organic wastes is volatile matter, the secondary reactions of volatile matter in the gas phase play a critical role in waste gasification processes. As discussed in the following sections, an increase in the temperature attained by the gaseous pyrolysis products (which are formed at temperatures between 300° and 400°C for most gasification systems) from 500° to 700°C can increase combustible gas yields by a factor of ten or more.

It is unfortunate that essentially no experimental data exist on the gas phase reactions of pyrolytic volatile matter. This section describes the results of an experimental research program designed to study the effects of temperature and residence time on the products and rates of the secondary, gas phase reactions of volatile matter derived from cellulose pyrolysis. The forthcoming MSE theses of Messrs. Timothy Mattocks and Virendra Kothari will provide similar data for the gas phase reactions of volatile matter derived from hard and softwoods, and cow manure in steam.

There is a strong resemblance between the results described in this section and those obtained from steam cracking ethane, naphthas, gas oils and other hydrocarbons to olefins. Early work on steam cracking was reviewed by Nelson[66], and an overview of more recent research was given by Zdonik et al.[67]. Goosens et al.[68] describe state-of-the-art pyrolysis simulation programs which use chemical kinetic models based on free radical mechanisms combined with heat and mass transfer models to predict olefin yields from steam crackers.

EXPERIMENTAL PROCEDURE

For the experiments described below dry, Whatman #1 filter paper stored in a desiccant bottle was used as feedstock material. The use of an oven to obtain "bone dry" material was found to be futile due to the hygroscopic nature of the cellulose. The cellulose was assumed to have the chemical composition of 0.444 C, 0.062 H, 0.494 O on a mass fraction basis, and the char composition was determined to be 0.7835 C, 0.04 H, and 0.1765 O by an independent laboratory.

---

*This material was published in Reference 14.

A specially designed quartz, tubular plug flow reactor was fabricated by studying the gas phase reactions. Rates of gas formation by species can be measured using the reactor either in a differential or an integral mode. Results described here emphasize the integral aspects of the tubular reactor since they are the easiest to interpret.

A schematic of the experimental layout is given in Figure 28. A typical experiment using the reactor follows the procedure outlined below:

1. With all three furnaces cold, a small (0.1 to 0.3g) sample of the material to be pyrolyzed is placed in the center of the pyrolysis reactor.

2. An inert gas is bled through ports D and E to cool the sample and purge the reactor, while furnaces 1 and 3 bring the steam superheater and the gas phase reactor to the desired temperature.

3. The peristaltic pump is actuated and pumps water into the steam generator at a measured rate. Concurrently, a small amount of inert tracer gas (argon) is continuously injected through port A into the rear of the reactor.

4. When condensed water first begins to appear in the pyrolysis reactor, Furnace 2 (which was preheated to the desired pyrolysis temperature) is moved into place around the pyrolysis zone of the reactor.

5. When pyrolysis temperatures are reached the six-port Valco valve is switched and the 34-port Valco valve automatically takes 15 samples of the gas stream for later analysis in the Hewlett-Packard 5834a Gas Chromatograph (HPGC). Unsampled gas is collected in a Teflon bag for later analysis.

6. When all 15 samples have been taken, the six-port valve is switched again and the samples are automatically analyzed by the HPGC. Gases collected in the Teflon bags are sampled using a gas-tight syringe and analyzed by the HPGC.

7. The char and tars produced during the experiment are collected and weighed. Water collected in the condenser is also weighed.

Temperatures within the reactor are controlled by various temperature controllers and monitored by type K thermocouples with continuous recording on chart recorders. Measured temperature variations along the length of the gas phase reactor are given in Figure 29.

The evolved gas composition was observed to undergo considerable variation during the course of the experiment; consequently ten gas standards were acquired to calibrate the HPGC for quantitative analysis of the following gases: Ar, N_2, H_2, CO, CO_2, CH_4, C_2H_4, C_2H_6, C_3H_6 , C_4H_8, C_4H_{10}, C_5H_{12}, and C_6H_{14}. Identification of the higher hydrocarbons ($>C_3$) is obscured by the fact that some other pyrolysis products have similar retention

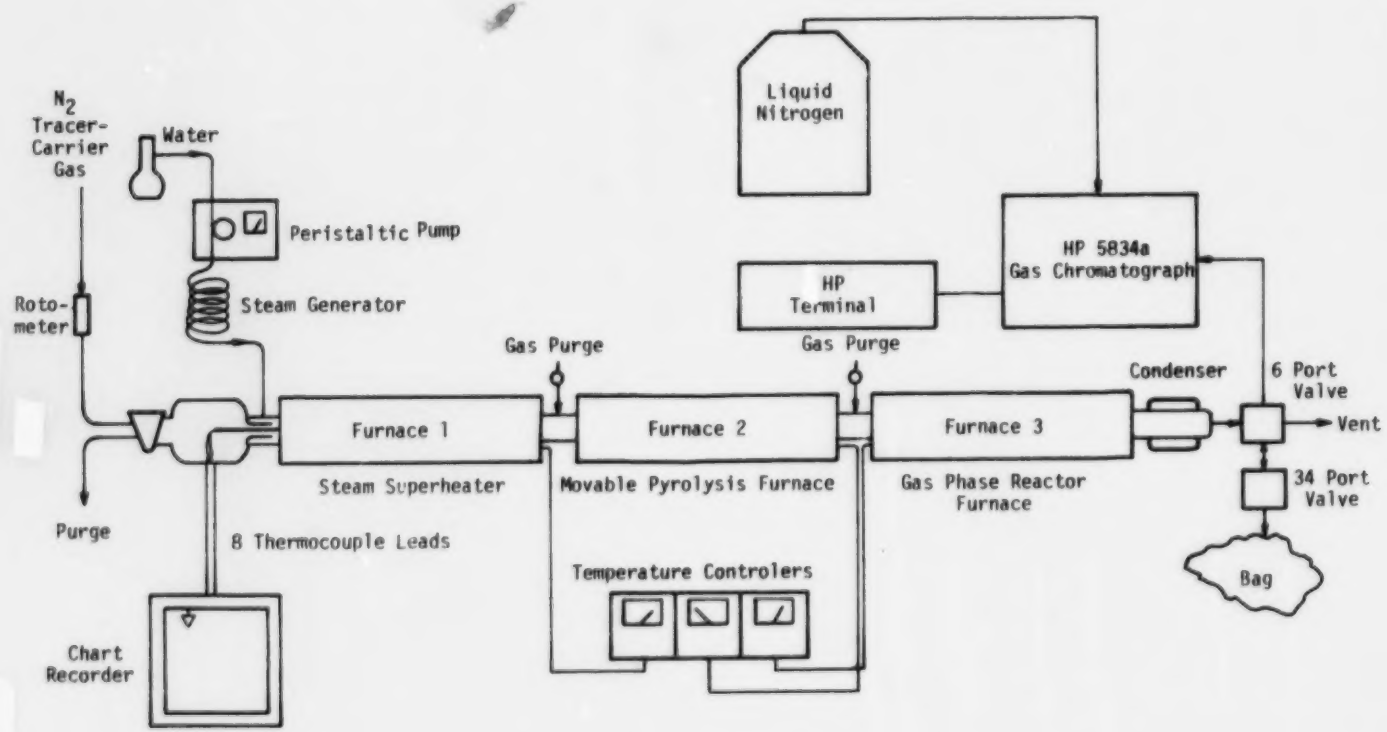

Figure 28

SCHEMATIC OF THE TUBULAR QUARTZ REACTOR EXPERIMENT

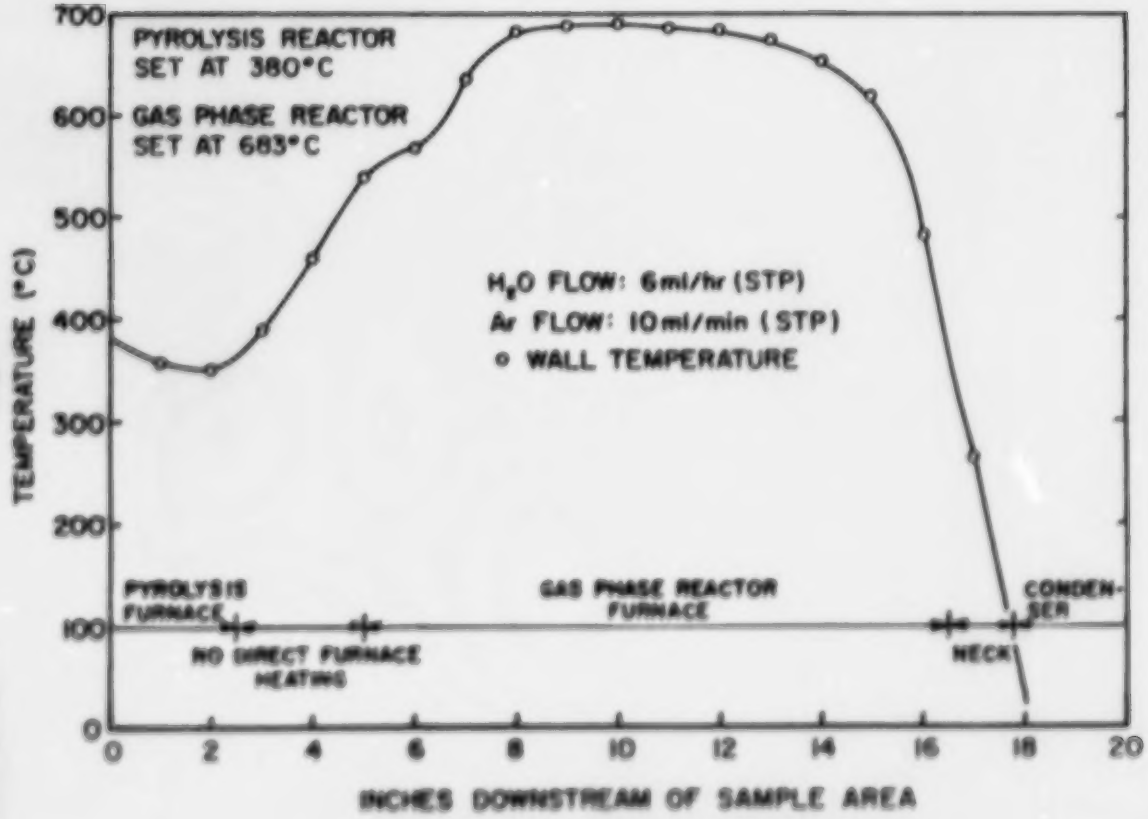

TEMPERATURE MAP OF TUBULAR PLUG FLOW REACTOR

Figure 29

times. Analyses given in this section for light hydrocarbons (< C_3) have been checked using a mass spectrometer. The HPGC uses a Poropak QS in series with a Porosil column operating between -50°C (cryogenic) and 200°C for gas analysis with a thermal conductivity detector (TCD). The carrier gas is a 8-1/2% H_2, 91-1/2% He mixture. A typical gas analysis takes 14 minutes.

The complete recovery of moisture and tars from the reactor sometimes poses difficulties. The moisture is absorbed on dry paper towels and weighed; whereas the tars condense on a rolled piece of aluminum foil inserted in the condenser. Mass balances are always better than 0.8, but can be misleading because much more water is used during the course of an experiment than solid reactant.

The carbon balance is a better measure of the experiment's quality, and usually ranges between 0.7 and 1.0 for the results reported here. Our inability to close the carbon balance in part reflects the formation of water soluble carbonaceous compounds which are not subject to analysis by our existing instrumentation. Their presence is manifested by the color and smell of the collected water, which ranges from clear with an odor resembling automobile exhaust, to deep amber with a stronger, more noxious odor.

As designed the reactor bears some resemblance to a dilute phase transport reactor in that the solids and volatile pyrolysis products are present only in low concentrations in the flowing steam. During pyrolysis the composition of gas in the gas phase reactor using the lowest steam flow and a 0.1g sample is nominally 68% steam, 28% volatiles, and 4% argon carrier (on a volume percent basis). Somewhat larger samples, leading to an increase in volatile concentrations, do not markedly affect the results reported here.

Rates of gas production can be measured using the reactor in either a differential or an integral mode. The differential mode employs the Valco valve system to obtain fifteen 0.6 ml samples of gas evolved during the course of the experiment. With Ar tracer gas injected at a measured rate, the dilution of the tracer gas sample can be directly related to the "instantaneous" rate of volatile gas production in the reactor. For example, with a tracer gas flow of 5 ml per min., a dilution of 50% in the gas sample would correspond to an "instantaneous" volatile gas production rate of 5 ml per min. Unfortunately, departures from true plug flow of gas flow within the reactor (primarily due to the effect of the condenser on gas flow) make the differential mode experimental data more difficult to interpret than indicated above. Research described here emphasizes the integral aspects of the reactor design.

When used in the integral mode total gas production by species is measured using Teflon bags to collect all the reactor effluent. The dependence of total gas production on gas phase residence time in the gas phase zone of the reactor is determined using the combined data of many experiments. As discussed in the following section, this data can be used to infer rates of gas production within the gas phase reactor. Kinetic models of gaseous species formation can be obtained through a study of the affects of both temperature and residence time on species production.

Kinetic Interpretation of Reactor Data

Consider the pyrolysis of a small sample of organic material in the pyrolysis zone of the tubular reactor system. At any time t the rate of evolution of gaseous volatile matter ($\dot{m}_v$) from the pyrolyzing sample is given by

$$\dot{m}_v(t) = m\frac{dV}{dt} = mk(V^*-V(t))^n;\ k = A\exp(-E/RT) \tag{11}$$

where m is the time dependent sample mass, m_i is the initial sample mass, m_f is the final sample mass, $V^* = (m_i - m_f)/m_i$, $V = (m_i - m)/m_i$, A is the pre-exponential constant, E is the apparent activation energy, R the Universal Gas Constant, T the time dependent absolute temperature, and n the apparent order of the reaction. The concentration of volatile matter (C_v) in the flowing stream is given by

$$C_v(t) = \frac{\dot{m}_v}{\dot{m}_s/\rho_s + \dot{m}_v/\rho_v} \tag{12}$$

where $\dot{m}_v$ is the mass flow of volatile matter and where $\dot{m}_s$ is the mass flow of steam in the tubular reactor and ρ_s and ρ_v are the densities of steam and volatile matter (respectively). Assuming plug flow, the volatile matter evolved at the time τ enters the gas phase reactor at time $\tau + \tau_i$ and leaves the gas phase reactor at time $\tau + \tau_o$. The residence time $\theta = \tau_o - \tau_i$ of the volatiles in the gas phase is given by

$$\theta = L^2/\int_0^L v(x)dx \approx \sigma L/\dot{V} \tag{13}$$

where L is the length of the gas phase reactor, v is the spatially dependent gas velocity in the reactor, $\dot{V}$ is the volumetric flow of volatiles plus steam in the reactor at the gas phase reactor temperature T, and σ is the reactor's effective cross sectional area.

Suppose that the rate of disappearance of condensible volatiles (due to cracking, reforming, etc. and treating the condensible volatiles as a single chemical species) in a differential volume element $\sigma\bar{v}\delta\tau$ of gas moving with average velocity $\bar{v} = L/\theta$ satisfies a first order rate law:

$$\frac{dC_v}{d\tau} = -C_v r_v \tag{14}$$

where the rate constant r_v is given by the Arrhenius expression

$$r_v = A_v\exp(-E_v/RT). \tag{15}$$

The time variable τ can be thought to "track" the position of the differential volume element with initial volatile concentration $C_V(t)$ as it moves through the gas phase reactor. The production of permanent gases produced by cracking/reforming reactions is also assumed to satisfy a first order rate law:

$$\frac{dC_j}{d\tau} = C_V r_j \tag{16}$$

where r_j is the rate constant associated with the j^{th} permanent gas and

$$r_j = A_j \exp(-E_j/RT). \tag{17}$$

As a first approximation the gas phase zone can be treated as an isothermal reactor (however, see the following section), leading to the expressions

$$C_V(t+\tau_o) = C_V(t)\ \exp(-r_V(\tau_o-\tau)) \tag{18}$$

$$\begin{aligned} C_j(t+\tau_o)-C_j(t) &= \int_{\tau_i}^{\tau_o} C_V(t) r_j \exp(-r_V(\tau-\tau_i))d\tau \\ &= C_V(t)(r_j/r_V)\ \left[1-\exp(-r_V(\tau_o-\tau_i))\right] \end{aligned} \tag{19}$$

where r_V and r_j are constant (by assumption of constant T), and it is also assumed that the temperature of the pyrolysis zone is sufficiently "cold" so that the cracking/reforming reactions do not commence until the differential volume element enters the gas phase reactor.

The mass of species j in the differential volume element emerging from the reactor at time $t+\tau_o$ is given by

$$\sigma\ v\ \delta t\ C_j(t+\tau_o) \tag{20}$$

and the total mass m_j of species j produced during the experiment is given by

$$\begin{aligned} m_j &= \sigma \int v(t) C_j(t+\tau_o)dt \\ &\simeq \bar{v}\sigma \int C_j(t+\tau_o)dt = \bar{v}\sigma(r_j/r_V)\left[1-\right. \\ &\qquad \left.\exp(-r_V(\tau_o-\tau_i))\right] \int C_V(t)dt \\ &\quad + \bar{v}\ \sigma\ \int C_j(t)dt\ . \end{aligned} \tag{21}$$

For short residence times ($r_V(\tau_o-\tau_i)<<1$) Equation 21 becomes

$$m_j \simeq \bar{v}\sigma r_j(\tau_o-\tau_i)\int C_V(t)dt + \bar{v}\,\sigma \int C_j(t)dt \ . \qquad (22)$$

A plot of m_j vs. residence time $(\tau_o-\tau_i)$ should yield a straight line with temperature dependent slope $\bar{v}\sigma r_j \int C_V(t)dt \equiv k_j$. A subsequent plot of $\ell n(k_j)$ vs. T^{-1} should yield straight lines whose slopes are the apparent activation energy E_j associated with the rate of production of species j. Thus the data obtained from the tubular reactor is susceptible to kinetic interpretation.

It should be noted that this analysis only provides an insight into the initial rates of the cracking reactions. Tertiary gas phase reactions tend to obscure the interpretation of the kinetic data derived from the reactor. Moreover, the initial rate measurements for the cracking reactions are meaningful only for short residence times ($r_V(\tau_o-\tau_i)<<1$). Because the cracking reactions occur rapidly this constraint is difficult to satisfy.

Departures From an Ideal Isothermal Reactor

The tubular quartz reactor was designed anticipating the need to provide for long (5 seconds or more) gas phase residence times in order to reform the oily volatile matter. Surprisingly, the observed reaction rates were so high that residence times on the order of 0.5 seconds or less were needed to satisfy the condition $r_V(\tau_o-\tau_i)<<1$. To obtain such short residence times, large mass flows were required which caused the reactor to deviate from its intended use as an ideal isothermal system. In addition, the Lindburg furnaces were observed to be less uniform in temperature than expected. Consequently, heat transfer plays a critical role in determining the residence time of the volatiles at temperature. The following paragraphs outline our "first order" approach towards recognizing the effects of heat transfer on the kinetic interpretation of the experimental data.

A simple energy balance for laminar fluid flow in a long tube leads to the equation

$$\frac{dT}{dx} + \alpha T = \alpha T_w \qquad (23)$$

where $\alpha = \frac{\pi D h}{\dot{m} c_p}$, and T(x) is the bulk gas temperature along the length x of the tube, T_w is the constant wall temperature, D is the tube's diameter, h is the heat transfer coefficient, $\dot{m}$ is the mass flow of the gas and c_p is the specific heat of the gas. Equation 23 can be solved to determine the distance ℓ required for the gas to reach temperature T, with the result

$$\ell = -\left(\frac{\dot{m} c_p}{\pi k N_{Nu_D}}\right) \ell n\left(\frac{T_w - T}{T_w - T_i}\right) \qquad (24)$$

where $h = kN_{Nu_D}/D$, k is the thermal conductivity of the gas, and N_{Nu_D} is the Nusselt number.

In order to obtain an approximate residence time ($\tau_o - \tau_i$) for the volatiles in the gas phase reactor, the length ℓ was calculated assuming $T_w - T = 5°C$. An error of 5°C in the gas phase temperature measurement gives rise to about a 10% error in the determination of E_j. The residence time of the volatiles at temperature was then calculated using the formula

$$\tau_o - \tau_i = \frac{(L-\ell)\sigma}{\dot{m}_s/\rho_s + \dot{m}_v/\rho_v} \qquad (25)$$

where L is the total length of the gas phase section of the reactor, and σ is the apparent cross sectional area of the reactor.

Table 11 lists values of ℓ as a function of T_w for a steam flow of 0.34 g/min (used in the short residence time kinetic experiments). From this data it is apparent that at the higher gas phase temperatures the volatiles spend about 50% of their time in the gas phase reactor being heated to isothermal conditions. Consequently, kinetic measurements at the higher temperatures represent integrated values of the rates at lower temperatures, in addition to the (assumed) constant rate at T_w. This result clouds the kinetic interpretation of the reactor data. Although more effort could be made to explicitly account for the warmup time in the kinetic model for the reactor data, we have chosen to focus our effort on the design of a "second generation reactor" which will provide sufficient heat transfer rates to insure nearly isothermal conditions for the shortest residence time experiments.

Some efforts have also been made to experimentally measure the temperature rise of the steam entering the gas phase reactor. Qualitative agreement with the results of the heat transfer calculations was found; however a brief calculation of the effect of radiation on the thermocouple's measurement of the gas temperature pointed to a significant error in the measurement. For example, with a steam flow of 0.12 g/min and a gas phase temperature of 600°C the thermocouple temperature was calculated to exceed that of the gas by 13°C. Carefully constructed radiation shields are needed to eliminate this effect. Because our research effort in this area was drawing to a close, it was decided to use the methodology described earlier (Equation 25) to estimate the residence time of the volatiles at temperature.

Departures From An Ideal Plug Flow Reactor

Both turbulence and molecular diffusion cause tubular reactors to depart from ideal plug behavior. It is standard practice to account for the two effects by a single dimensionless parameter $\mathcal{D}/vL$, called the vessel dispersion number. This number is usually determined experimentally, and its magnitude indicates the degree of departure of the reactor from plug flow ($\mathcal{D}/vL < 0.01$ for plug flow). A good discussion of the effects of

TABLE 11. VARIOUS PARAMETERS USED TO CALCULATE GAS PHASE RESIDENCE TIME

T_w	ℓ	Effective reactor volume	Effective insert volume
750°C	13.4 cm	46.4 cm^3	30.2 cm^3
700°C	13.9	48.1	31.3
675°C	14.2	49.2	32.0
650°C	14.5	50.2	32.6
625°C	14.8	51.3	33.3
600°C	15.2	52.7	34.2
575°C	15.6	54.0	35.1
550°C	16.1	55.8	36.2
500°C	17.2	59.6	38.7

$L = 29.2$ cm

$\sigma = 3.464$ cm^2

bulk volume of insert $\cong 70$ cm^3

length of insert $\cong 31.1$ cm

dispersed plug flow on the kinetic interpretation of reactor data is given by Levenspiel (69).

The value D/vL = 0.122 was measured by T. Mattocks as part of his MSE thesis research. Although this value suggests significant departures from plug flow, we believe most of the dispersion occurs in the condenser without affecting the kinetic measurements presented here.

Results and Discussion

Figures 30, 31, and 32 display the dependence of gas production (g gas per g cellulose or % conversion) by species on gas phase residence time for various gas phase reactor temperatures. For these experiments the steam superheater was maintained at 350°C, and the pyrolysis furnace at 500°C. This latter setting gave rise to a measured sample heating rate of 100°C/min. Residence times were altered by varying the peristaltic pump's water flow rate between 0.06 and 0.34 g/min,, and by inserting a closed quartz cylinder into the gas phase reactor to reduce its apparent volume.

Data points reported in Figures 30-32 were accumulated over a period of eight months using experimental techniques which evolved and improved during that time period. Data points with residence times of two to three seconds were obtained using a water flow rate of 0.34 g/min for a 0.25 g sample. Shorter residence times were obtained using a quartz insert to reduce the gas phase reactor's apparent volume. Longer residence times were obtained by reducing the water flow rate and cellulose sample size proportionately. Thus, all the data represent the same steam flow/cellulose weight ratio.

Since cellulose pyrolysis occurs in about one minute with a heating rate of 100°C/min., the data correspond to a steam dilution ratio of about 1.4 g steam per 1 g cellulose feed. Available evidence suggests that higher steam dilution ratios have little effect on the gasification results. Efforts are presently being made to more fully elucidate the effects of dilution ratio on steam gasification products.

Of the various gases represented in Figures 30-32 the behavior of carbon dioxide is simplest to interpret, since it shows the least dependence on gas phase residence time or temperature. Apparently the primary mechanism for CO_2 formation rests in the initial pyrolysis process. Secondary, gas phase reactions at temperatures above 500°C contribute less to CO_2 formation. In order to increase gasification efficiency by reducing CO_2 formation (each molecule of CO_2 formed represents a net loss of carbon from the combustible products of the process), the conditions affecting the pyrolysis step of gasification must be carefully examined. For example, the use of high solids heating rate may reduce CO_2 formation.

Methane formation is also relatively easy to interpret. Increasing temperatures and increasing residence times result in increased methane formation. The slope of the dashed lines in Figure 31 gives the apparent rate of methane production at the various temperatures studied. The dependence of this production rate on temperature is used later in this section to estimate the activation energy for methane formation. Efforts

to elucidate the mechanism of methane formation (most probably the pyrolysis/hydrogenation of higher hydrocarbons) are presently underway.

Carbon monoxide and hydrogen production data behave similarly to one another, and reach a maximum at about 5 seconds residence time and 700° to 750°C. Data for C_2H_6 production show some similarity to that of CH_4; however C_2H_6 production reaches a maximum at temperatures of 650° to 700°C and residence times of about 2 seconds. Competitive rates of formation by pyrolysis and consumption by pyrolysis or dehydrogenation reactions probably explain this observed behavior.

Ethylene production is maximized by temperatures of 700° to 750°C and residence times of about 6 seconds; whereas propylene formation is favored by lower temperatures (650°C) and shorter residence times (2 seconds).

In general, these results indicate that the gas phase reaction temperature is the most significant determinant of gasification results. The role of primary pyrolysis conditions and gas phase residence times is much less significant. Moreover, for temperatures above 650°C the initial rates of species formation are very high, so that much of the gas formation is complete in less than 0.5 sec. These very high rates of gas formation due to secondary reactions are of great significance for reactor design.

The preceding conclusions are substantiated by Figure 33, which shows the effect of gas phase temperature and residence time on the carbon, hydrogen and oxygen gasification efficiencies (carbon efficiency = carbon in gas ÷ feedstock carbon). Again, the gas phase reactor temperature most significantly affects the carbon and hydrogen efficiencies of the system.

Under the best conditions examined to date, 83% of the feedstock's energy was carried by the gaseous products of the process, and tar production was reduced to 3% of the feedstock weight. The gas had a heating value of 490 Btu/scf. Other pertinent statistics are given in Table 12.

Initial experiments in flowing argon with no steam present yield essentially the same results as the comparable steam runs. From this it appears that the gasification process is dominated by cracking reactions and not steam reforming reactions. Variations in heating rate of the cellulose from 50°C/min. to 200°C/min. do not markedly affect results.

Using gas phase residence times at temperature ranging from 0.46 to 0.97 sec (750° and 500°C respectively), apparent rates of production were measured for seven gaseous species: CO_2, H_2, CO, CH_4, C_2H_4, C_2H_6 and C_3H_6. Figures 34 and 35 are graphs of log (k_j/M_j) vs. T^{-1}, where k_j is the experimentally determined rate of production of gas species j. As indicated in Figures 34 and 35, the slope of the lines connecting the values of log (k_j/m_i) gives the apparent activation energy E_j associated with the rate of production of each species j. Values for each E_j are given in Table 13.

Several important conclusions can be drawn from Figures 34 and 35. At high temperatures (and short residence times) the rate of conversion of

FIGURE 30

NON HYDROCARBON GAS PRODUCTION VS RESIDENCE TIME
FOR VARIOUS GAS PHASE TEMPERATURES

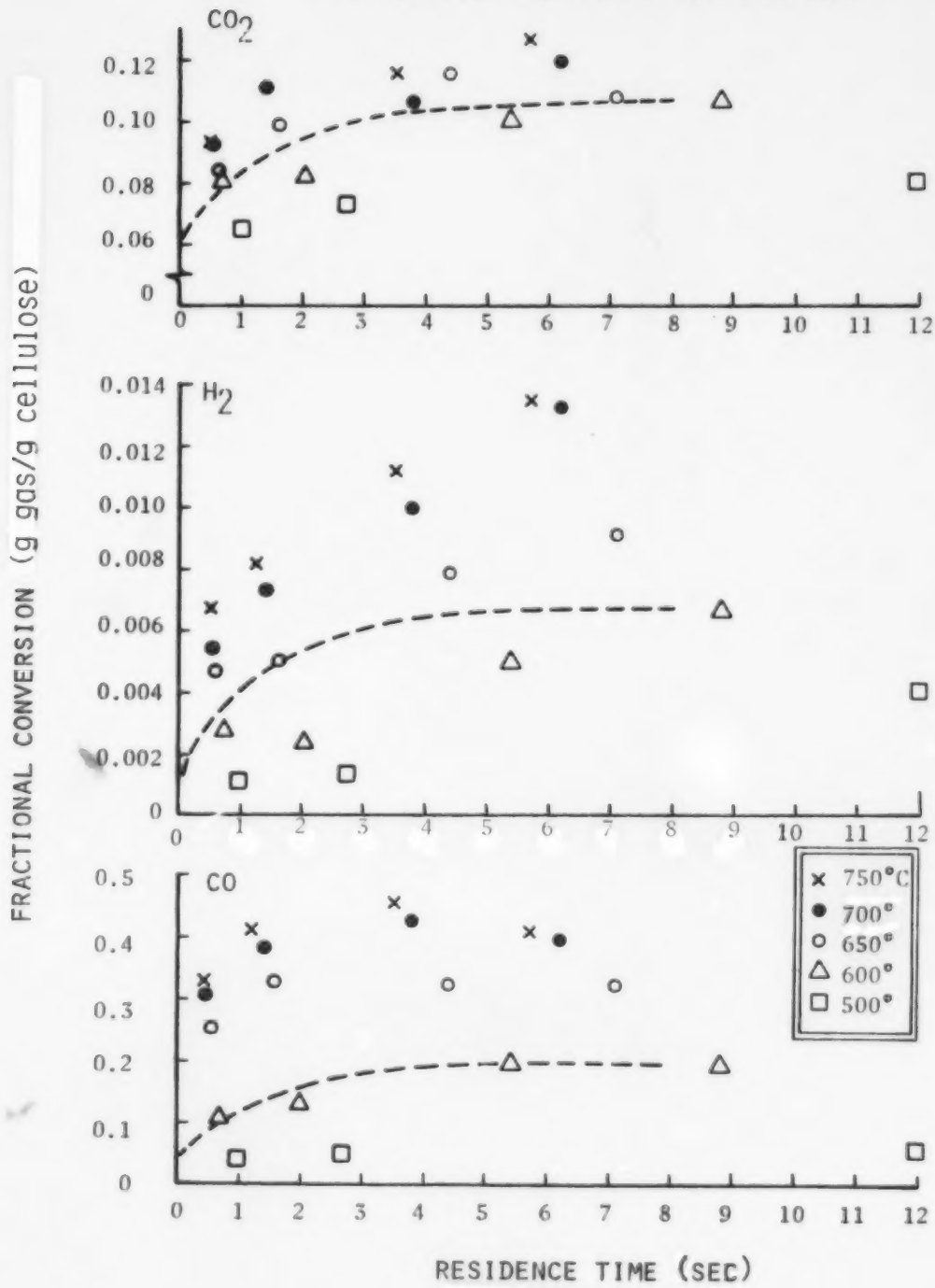

FIGURE 31

PARAFFINIC HYDROCARBON GAS PRODUCTION VS. RESIDENCE TIME FOR VARIOUS GAS PHASE TEMPERATURES

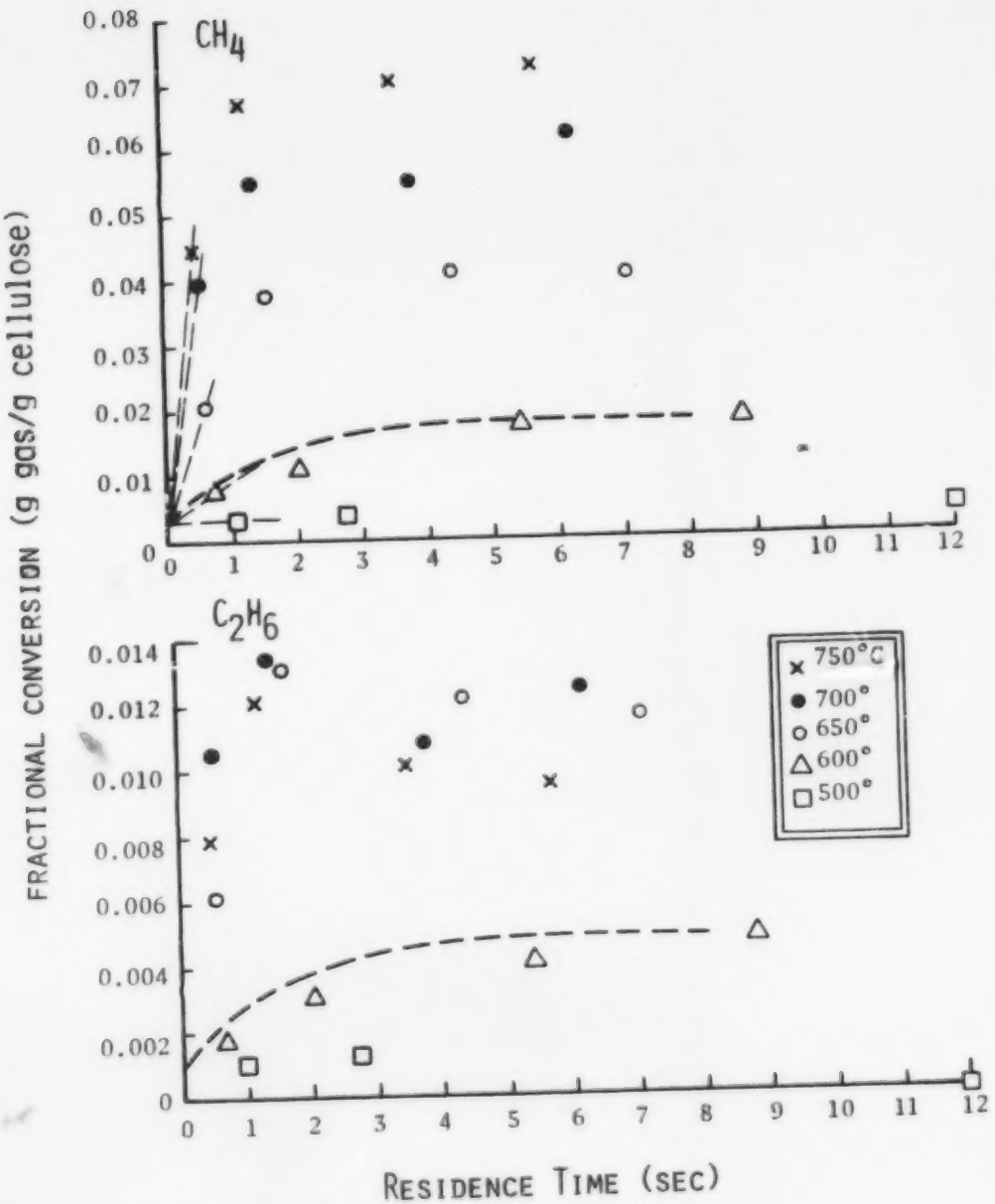

FIGURE 32

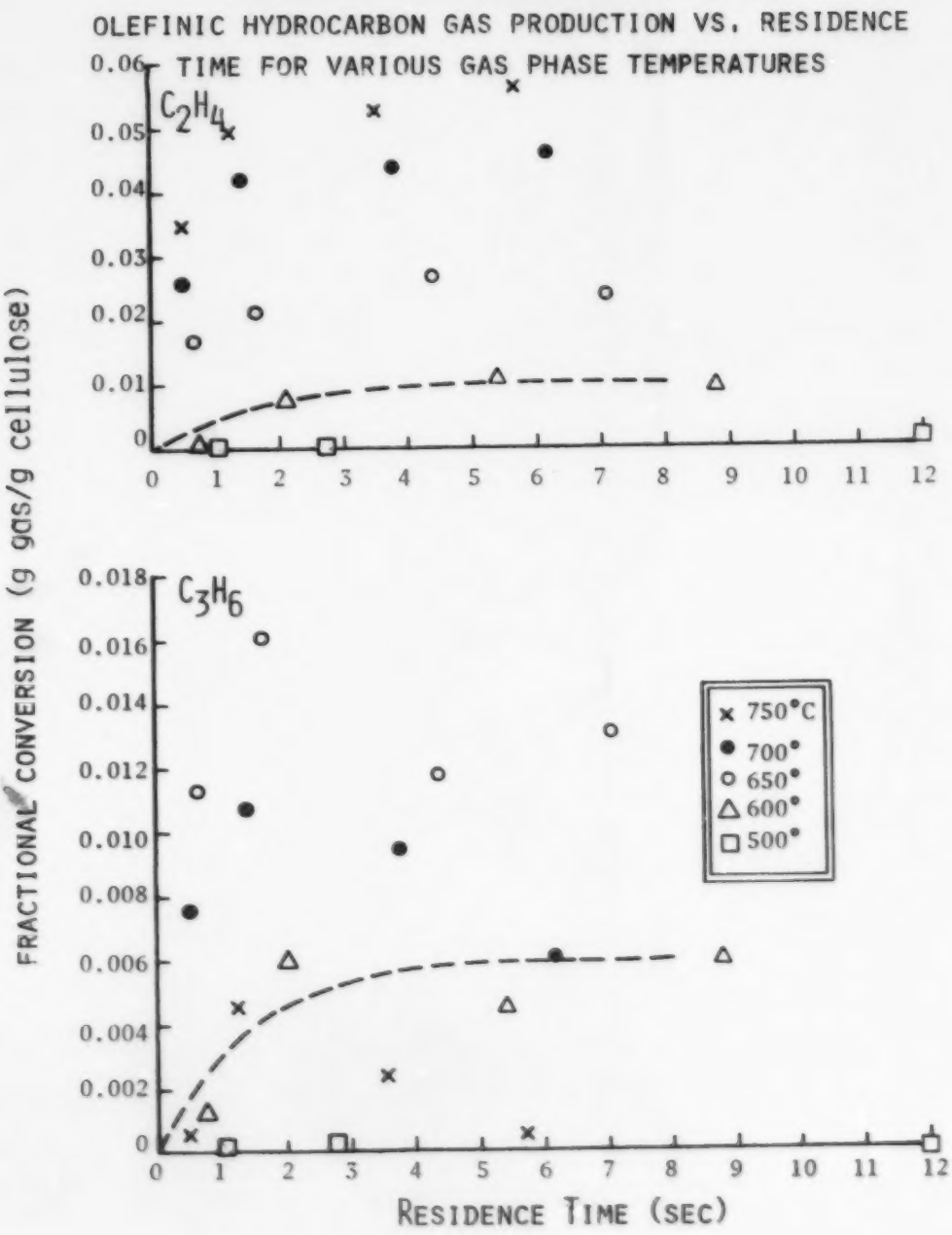
OLEFINIC HYDROCARBON GAS PRODUCTION VS. RESIDENCE TIME FOR VARIOUS GAS PHASE TEMPERATURES
C_2H_4
C_3H_6
FRACTIONAL CONVERSION (g gas/g cellulose)
RESIDENCE TIME (SEC)
750°C
700°
650°
600°
500°

FIGURE 33

CARBON, HYDROGEN AND OXYGEN EFFICIENCY VS. RESIDENCE TIME FOR VARIOUS GAS PHASE TEMPERATURES

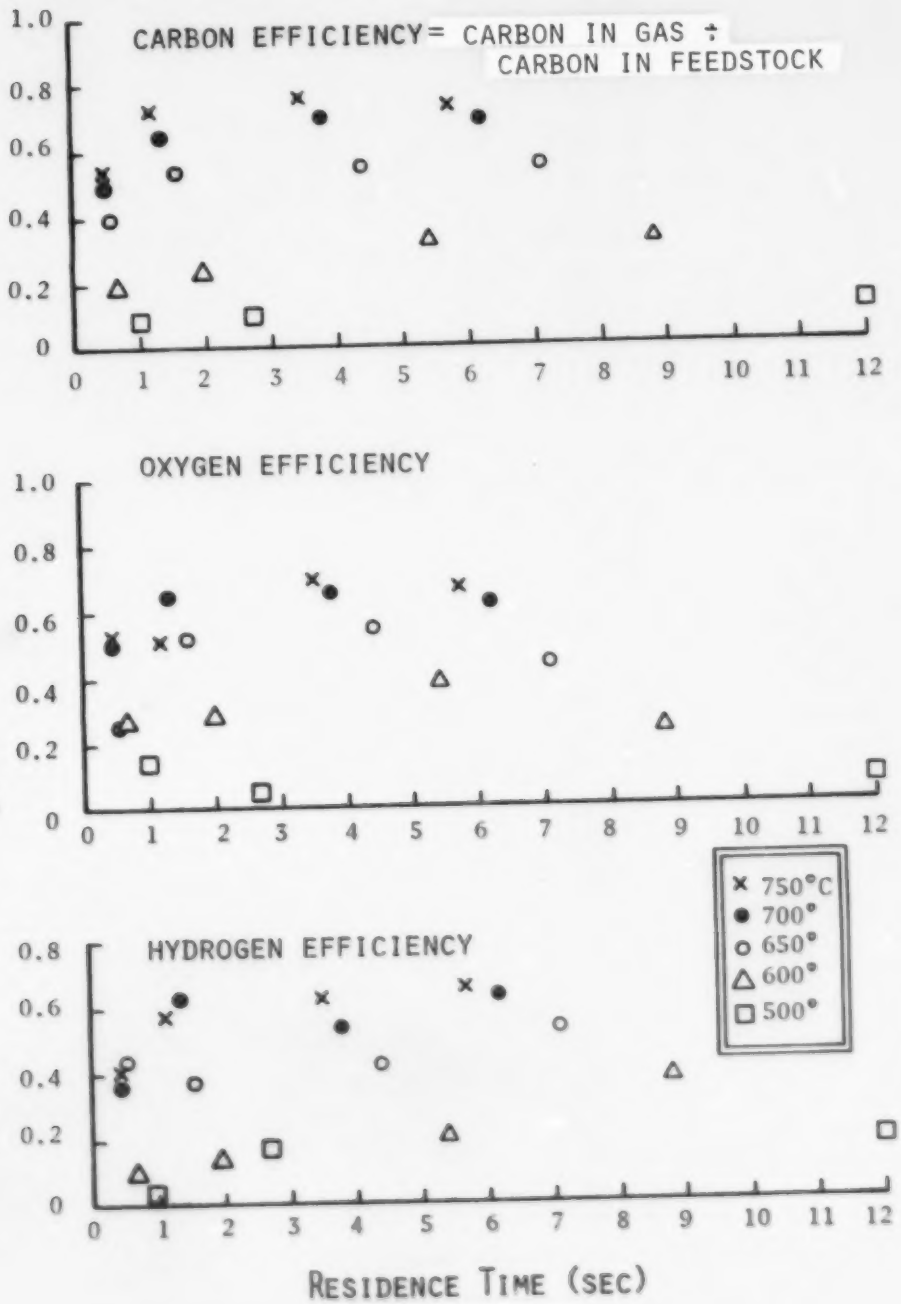

TABLE 12. SELECTED GASIFICATION RESULTS FOR CELLULOSE

Steam Superheater Temperature	350°C
Pyrolysis Reactor Temperature	500°C
Gas Phase Reactor Temperature	700°C
Gas Phase Reactor Residence Time	3.5 sec
Sample Weight	0.125 g
Char Residue Weight	0.012 g
Char Residue Weight Percent	10%
Tar Residue Weight	0.003
Tar Residue Weight Percent	2%
Gas Volume Produced	84 ml
Gas Heating Value	490 Btu/scf
Calorific Value of Gases	13.7 MM Btu/ton
Calorific Value of Char	2.8 MM Btu/ton
Calorific Value of Tars	0.5 MM Btu/ton
Mass Balance	0.84
Carbon Balance	0.96
Gas Analysis (Vol %)	
CO	52
H_2	18
CO_2	8
CH_4	14
C_2H_4	6
C_2H_6	1
C_3H_6	0.1
other	0.9

TABLE 13. APPARENT LOW TEMPERATURE (500°C $\leq$ T $\leq$ 675°C) ACTIVATION ENERGY (E_j) FOR VARIOUS GAS SPECIES

Gas Species	E_j
CO_2	21 kcal/gmol
H_2	35
C_2H_6	38
C_2H_4	55
C_3H_6	55
CO	60
CH_4	67

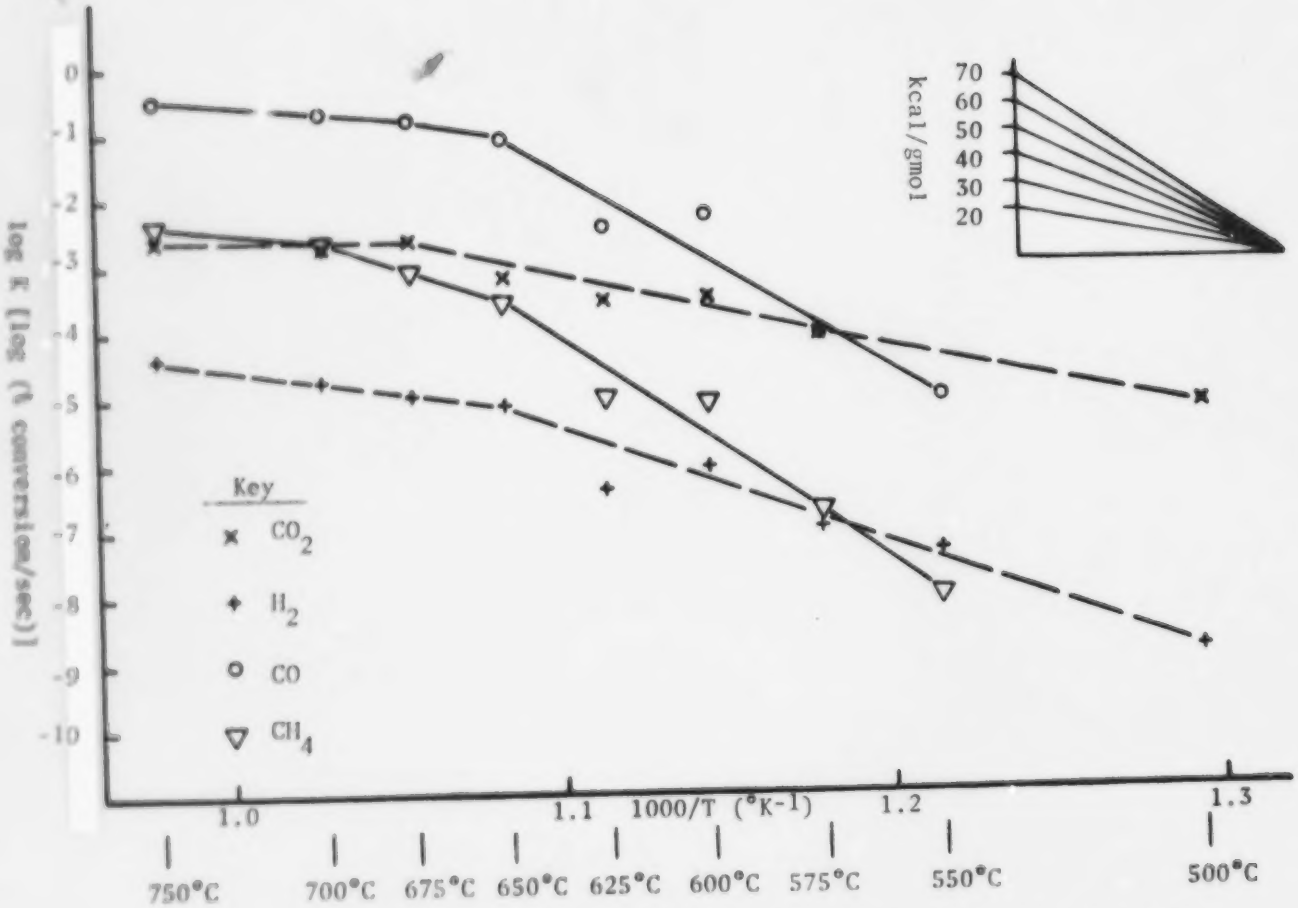

Arrhenius Plot of the Gas Phase Production Rate for Various Gas Species

Figure 34

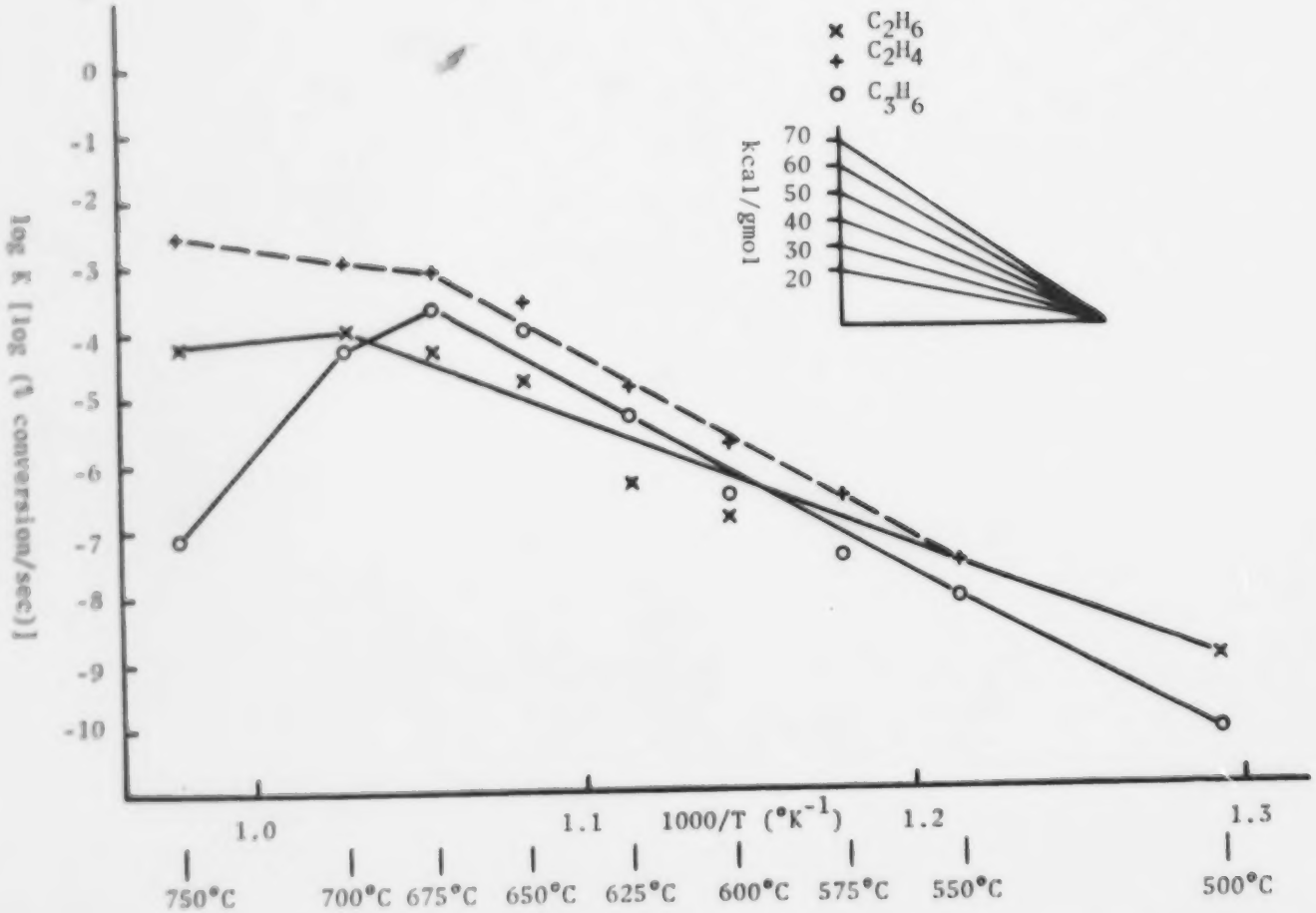

Arrhenius Plot of the Gas Phase Production Rate for Various Gas Species

Figure 35

volatile matter to ethylene is second only to CO and CH_4 in importance. Thus large yields of ethylene can be expected from a well designed biomass gasifier. In contrast to ethylene, the rate of production of propylene peaks at 675°C and rapidly declines at higher temperatures. As expected, both the rates of production of hydrogen and carbon monoxide are favored by high temperatures.

The rate curves for methane and ethylene "track" each other closely, suggesting that the same mechanism may be responsible for the formation of the two gases. All the rates exhibit a break at about 675°C, with lower apparent E_j above 675°C. This may indicate a change in the cracking mechanism, or it may be an artifact of poor heat transfer in the gas phase reactor. A more explicit mechanistic interpretation of the data is made difficult by the effects of heat transfer and non-ideal plug flow on the kinetic interpretation of the experimental data. Nevertheless, the data are quite useful for engineering design purposes, and suggest criteria to be used for the design of second generation reactors intended to provide more accurate measurements of gas phase cracking rates.

Finally, Figures 30-32 also exhibit the fit (dashed line) of Eq.21 to the experimental data for a gas phase temperature of 600°C. Values for $\bar{v}\sigma\int c_j(t)dt$ and $\bar{v}\sigma(r_j/r_v)\int c_v(t)dt$ at 600°C used in Eq. 21 are listed in Table 14. The relatively good agreement of the model embodied in Eq. 21 with the experimental data given in Figures 30-32 is not entirely fortuitous, but is less good at higher temperatures where the constraint $r_v(\tau_o-\tau_i)<<1$ is not satisfied. A mechanistic interpretation of the gas phase phenomena is needed to improve our ability to mathematically predict the products of gasification under a variety of conditions.

CONCLUSIONS

This research has shown biomass gasification to be dominated by the cracking of evolved volatile matter in the gas phase. At temperatures above 700°C these cracking reactions proceed to completion in a time scale of one second or less. Careful control of the time/temperature history of the volatile matter evolved by pyrolyzing biomass can be used to favor the formation of more valuable chemicals and fuels: propylene, ethylene and methane. Based on these results, considerably more research on the secondary, gas phase cracking mechanisms and kinetics is recommended in order to isolate the optimal conditions for converting biomass into a selected product slate of fuels and chemicals.

TABLE 14. NUMERICAL VALUES USED IN THE GAS PHASE KINETIC MODEL

	$\bar{v}\sigma\int c_j(t)dt$	$\bar{v}\sigma(r_j/r_v)\int c_v(t)dt\Big\|_{T = 600°C}$
CO_2	0.061	0.046
H_2	0.001	0.0057
CO	0.045	0.155
CH_4	0.0035	0.0145
C_2H_6	0.0009	0.0039
C_2H_4	0.0	0.010
C_3H_6	0.0002	0.0058

SECTION VII

MODEL COMPOUND STUDIES

INTRODUCTION

Exploratory studies of the cracking characteristics of certain model compounds were initiated using a Chemical Data System (CDS) pyrolysis-analysis system originally acquired for Princeton's coal research program. The CDS pyrolysis-analysis system is a rather complex arrangement of components which may be used in a variety of ways. For purposes of this research it can be considered as a temperature programmed pyrolyzer, followed by a stop-flow gas chromatograph (GC), and then by a system which helps to identify the products separated by GC. Temperatures of many of the components may be controlled by separate circuits, and the bulk of the system is maintained at temperatures in the range of 250 to 350°C. Descriptions of the various subsystems follow (see Figure 36).

The model 120 Pyroprobe is a heated quartz-lined interface (up to 300°C) where a flat platinum filament or a platinum coil may be resistively heated. A programmer permits the flat filament to be heated at rates of 5, 10, 20, 30, and 40°C/min, and 0.1, 0.2, 0.5, 1, 2, 5, 10, and 20°C/msec. The total heating time and final temperature are also preselected; the latter up to 1400°C. The platinum coil is designed to house a quartz tube as a container for samples that cannot be fastened to the flat filament. The mass of the quartz tube permits only heating rates up to 0.5°C/msec to be used. The temperature is that of the platinum element, rather than that of the sample. Up to four gases at separately controlled flow rates may be mixed and flowed over the pyrolysis sample. Reactive gases are permitted by the construction of the pyrolysis system. The pyrolysis gases may be taken out of the system, passed through a sorption trap, or may be injected into a GC column. The trap is filled with Chromosorb 102 and the GC with Poropak Q, but other column materials can be substituted, as required.

The GC is of the two-column temperature programmed type with flame ionization detectors (FID) at the exit of both columns and a thermoconductivity detector (TCD) at the exit of the sample column. A second TCD is between the trap and the sample GC column inlet. A stop-flow feature permits single GC peaks to be analyzed by auxiliary methods while the materials still in the GC column are held stationary. The temperature of the GC column may be fixed during stop-flow operation, and programmed increase may continue when flow is resumed.

FLOWCHART OF CDS SYSTEM

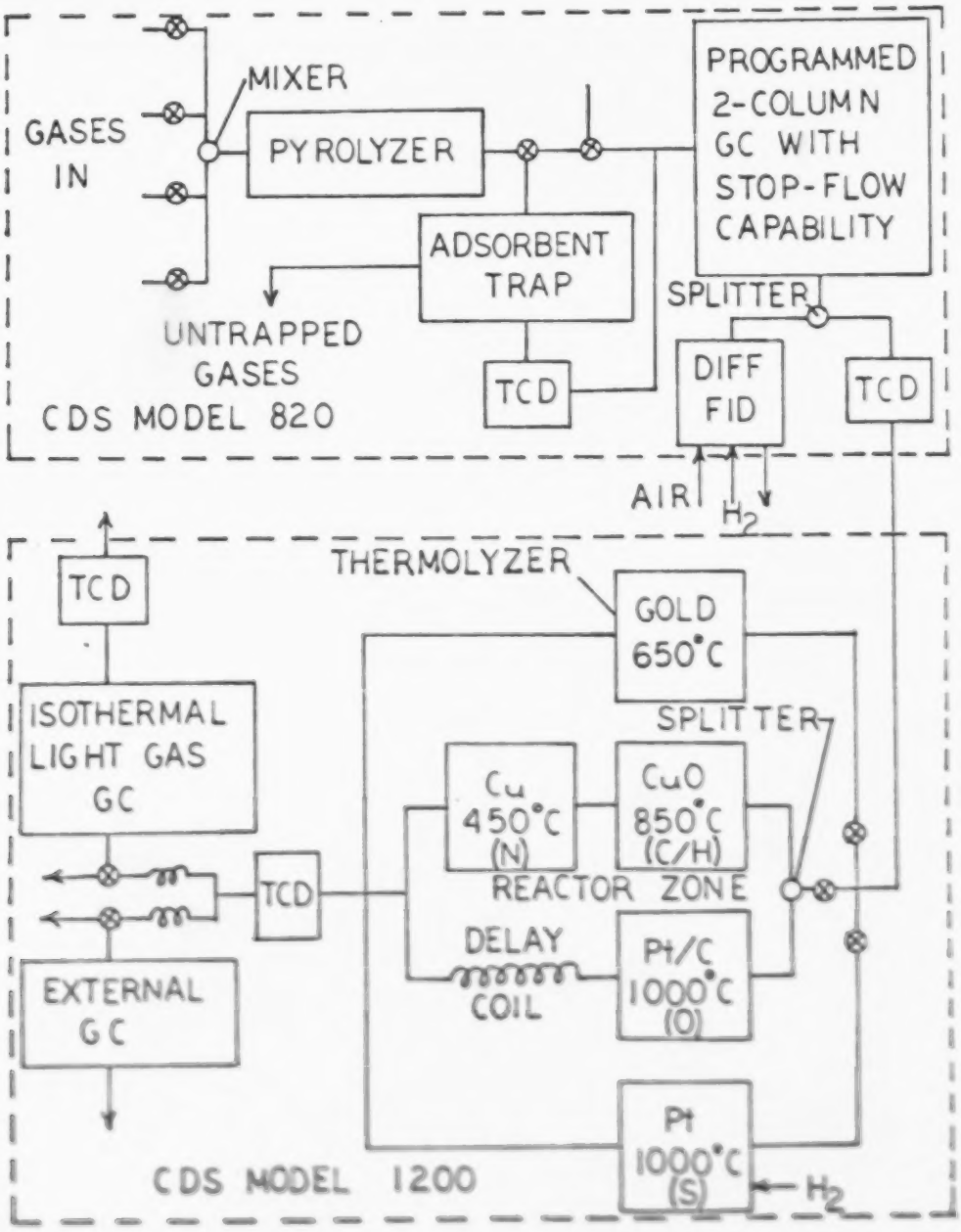

Figure 36

The Pyroprobe, trap, GC, and detectors are housed in the CDS model 820DEB unit. The GC peak identifier is the CDS model 1200, which will be described later. A number of experiments have been carried out to familiarize us with the use of this system, including pyrolysis of Whatman filter paper and of coal. Since the detectors are very sensitive, very small samples are required -- 10 to 50 mg being suggested by CDS. A tuft of quartz wool is inserted into the quartz tube, and the tube and wool are heated in air to 1400°C for 10 sec. After cooling, the paper or coal are inserted, so as to be centered with respect to the coil, and the probe is inserted in the coal interface. The air is then flushed out by the helium carrier gas, and the interface is warmed to reduce condensation of the less volatile products. With fast heating, i.e., gas generation time << GC separation time, direct injection to the GC unit is desirable. Otherwise, trapping and/or external collection and analysis are necessary. The Chromosorb 102 filler does not, however, retain the lighter gases at room temperature, and could probably not retain hydrogen, even if cooled. CDS has advised the use of powdered carbon dioxide ice to cool the trap and/or the use of Carbosieve B as the adsorbent for the light gases. The Poropak Q GC column has been unable to separate the light gases at room temperature, however later analysis with the CDS model 1200 unit is possible, as will be described below. It may be necessary to change to a different column, or to carry out analysis in two separate pyrolyses. In carrying out pyrolysis it was observed that products that condensed in the vicinity of the probe contributed to products of later pyrolysis. Therefore, it may be necessary to clean the probe and interface following some pyrolyses. It was found that heating the interface at 290°C in air for two hours, with periodic 1400°C - 10 sec probe flashing, cleaned the apparatus. CDS now has an option of replacing the 300°C interface with a programmed higher temperature interface; this replacement will be made, if needed.

The separated peaks of the GC (i.e., effluence for $\leq$ 15 sec) flow through a heated line to series of reactors designed for elemental or pyrolytic analysis. Once past the reactors the gases flow past a TCD to a splitter, and then to a pair of delay coils from which they may be injected into an isothermal light gas GC and/or into an external programed GC. The isothermal light gas GC contains mixed porous polymers, and searates gases up to butanes. A backflushing capability permits heavier gase to be ejected from this GC. The external GC provision would be usedif heavier pyrolysis products than C_4 are generated. The pyrolytic reactr is filled with gold (recommended temperature 650°C), and converts the enering material to a series of products that are characteristic of tht material. Injection of knowns directly into the reactor inlet stream wil aid in the identification of the GC effluent.

An alternate method of identification is elemental analyss. C, H, O, N, and S analysis may be accomplished in several different stzes. The first four elements are analyzed as follows. The GC effluent s divided into two equal portions that enter two reactor lines. The C-HN line is composed of two reactors in series. The first (CuO at 850°C) oxidizes C to CO_2 and H to H_2O and the second (Cu at 450°C) converts nitrgen

containing gases from the first reactor to N_2. The second reactor contains platinized carbon at 1000°C, and converts O to CO. Alternatively, the GC effluent may be directed to a platinum reactor at 1000°C, where it is mixed with H_2, and the S is converted to H_2S. By calibrating with known amounts, the isothermal GC results may be converted to quantitative elemental analyses, so that the chemical composition of the GC effluent may be further characterized. Thus three methods of identification are available; namely, (1) by the retention time through the GC in the model 820 DEB unit, (2) by comparing pyrolysis products in the GC of the model 1200 unit and/or an external programmed GC, and (3) by elemental analysis in the model 1200 unit.

As described earlier, with rapid pyrolysis directly into the GC, the Poropak Q column will not resolve H_2, N_2, O_2, and CO. Tests with some of these gases indicate that they may be analyzed with the reactor/isothermal light gas GC of the model 1200 unit, wherein H_2 is converted to H_2O, O_2 is converted to CO, and CO is converted to CO_2. An alternative method is to allow these light gases to bypass the model 1200 system and go into an auxiliary GC equipped with a light gas GC column; e.g., molecular sieve or Carbosieve B.

When the gases flow from the trap to the GC, they pass the reference side of the TCD. Since the lightest gases pass through the GC column very rapidly, some may arrive at the GC sample TCD before the reference detector has returned to baseline. Although we will probably not do any qualitative or quantitative analysis of the light gases at this stage, at least one of several modifications would have to be made to do so, including: (1) increasing GC retention time by changing column material, length, or operating conditions, (2) installing a delay line between the reference TCD outlet and the GC inlet, or (3) removing the reference TCD from this part of the system and connecting elsewhere; e.g., at the end of the reference GC column or at the trap vent. In the latter position, the sorption trap could be cooled by dry ice, with H_2 detection by the reference TCD taking place during gas collection. Accuracy would be limited by such factors as low detector sensitivity, relatively long times for evolution for relatively slow heating, and baseline drift.

During this period, some ghost peaks were observed, which were attributed to vapors evolved from condensed materials on various hot surfaces. Ghosts were removed by solvent injection through a septum installed at the pyrolyzer insertion position. One-half mg samples of Whatman No. 1 filter paper were pyrolyzed in flowing helium in the quartz furnace tube at platinum coil temperatures of 900 and 1400°C for 20 sec., with direct injection to the GC. The GC column was 1/8 in. dia. x 6 ft. of Poropak Q with a flow rate of approximately 30 ml/min programmed for 9 min at 40°C, heated from 40 to 220°C at a rate of 10°C/min, and then held at 220°C for about 45 min. It was found that some different products formed at the two heating rates, and there were different yields of the same products. Samples of various coals which were pyrolyzed at 1400°C, as part of another study, showed the formation of essentially the same products as paper at the same temperature, but with different yields.

In comparing all of the GC curves, it was found that reproducibility was quite good on the temperature ramp, but was much poorer during isothermal portions. Investigation of the starting temperature showed that the GC system was so hot that 40°C was a rather poor starting temperature, so current GC programs are being started at 60°C. Furthermore, rather continuous flow monitoring is being used to determine the uniformity of flow and effects of its variation.

Calibration experiments were carried out for some 25 compounds, some of which had similar retention times as observed in the pyrolysis/GC runs.

In examining the various pyrolysis GC results, it is evident that most significant products are so minor that the elemental analysis system would not be able to furnish sufficient accuracy to help identify the GC effluents due to its use of a thermal conductivity detector (TCD), with its inherently low sensitivity. Therefore, it may be more useful to consider using the identification approach of thermolysis followed by a second GC which employs flame ionization detection (FID), although CO, CO_2, and H_2O as thermolysis products would still require TCD, since they do not respond to FID. In thermolysis, pyrolysis of the effluent from the first GC system would yield characteristic secondary products in the second GC, so that comparison with thermolysis products of known compounds would help to identify the effluents from the first GC.

Since it has been suggested that the pyrolysis products of cellulose may well be produced from the decomposition of levoglucosan[3] we examined the effect of heating rate on product distribution. About 0.5 mg samples of levoglucosan (m.p 174-177°C) were decomposed at 5,000 and 20,000°/sec up to 1000°C in the inert atmosphere of the CDS unit. Under these conditions CO, CO_2, and CH_4 accounted for 85-90% of all volatile products and the CO/CO_2 ratio increased from 14 $\pm$ 2 to 21.5 $\pm$ 3.7 with an increase in heating rate. The higher heating rate also favored methane formation.

ETHANOL PYROLYSIS

To gain an insight into the gas phase chemistry of the pyrolysis products of cellulosics the thermolysis of ethanol was examined as one model compound for levoglucosan - the principal cellulose intermediate.

The pyrolysis reactions were carried out in the thermal reactor of the CDS system. In each experiment 0.5 µl of ethanol (99.12 w/w%) was injected and the products analyzed on a Poropak Q-chromosorb 104 column. The product mixture was composed of CO, CH_4, C_2H_4, C_2H_6, H_2O, CH_3CHO, unreacted ethanol and a trace of propene and propane. Product composition was calculated from the response factors given in the literature[37,71,72] and the residence times and rate constraints by the method of Rensfelt et al[73]. The results of this investigation are outlined below.

1. Product Distribution

Reactor Temperature	647°C	660°C
Residence Time	2.95 sec	3 sec
% Ethanol Converted	53	72
Products (Mole %)	Run 1	Run 2
CO	14.7	27.4
CH_4	15.2	25.3
C_2H_4	7.16	8.52
C_2H_6	0.65	1.42
H_2O	9.65	10.7
CH_3CHO	15.4	11.2
C_2H_5OH	37.3	15.46

2. Approximate Balanced Equation

$$C_2H_5OH \longrightarrow CO + CH_4 + C_2H_4 + C_2H_6 + H_2O + CH_3CHO + H_2^*$$

Coefficients -							
	647°C	0.38	0.40	0.185	0.017	0.255**	0.40 + (0.71)
	660°C	0.57	0.53	0.18	0.03	0.23**	0.24 + (0.8)

3. Overall Reaction Scheme

A. Major Products

$$CH_3CH_2OH \xrightarrow{ke} C_2H_4 + H_2O$$

$$CH_3CH_2OH \xrightarrow{kc} CH_3CHO + H_2$$

$$CH_3CHO \longrightarrow CH_4 + CO$$

B. Minor Products (< 1 mole %)

$$(CH_3CHO \longrightarrow CH_3^{\bullet})$$

$$2CH_3^{\bullet} \longrightarrow C_2H_6$$

$$CH_3^{\bullet} + C_2H_4 \longrightarrow CH_3CH_2CH_2 \xrightarrow{-H^{\bullet}} CH_3CH = CH_2$$

$$CH_3CH_2CH_2 \xrightarrow{+H^{\bullet}} CH_3CH_2CH_3$$

4. Conclusions

A. Stoichiometry of Above Reactions Requires:

a) one H_2 for each CH_3CHO formed

b) one CH_4 and CO for each CH_3CHO that disappears

	647°C	660°C
1. Total amount of CH_3CHO from 1 ETOH	0.40	0.24
2. Amount of C_2H_4 expected (found)	0.22 (0.185)	0.19 (0.18)
3. Amount of H_2O expected (found)	0.22 (0.23)	0.19 (0.21)
4. Amount of H_2 expected (amount used to balance equations)	0.78 (0.71)	0.81 (0.8)

B. About 20% of alcohol pyrolyses to give olefins and 80% to give aldehydes and synthesis gas, or dehydrogenation is about 4 times faster than dehydration (this distribution is catalytically sensitive)

$$\frac{kc}{ke} = \frac{(CH_3CHO)}{(C_2H_4)} = \frac{0.81}{0.19} \simeq 4.2$$

C. At 660°C, slightly less CH_4 than CO is formed and is explained by reaction scheme 3B (minor products).

---

* Untracted but necessary to balance equations.

**Includes 0.02 H_2O in starting ethanol.

D. The heat of reaction for the balanced equation (647°C).

$$\Delta H_2(25°C) = +10.2 \text{ kcal/mol EtOH}$$

or $\Delta H_2 \approx 220$ cal/g starting material if ethanol is typical of gas phase thermochemistry.

5. Kinetics

In order to establish kinetics of pyrolysis, additional runs were made at 647°C.

A. Plot of log (C/CO)* vs t is linear up to about 70% reaction with $k_{obs} = 0.19 \text{ sec}^{-1}$

B. Rate Law for EtOH Disappearance

$$\frac{-d(EtOH)}{dt} = (ke + kc)EtOH$$

where $$\frac{kc}{ke} = \frac{[CH_3CHO]_t}{[C_2H_4]_t} \simeq 4.2 \quad \text{(see 4B)}$$

$$k_{obs} = (ke + kc) = 0.19 \text{ sec}^{-1}$$

$$\therefore ke \simeq 0.036 \text{ sec}^{-1}$$

$$\text{and } kc \simeq 0.154 \text{ sec}^{-1}$$

From Literature

1. Aldehyde formation

$$kc \simeq 10^{10 \pm 0.4} e^{-\frac{46,200}{RT}} \text{ sec}^{-1}$$

$\therefore$ at 647°C $kc \simeq 0.11 \pm 0.15 \text{ sec}^{-1}$

our experimental kc is in good agreement with literature.

2. Olefin formation

$$ke \simeq 0.036 \simeq **10^{13.3} e^{-\frac{E_a}{R \times 920}} \text{ sec}^{-1}$$

and $E_a \simeq 52$ kcal/mol.

---

* C/CO = % Remaining

**A factors for alcohol elimination are about $10^{13.2-13.4}$

Similar data

$$E_e(\text{i-propyl alcohol}) = 67 \text{ kcal/mol}.$$

C. Other products

Concentrations of CO, CH_4, C_2H_4, C_2H_6, H_2O, and CH_3CHO increase during the experiment. The very small amount of propane, propene is ignored.

1. As expected from the stoichiometry of reaction 3A, CO and CH_4 are formed in the same amount.

2. The constancy of the CH_3CHO plot indicates a steady state assumption.

$$k_c(EtOH) = \frac{d(CH_3CHO)}{dt} = \frac{d(CH_4)}{dt} = \frac{d(CO)}{dt} \quad .$$

SECTION VIII

PRESSURIZED STEAM GASIFICATION STUDIES

A heavily instrumented, micro-reactor system was developed with U.S. EPA support to study pressurized steam gasification of biomass. The system uses a Setaram Differential Scanning Calorimeter (DSC) to monitor the rates and heats of pyrolysis of the solid phase reactant. The unique features of the DSC, and the role it plays in the reactor system, are described in Table 15. Some early data was gathered in Setaram's Lyon laboratory on the effects of pressure on biomass pyrolysis. These preliminary results were reported in reference 14.

Figure 37 depicts an early design of the entire reactor system. Unfortunately, the steam generator was unable to generate reproducible, small flows of steam under pressure. Ultimately, the steam generator system was replaced by a commercially available steam generator which performs well up to a pressure of 5 atm.

Figure 38 is a schematic of the two micro-reactors, fabricated from type 316 stainless steel. These reactors were designed to provide: 1) reactor contact with the calorimeter sensor, 2) minimum lateral heat flux along the tube, and 3) capability of repeated operation at 150 psi and 800°C. As in our earlier work, the reactor is zoned to provide for separate study of the solid phase (occuring in the DSC) and gas phase chemistry (occuring in the reactor zone surrounded by the heating block).

Table 16 lists the results of a series of shakedown experiments using the micro-reactor system without the Setaram DCS. Both experiments utilized a solid's heating rate of 100°C/min to 500°C. The data reveal a marked increase in char yield with increasing pressure, and a decrease in the carbon efficiency (carbon efficiency = carbon in gas ÷ carbon in feed) from 0.77 to 0.36. Apparently, increased pressure leads to a dramatic decrease in gas production by pyrolysis. Pressurized biomass reactors will have to operate at elevated temperatures with longer solids residence times in order to gasify the char residue by the water and gas Boudouard reactions.

TABLE 15

THE SETARAM DIFFERENTIAL SCANNING

CALORIMETER (DSC)

1. Is a calorimeter. It measures the rate of heat influx or outflow from a small reactor volume enclosed in a furnace.

2. Scans in temperature. It can heat the reactor volume from subambient to 827°C at heating rates up to 20°C/min.

3. Is actually two opposed calorimeters. It measures differences in heat flow between a control volume and a sample volume.

4. Is capable of "seeing" into a pressurized tubular steel reactor and reporting rates of chemical reactions occurring within it.

5. Is capable of measuring the total heat of reaction of the pyrolysis/ steam gasification process.

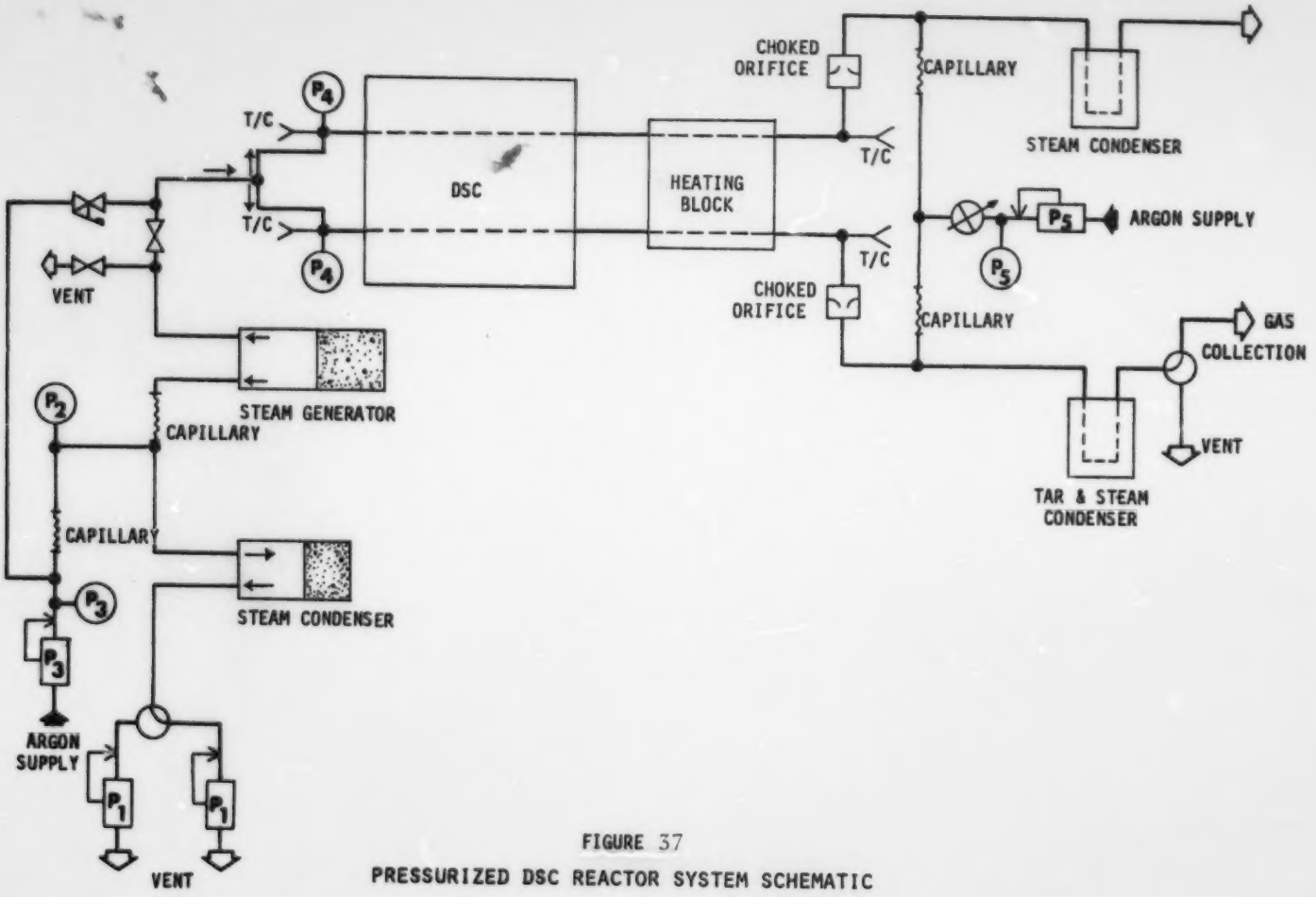

FIGURE 37

PRESSURIZED DSC REACTOR SYSTEM SCHEMATIC

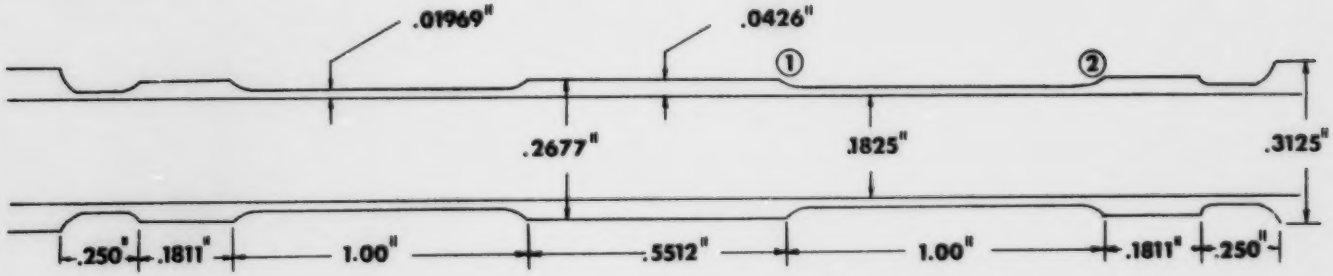

FIGURE 38

TUBULAR REACTOR SCHEMATIC

TABLE 16

CELLULOSE GASIFICATION RESULTS AT ATMOSPHERIC

AND ELEVATED PRESSURES

Pressure	0.1 MPa*	0.2 MPa
Gas Phase Reactor Temperature	700°C	700°C
Gas Phase Reactor Residence Time	1.3 s	1.8 s
Sample Weight	0.0146 g	0.0165 g
Char Residue Weight	0.0005 g	0.003 g
Gas Volume Produced	11.4 mℓ	8.9 mℓ
Gas Heating Value	392 Btu/scf	378 Btu/scf
Calorific Value of Char	1.0 MM Btu/mt	5.3 MM Btu/mt
Calorific Value of Gases	12.7 MM Btu/mt	8.5 MM Btu/mt
Mass Balance	0.87	0.81
Carbon Balance	0.83	0.89
Gas Analysis (Vol %)		
CO	38.8	37.6
H_2	28.9	24.7
CO_2	19.8	24.5
CH_4	6.8	8.3
C_2H_4	3.6	2.7
C_2H_6	0.9	0.8
C_3H_6	1.0	1.2
other	0.2	0.2

*0.1 MPa = 1 atmosphere

REFERENCES

1. Gordon, S. and B. J. McBride (1971). Computer program for calculation of complex chemical equilibrium compositions, rocket performance, incident and reflected shocks, and Chapman-Jouquet detonations. NASA-SP 273, Cleveland, Ohio.

2. Tillman, D. A. (1978). Wood as an energy source. Academic Press, New York.

3. Anderson, L. L. and Tillman, P. A. (1977). Eds. Fuels from Waste, Academic Press, New York.

4. Shafizadeh, F., Sarkanen, K. V. and Tillman, D. A. (1976). Eds. Thermal uses and properties of carbohydrates and lignins. Academic Press, New York.

5. Weinstein, N. J. and Toro, R. F. (1976). Thermal processing of municipal solid waste for resource and energy recovery. Ann Arbor Sci., Ann Arbor, Mich. p. 192.

6. Cheremisinoff, P. N. and Morresi, M. A. (1977). Energy from wood waste. Environment, 19, No. 4.

7. Antal, M. J., Feber, R. C., and Tinkle, M. (1976). Synthetic fuels from solid wastes and solar energy. Proceedings of the World Hydrogen Energy Conference, Miami.

8. Antal, M.J. (1976). Tower power: producing fuels from solar energy. Bulletin of the Atomic Scientists, 32, 59.

9. Feber, R. C. and Antal, M. J. (1977). Synthetic fuel production from solid wastes. Environmental Protection Technology Series, EPA-600/2-77-147.

10. Antal, M. J. (1977a). The conversion of urban wastes. Proceedings of the International Symposium on Alternative Energy Sources, Barcelona.

11. Antal, M. J. (1977b). A comparison of coal and biomass as feedstocks for synthetic fuel production. Miami International Conference on Alternative Energy Sources, Miami.

12. Antal, M. J. (1978a). Biomass energy enhancement. Report to the President's Council on Environmental Quality.

13. Antal, M. J. (1978b). Synthesis gas production from organic wastes by pyrolysis/steam reforming. IGT's Conference on Energy from Biomass and Wastes, Washington.

14. Antal, M. J. (1979). The effects of residence time, temperature and pressure on the steam gasification of biomass. Preprints of the ACS Honolulu Meeting.

15. Diebold, J. and Smith, G. (1978). Conversion of trash to gasoline. NWC Tech. Pub. 6022, China Lake.

16. Stamm, A. J. (1956). Thermal degradation of wood and cellulose. Ind. Eng. Chem., 48, 413.

17. Mackay, G. D. M. (1967). Mechanism of thermal degradation of cellulose: a review of the literature. Forestry Branch Dept. Publ. No. 1201, Canada Dept. of Forestry and Rural Development.

18. Roberts, A. F. (1970). A review of kinetic data for the pyrolysis of wood and related substances. Combust. Flame, 14, 261.

19. Welker, J. R. (1970). The pyrolysis and ignition of cellulosic materials: a literature review. J. Fire Flamm., 1, 12.

20. Beall, F. C. and Eickner, H. W. (1970). Thermal degradation of wood components: a review of the literature. Forest Prod. Laboratory Res. Paper 130, U.S. Forest Service.

21. Golova, O. P. (1975). Chemical reactions of cellulose under the action of heat. Usp. Khim, 44, 1454.

22. Madorsky, S. L. (1964). Thermal degradation of organic polymers. Interscience, New York, p. 238.

23. Madorsky, S. L., Hart, V. E. and Straus, S. (1956). Pyrolysis of cellulose in a vacuum. J. Res. Nat. Bur. Std., 56, 343.

24. Schwenker, R. F. , Jr. and Pascu, E. (1958). Chemically modifying cellulose for flame resistance. Ind. Eng. Chem., 50, 91.

25. Murphy, E. J. (1962). Thermal decomposition of natural cellulose in vacuo. J. Polym. Sci., 58, 649.

26. Berkowitz-Mattuck, J. B. and Noguchi, T. (1963). Pyrolysis of untreated and APO-THPC treated cotton cellulose during one-second exposure to radiant flux levels of 5-25 cal/cm^2-sec. J. Appl. Polym. Sci., 7, 709.

27. Schwenker, R. F., Jr. and Beck. L. R. (1963). Study of the pyrolytic decomposition of cellulose by gas chromatography. J. Polym. Sci., C2, 331.

28. Martin, S. (1965). Diffusion controlled ignition of cellulose materials by intense radiant energy. Tenth Symp. (Int'l.) on Combust., The Combustion Inst., Pittsburgh, 877 (1965).

29. Lipska, A. E. and Woodley, F. A. (1969). Isothermal pyrolysis of cellulose: kinetics and GC-MS analysis of the degradation products. J. Appl. Polym. Sci., 13, 851.

30. Shafizadeh, F. (1975). Industrial pyrolysis of cellulosic materials. J. Appl. Polymer. Sci., Symp. No. 28, pp. 153-174.

31. Kilzer, F. J. and Broido, A. (1965). Speculation on the nature of cellulose pyrolysis. Pyrodynamics 2, 151.

32. Broido, A. (1966). Thermogravimetric and differential thermal analysis of potassium bicarbonate contaminated cellulose. Pyrodynamics 4, 243.

33. Weinstein, M. and Broido, A. (1970). Pyrolysis-crystallinity relationships in cellulose. Comp. Sci. and Tech. 1, 287.

34. Arseneau, D. F. (1971). Competitive reactions in the thermal decomposition of cellulose. Can. J. Chem. 49, 632.

35. Arseneau, D. F. and Stanwick, J. J. (1971). A study of reaction mechanisms by DSC and TG. Thermal Analysis, Vol. 1, Proceedings Third ICTA, Damos.

36. Broido, A. and Nelson, M. A. (1975). Char yield on pyrolysis of cellulose. Combust. Flame 24, 263.

37. Broido, A. (1976). Kinetics of solid phase cellulose pyrolysis in thermal uses and properties of carbohydrates and lignins. (F. Shafizadeh, K. Sarkanen and D. Tillman, ed.) Academic Press, New York.

38. McCarter, R. J. (1972). The pyrolysis of cellulose at rates approaching those in burning. Textile Res. J. 42, 709.

39. Chatterjee, P. K. (1968). Chain reaction mechanism of cellulose pyrolysis. J. Appl. Polym. Sci. 12, 1859.

40. Chatterjee, P. K. and Conrad, C. M. (1966). Kinetics of the pyrolysis of cotton cellulose. Textile Res. J. 36, 487.

41. Madorsky, S. L., Hart, V. E. and Straus, S. (1958). Thermal degradation of cellulosic materials. J. Res. Nat'l. Bur. Std. 60, 343.

42. Lewellen, P. C., Peters, W. A. and Howard, J. B. (1976). Cellulose pyrolysis kinetics and char formation mechanism. Sixteenth Int'l. Symp. on Combust., Massachusetts Inst. of Technology, August 1976.

43. Tang, W. K. (1967). Effects of inorganic salts on pyrolysis of wood, x-cellulose, and lignin, determined by DTA. Forest Prod. Laboratory Paper 71, Madison, Wis.

44. Tang, W. K. and Neill, W. K. (1964). Effects of flame retardants on pyrolysis and combustion of x-cellulose. J. Polym. Sci. 6, 65.

45. Lipska, A. E. and Parker, W. J. (1966). Kinetics of pyrolysis of cellulose in the temperature range 250-300°C. J. Appl. Polym. Sci. 10, 1439.

46. Gross, D. and Robertson, A. F. (1958). Self ignition temperatures of materials from kinetic reaction data. J. Res. Nat'l. Bur. Std. 61, 413.

47. Roberts, A. F. and Clough, G. (1963). Thermal decomposition of wood in an inert atmosphere. Ninth Symp. (International) on Combustion, p. 158, Academic Press, New York.

48. Murty, K. A. and Blackshear, P. L., Jr. (1966). An X-ray photographic study of the reaction kinetics of x-cellulose decomposition. Pyrodynamics 4, 285.

49. Kanury, A. M. (1972). Thermal decomposition kinetics of wood pyrolysis. Combust. Flame 18, 75.

50. Baker, R. R. (1975). Thermal decomposition of cellulose. J. Thermal Anal. 8, 163.

51. Maa, P. S. and Bailie, R. C. (1978). Experimental pyrolysis of cellulosic material. The 84th Nat'l. Meeting AIChE, Atlanta, Georgia, February 1978.

52. Ruth, L. A., Squires, A. M. and Graff, R. A. (1972). Desulfurization of fuels with half-calcined dolomite. Environmental Sci. and Tech. 6, 1009.

53. Sestak, J., Satava, V. and Wendlandt, W. (1973). The study of heterogeneous processes by thermal analysis. Thermochim. Acta 7, 333.

54. Lucci, A. and Tamanini, M. (1975). Methods of non-isothermal kinetic analysis by DSC curves. Thermochim. Acta 13, 147.

55. Battezzate, L. Lucci, A. and Riontino, G. (1978). A computer method to determine the kinetic law of solid-state reactions from DSC curves. Thermochim Acta 23, 213.

56. Chen, D. T. Y. and Fong, P. H. (1977). Evaluation of kinetic parameters from TG curves. Thermochim. Acta. 18, 161.

57. Criado, J. M. (1978). Kinetic analysis of DTG data from master curves. Thermochim. Acta. 24, 186.

58. Friedman, H. L. (1964). Kinetics of thermal degradation of char-forming plastics from thermogravimetry. J. Polym. Sci. C6, 183.

59. Ozawa, T. (1965). A new method of analyzing thermogravimetric data. Bull. Chem. Soc., Japan 38, 1881.

60. Flynn, J. H. and Wall, L. A. (1966). A quick direct method for the determination of activation energy from TGA data. Polym. Letters 4, 323.

61. Freeman, E. S. and Carroll, B. (1958). The application of thermoanalytical techniques to reaction kinetics. The TG Evaluation of the Kinetics of the Decomposition of Calcium Oxalate Monohydrate. J. Phys. Chem. 62, 394.

62. Altorfer, R. (1978). Estimation of kinetic parameters from conversion curves determined of constant heating rate. Thermochim. Acta 24, 17.

63. Sharp, J. H. and Wentworth, S. A. (1969). Kinetic analysis of thermogravimetric data. Anal. Chem. 41, 2060.

64. Beall, F. (1968). Thermal degradation analysis of wood and wood components. Ph.D. Thesis, Syracuse University, Syracuse, New York.

65. Timell, T. E. ( ). Recent studies on the molecular morphology of wood. Second Can. Wood Chem. Symp. CPPA and CIC, pp. 5-6, Ste. Marguerite, PQ.

66. Nelson, W. L. (1958). Petroleum refinery engineering. Fourth Edition, McGraw Hill Book Co., New York.

67. Zdonik, S. B., Green, E. J. and Hallee, L. P. (1970). Manufacturing ethylene. Petroleum Publishing College, Tulsa.

68. Goosens, A. G., Dente, M. and Ranzi, E. (1978). Improve steam cracker operation. Hydrocarbon Processing, September 1978.

69. Levenspiel, O. (1972). Chemical reactor engineering. Second Edition, John Wiley and Sons, Inc., New York.

70. Wodley, F. A. (1969). U.S. Naval Radiological Def. Lab., AD 704 145, August 1969.

71. Antal, M. J. (1977-78). Quarterly Progress Reports to U. S. EPA, Princeton University, Princeton, N.J.

72. Antal, M. J., Friedman, H. L. and Rogers, F. E. (1977). Kinetic rates of cellulose pyrolysis in nitrogen and steam. Eastern States Section, The Combustion Institute Fall Meeting, Hartford, Conn.

73. Rensfelt, E., Blomkvist, G., Ekstrom, C., Engstrom, S., B-G. Espenas and Liinanki, L. (1978). Basic gasification studies for development of biomass medium Btu gasification process. IGT Conference on Energy from Biomass and Wastes, Washington, D. C., August 1978.

APPENDIX I

The following schematic attempts to summarize the findings of previous workers on the mechanism of cellulose pyrolysis. It represents a consensus of the literature and a modification of that due to Broido and Weinstein[33].

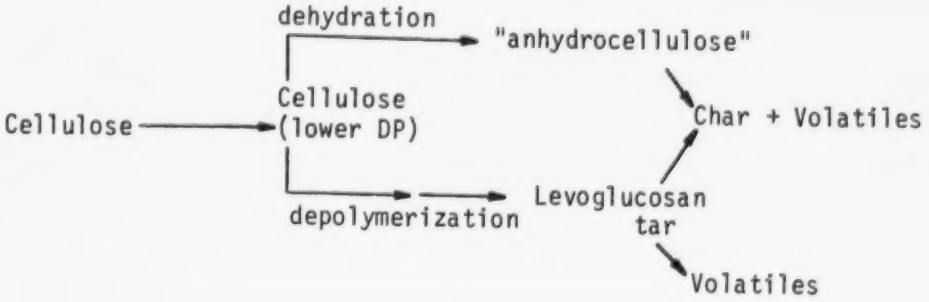

The first step is a decrease in the degree of polymerization (DP) to about 200 with no detectable weight loss[17,33,37]. From this point on, the pyrolysis mechanism appears to branch on the assumption that a molecule as complex as cellulose should have more than one chemical decomposition pathway available, and the implementation of one of these pathways increases or decreases the likelihood of another taking place. A dehydration or thermal autocrosslinking reaction leads to the formation of anhydrocellulose which shows increased C = O and C = C bond activity in the infrared[17,34]. The anhydrocellulose may continue to react further to form most of the char and some volatile species.

Competing with the anhydrocellulose reaction is a series of sequential depolymerization reactions[40] which eventually produce a levoglucosan tar. This tar may either form char and some volatiles, or mainly volatiles depending on the experimental conditions. The presence of acids or bases may catalyze the conversion of levoglucosan tar to char[30]. Pyrolysis conditions utilizing high temperatures, high heating rates, short residence times, and small samples virtually eliminate the char forming route and bring about the complete conversion of cellulose to volatile species[42]. If cellulose is conditioned at low temperatures (200-250°C), so that some anhydrocellulose is formed, then not even rapid pyrolysis of the samples precludes some char formation via the anhydrocellulose route[42].